

Arylboronic Acid-Catalyzed Hydrolyses of Salicylaldehyde Imines

**By**

**Sheuli Zakia**

A Dissertation Submitted to the Graduate Faculty in Chemistry in partial fulfillment of the requirements for the degree of Doctor of Philosophy, The City University of New York.

2011

2011

Sheuli Zakia

All rights Reserved

This manuscript has been read and accepted for the  
Graduate Faculty in Chemistry in satisfaction of the  
dissertation requirement for the degree of Doctor of Philosophy

Dr. Manfred Philipp

\_\_\_\_\_  
Date

\_\_\_\_\_  
Chair of Examining Committee

Dr. Mahesh K. Lakshman

\_\_\_\_\_  
Date

\_\_\_\_\_  
Executive Officer

Dr. Robert Engel

\_\_\_\_\_  
Dr. Adam Profit

\_\_\_\_\_  
Dr. Andrei Jitianu

\_\_\_\_\_  
Supervisory Committee

THE CITY UNIVERSITY OF NEW YORK

## ABSTRACT

### Arylboronic Acid-Catalyzed Hydrolyses of Salicylaldehyde Imines

By

**Sheuli Zakia**

Adviser: Prof. Manfred Philipp

Boronic acids accelerate hydrolyses of the Schiff's bases derived from salicylaldehyde and primary amines. The accelerations of Schiff's base hydrolyses are due to the formation of a complex between the boronic acid and the imine followed by the break-down of the complex to products. The formation of a reversible complex between arylboronic acids and imines allows the rate of hydrolysis to display typical Michaelis-Menten enzyme-substrate kinetics, including situations where the imine is completely saturated with the boronic acid.

This thesis focuses on the ability of different arylboronic/benzeneboronic acids(BBAs) to catalyze the hydrolysis of different imines, most of them being salicylaldehyde imines made using primary amines or amino acids, an example being salicylidene-threonine.

In order to better understand the mechanism involved in the imine hydrolysis by arylboronic acids, I studied structure-activity relationships(SAR) for different substituted BBAs and of different imine substrates undergoing hydrolyses. Herein, I present the most important aspects of these SAR studies on both the catalysts(BBAs) and on their imine substrates. I hypothesized that electron withdrawing groups would enable BBAs to be more easily ionized, thus becoming better hydrogen bond donors and making it easier to have higher affinities for the imine substrates.

SAR experiments conducted with different fluoro-substituted benzeneboronic acids showed that all fluoro-BBAs have higher catalytic efficiencies of imine hydrolysis than the unsubstituted boronic acid except for the catalysts with two fluorine atoms substituted in the *ortho*-position with respect to the boron atom. The latter presumably induced steric hindrance. SAR on BBAs enabled me to discover novel catalysts for the hydrolysis of salicylidene-3-hydroxyaniline imine. The best ones are with 2,3,5-trifluoroBBA and 2,3,4,5-tetrafluoroBBA and their  $k_{cat}/K_M$  values go over 1000 fold higher than with the unsubstituted BBA.

Furthermore, SAR of different imine substrates highlights the most important structural determinants of the enhanced catalytic efficiency. The most important contribution to the efficiency of imine hydrolysis are shown to be the hydrogen bonding donors or acceptors (hydroxy or amino groups) in the imine substrates which are demonstrated to activate the catalytic turn-over ( $k_{\text{cat}}$ ) of the arylboronic acid catalyst.

The pH dependencies for BBA catalyzed hydrolysis of salicylaldehyde-3-hydroxyaniline shows that rate constants are maximal at lower pH values and decrease with increasing pH. The kinetics shows single proton ionizations, demonstrating that there is no other ionization event related to the imine itself which could affect catalytic efficiency. Moreover, the  $k_{\text{cat}}$ ,  $K_{\text{M}}$  and  $k_{\text{cat}}/K_{\text{M}}$  dependencies with pH shows that  $k_{\text{cat}}$  is independent of pH. This indicates the absence of hydroxide or hydronium ion involvement in the hydrolysis.

The plots of  $\text{Log}_{10}(K_{\text{M}})$ ,  $\text{Log}_{10}(k_{\text{cat}})$ ,  $\text{Log}_{10}(k_{\text{cat}}/K_{\text{M}})$ , vs. Hammett sigma substituent constants indicate that  $k_{\text{cat}}$ ,  $K_{\text{M}}$  and  $k_{\text{cat}}/K_{\text{M}}$  all dependent on electron withdrawing substituent groups present in the benzeneboronic acids.

The hydrogen bonding network provided by the hydroxyl or amino groups in the imine substrates during the hydrolysis could assist the BBA catalysts in binding tighter to the substrate, which in turn, are reflected in higher catalytic efficiencies. The presence of hydroxyl and amino groups in imine substrates of 2,3,4,5-tetrafluoroBBA resulted in 5- to over 100-fold increases in  $k_{\text{cat}}/K_{\text{M}}$  values. Thus the 2,3,4,5-tetrafluoroBBA-catalyzed  $k_{\text{cat}}/K_{\text{M}}$  value for salicylidene-threonine is  $33 \text{ M}^{-1}\text{sec}^{-1}$  and for salicylidene-lysine is  $17 \text{ M}^{-1}\text{sec}^{-1}$  whereas for salicylidene-valine, without an amino acid side chain hydroxyl or amino group, it is only  $8 \text{ M}^{-1}\text{sec}^{-1}$ .

The relative stabilities of the complexes between BBAs and imines are predicted through docking experiments with the software SCULPT provided by MDL. NMR spectroscopy experiments are performed to confirm the structures.

This thesis highlights the importance of the hydroxyl group substituted to the benzene ring in aniline or benzylamine based imines in inducing better catalytic efficiencies for their hydrolyses by fluoro-substituted BBAs. Examples are shown in the  $k_{\text{cat}}/K_{\text{M}}$  values for the hydrolysis of salicylidene-3-hydroxyaniline with 2,3,5-trifluoroBBA ( $232 \text{ M}^{-1}\text{sec}^{-1}$ ), and 2,3,4,5-tetrafluoroBBA ( $175 \text{ M}^{-1}\text{sec}^{-1}$ ).

## **ACKNOWLEDGEMENTS**

I am truly thankful to my thesis advisor, Prof. Manfred Philipp, whose encouragement, guidance and support from the initial engagement to his group to the final level enabled me to develop an understanding of the subject. And amazingly, he was always available to meet throughout the past years and encouraged me by creating projects right there and then.

I also offer my regards and blessings to all of those who supported me in any respect during the completion of the project. I am indebted to my colleagues to support me. Lastly, I am thankful to my mother who has been patiently waiting for this degree after I had deserted being a medical doctor earlier. And I am thankful to my daughter who so far in her life always seen me busy with my study. I am the first one in our close family net who is having a Ph.D. degree. Hopefully that remains as an encouragement for the youngsters.

## Table of Contents

1. Introduction .....	1
1.1.1 Enzyme models: .....	1
1.1.1a. Polymers as enzyme models.....	1
1.1.1b. Micelles as enzyme models.....	2
1.1.1c. Cyclodextrins as enzyme models .....	3
1.1.1d. Macrocyclic molecules as enzyme models .....	5
1.1.1e. RNA & DNA as enzyme models.....	5
1.1.2. Boric, boronic and arylboronic acid as enzyme model .....	7
1.1.3. Imines (Schiff's bases) as model hydrolysis substrates .....	11
1.2. Working model for the kinetics of imine hydrolysis by benzenboronic acids .....	12
1.3. Benzenboronic acids (BBA) as catalyst for the hydrolysis of imine.....	13
1.4. The imines as substrates for the hydrolysis with boronic acids .....	16
1.4.1. Imines with amino acids.....	17
1.4.2. Imines with non amino acid amine: .....	18
1.4.3. The spectral characteristics of the imines .....	20
1.5. Effect of benzenboronic acids as catalyst for the hydrolysis of imine. ....	21
1.5.1. Modeling with Sculpt.....	22
1.5.2. Effect of different substituents of benzenboronic acids on the hydrolysis of selected imine substrates .....	23
1.5.3. pH profile of the benzenboronic acid on the hydrolysis of imine .....	24
2. Materials & Methods.....	25
2.1.1. Synthesis of the imines.....	25
2.1.2. Hydrolysis conditions of imines by different BBAs .....	25
2.1.3. Instrumental discussion of the imines hydrolyses by BBA: .....	26
2.2. Experimental steps for the hydrolysis assay .....	26
2.2.1. Progress curve analysis of imine hydrolysis by BBA: .....	27
2.2.2. Determination of $K_M$ & $k_{cat}$ : .....	32
2.3. pH profiles for the imines hydrolysis.....	33
2.3.1. Description of pH profile .....	33
2.3.2. pK determination for BBA.....	34
2.3.3. pH profile example.....	36
2.4. Modeling with a SCULPT of different complexes between benzenboronic acids and imines .....	37

3. Results and Discussions .....	39
3.1.1. The effect of different concentrations of 2,3,4,5-tetrafluoroBBA on the catalytic efficiency of salicylidene-3-hydroxyaniline hydrolysis .....	39
3.2. SAR of different substituted benzeneboronic acids on the catalytic efficiency of imine hydrolysis .....	43
3.2.1. The fluoro-substituted BBA acids have higher catalytic efficiency of imine hydrolysis than the un-substituted BBA .....	45
3.2.2. The nitro substituted benzeneboronic acids have higher catalytic efficiency of imine hydrolysis than the un-substituted boronic acid .....	52
3.2.3. Benzeneboronic acids with mixed substitution have higher catalytic efficiency on imine hydrolysis than the un-substituted benzeneboronic acid .....	56
3.3 Structure-activity relationship (SAR) of different imines substrates and their effect upon the benzeneboronic acid catalytic efficiency. ....	59
3.3.1. SAR of different amino acids based imines substrates and their effect upon the benzeneboronic acid catalytic efficiency .....	60
3.3.2. The effect of meta-hydroxy-phenylglycine on the benzeneboronic acids catalytic efficiency .....	64
3.3.3. SAR of different primary organic amines based imine substrates and their effect upon the benzeneboronic acids catalytic efficiency .....	66
3.4.1. Effect of carboxyl group of imines on the catalytic efficiencies of benzeneboronic acids	71
3.4.2. Effect of hydroxyl-amine on the benzeneboronic acids catalytic efficiency. ....	78
3.5. Effect of substituents of benzeneboronic acid on the rate of imine hydrolysis.....	82
3.6. Sculpt Results.....	88
3.7.1. Effect of pH on the hydrolysis of salicylidene-3-hydroxy aniline by different boronic acids .....	91
3.7.2. The pH dependence of $k_{cat}$ and $K_M$ in the hydrolysis of the imine by the boronic acids ....	94
3.8. NMR analysis for the structure determination. ....	95
4. Conclusions .....	97
References: .....	106

## List of Tables:

<b>Table I:</b> Catalytic constants for the hydrolyses of salicylidene-L-isoleucine by various boronic acid catalysts..	14
<b>Table II:</b> Substituted arylboronic acids used in this dissertation.	15
<b>Table III:</b> Names and structures of the imines used for the hydrolysis.	19
<b>Table IV:</b> Maximum absorption band for different imines used to monitor the hydrolysis.	21
<b>Table V:</b> Rate constants for the hydrolysis of salicylidene-thronine with 2,3,4,5-tetrafluoroBBA.	31
<b>Table VI:</b> pH-dependent 278.5 nm absorbance values for 2,3,5-trifluoroBBA	35
<b>Table VII:</b> Catalytic constants for 2,3,4,5-tetrafluoroBBA-mediated hydrolyses of salicylidene-3-hydroxyaniline at different substrate and catalyst molar ratios.	42
<b>Table VIII:</b> Catalytic constants for the hydrolysis of salicylidene-3-hydroxyaniline by BBA and fluoro-substituted BBAs at different substrate and catalyst molar ratios.	49
<b>Table IX:</b> Catalytic constants for the hydrolysis of salicylidene-3-hydroxyanilin by BBA and two nitro –group-substituted BBAs.	55
<b>Table X:</b> Catalytic constants for the hydrolysis of salicylidene-3-hydroxyaniline by substituted.BBAs	58
<b>Table XI:</b> Kinetic constants for 2,3,4,5-tetrafluoroBBA catalyzed hydrolyses of various salicylidene-aminoacid imines	63
<b>Table XII:</b> BBA catalytic constants for the hydrolysis of salicylidene-3-hydroxyphenylglycine imine at stoichiometric molar ratios.	65
<b>Table XIII:</b> 2,3,5-trifluoroBBA catalytic constants for the hydrolysis of imines made from salicylaldehyde and various primary organic amines.	68
<b>Table XIV:</b> 2,3,4,5-tetrafluoroBBA catalytic constants for the hydrolysis of imines formed from salicylaldehyde and various primary organic amines	70
<b>Table XV:</b> Catalytic constants for the 2,3,4,5-tetrafluoroBBA mediated hydrolysis of carboxyl and carboxylamide substituted imines at stoichiometric molar ratios	72
<b>Table XVI:</b> Catalytic constants for the 2,3,4,5-tetrafluoroBBA mediated hydrolysis of two related imines at stoichiometric molar ratios	75

<b>Table XVII:</b> Catalytic constants for the 2,3,5-trifluoroBBA mediated hydrolyses of two related imines at stoichiometric molar ratios .....	75
<b>Table XVIII:</b> 2,3,5-trifluoroBBA catalytic constants for the hydrolyses of two hydroxyl functional group containing imines at stoichiometric molar ratios.....	79
<b>Table XIX:</b> Kinetic constants for the 2,3,4,5-tetrafluoroBBA-catalyzed hydrolyses of two structurally similar hydroxyl group-containing imines at stoichiometric molar ratios.....	79
<b>Table XX:</b> Kinetic constants for the 2,3,4,5-tetrafluoroBBA-catalyzed hydrolyses of two hydroxyl group-containing imines at stoichiometric molar ratios. ....	80
<b>Table XXI:</b> Kinetic constants for the 2,3,4,5 tetrafluoro BBA catalyzed hydrolyses of two hydroxyl functional group related imines at stoichiometric molar ratios. ....	80
<b>Table XXII:</b> Hammett-relationship values for the hydrolysis of salicylidene-3-hydroxyaniline by various BBAs .....	84
<b>Table XXIII:</b> SCULPT-derived interaction energies and structural images for complexes of BBAs with salicylidene-3-hydroxyaniline.....	89
<b>Table XXIV:</b> pK values derived from pH profiles for the hydrolysis of salicylidene-3-hydroxyaniline with different BBAs .....	91
<b>Table XXV:</b> $k_{cat}$ and $K_M$ values for various BBA's at different pH values .....	95

## List of Figures:

<b>Figure 1:</b> Kinetics for the autohydrolysis of salicylidene-amino acid imines.....	17
<b>Figure 2:</b> UV-Vis spectrum of 0.05M salicylidene-threonine. ....	20
<b>Figure 3:</b> Hydrolysis of salicylidene-threonine with different concentrations of 2,3,4,5-tetrafluoroBBA.....	27
<b>Figure 4:</b> Hydrolysis progress curves for salicylidene-threonine with different concentrations of 2,3,4,5-tetrafluoroBBA. ....	28
<b>Figure 5:</b> Steady state portion of the hydrolysis of 5.0 mM salicylidene-threonine with different concentrations of 2,3,4,5-tetrafluoroBBA.....	30
<b>Figure 6:</b> First order rate constants for the hydrolysis of salicylidene-threonine at different concentrations of 2,3,4,5-tetrafluoroBBA.....	32
<b>Figure 7:</b> Lineweaver-Burk plot for the hydrolysis of salicylidene-threonine with different concentrations of 2,3,4,5-tetrafluoroBBA. Catalytic constants are given next to the figure. ....	33
<b>Figure 8.</b> pH-dependent UV spectra for 2,3,5-trifluoroBBA.....	34
<b>Figure 9:</b> pH dependence of the absorption spectrum of 2,3,5-trifluoroBBA.....	35
<b>Figure 10:</b> Red (■) denotes theoretical plot and blue (◆) denotes experimental data points for the graph showing Log of $k_{cat}/K_M$ at different pH for the hydrolysis of salicylidene-3-hydroxyaniline .....	36
<b>Figure 11:</b> (a) Initial ester formation between the 2,3,5-trifluoroBBA and the salicylidene-3-hydroxyphenylglycine. b) Further ester bonds and a new boron-nitrogen covalent bond between the BBA and the imine are shown to be engaged in the complex.....	38
<b>Figure 12:</b> An example of a complex between salicylidene- <i>meta</i> -hydroxyphenylglycine and 2,3,5-trifluoroBBA.....	38
<b>Figure 13:</b> Structure and name of the substrate and the catalyst.....	40
<b>Figure 14:</b> Salicylidene-3-hydroxyaniline hydrolysis with 2,3,4,5-tetrafluoroBBA at a 1:10 molar ratio of BBA to imine .....	40
<b>Figure 15:</b> Salicylidene-3-hydroxyaniline hydrolysis with 2,3,5-trifluoroBBA at a 1:5 molar ratio of BBA to imine.....	41

<b>Figure 16:</b> a) Hydrolysis of salicylidene-3-hydroxyaniline with 2,3,4,5-tetrafluoroBBA at (1:1) stoichiometric BBA to imine ratio .....	41
<b>Figure 17:</b> Hydrolysis of salicylidene-3-hydroxyaniline using different concentrations of BBA .....	44
<b>Figure 18:</b> Hydrolysis of salicylidene-3-hydroxyaniline with different concentrations of a) 2,3,5-trifluoroBBA and b) 2,3,4,5-tetrafluoroBBA .....	46
<b>Figure 19:</b> The hydrolysis of salicylidene-3-hydroxyaniline with different concentrations of a) 2,3,5-trifluoroBBA and b) 2,3,4,5-tetrafluoro BBA .....	47
<b>Figure 20:</b> Lineweaver-Burk plots for the hydrolysis of salicylidene-3-hydroxyaniline with different concentrations of a) 2,3,5-trifluoroBBA and b) 2,3,4,5-tetrafluoroBBA.....	47
<b>Figure 21:</b> Lineweaver-Burk plots for the hydrolysis of salicylidene-3-hydroxyaniline with different concentrations of a) 3,5-Bis(trifluoromethyl)BBA and b) 3,4,5-trifluoroBBA .....	48
<b>Figure 22:</b> The hydrolysis of salicylidene-3-hydroxyaniline with different concentrations of a) 3-nitroBBA and b) 3,5-dinitro-2-methylBBA.....	53
<b>Figure 23:</b> Lineweaver-Burk plots for the hydrolysis of salicylidene-3-hydroxyaniline with different concentrations of a) 3-nitroBBA and b) 3,5-dinitro-2-methylBBA .....	53
<b>Figure 24:</b> The hydrolysis of salicylidene-3-hydroxyaniline with different concentrations of 3-carboxy-5-nitro-benzeneBBA.....	57
<b>Figure 25:</b> The hydrolysis of salicylidene-3-hydroxyaniline with different concentrations of 3-aminoBBA. ....	57
<b>Figure 26:</b> The hydrolysis of salicylidene-lysine with different concentration of 2,3,4,5-tetrafluoroBBA.....	61
<b>Figure 27:</b> The hydrolysis of salicylidene-threonine with different concentrations of 2,3,4,5-tetrafluoroBBA.....	61
<b>Figure 28:</b> The hydrolysis of salicylidene-threonine with different concentrations of 2,3,4,5-tetrafluoroBBA.....	62
<b>Figure 29:</b> The hydrolysis of a) salicylidene-L-isoleucine b) salicylidene-L-isoleucinamide with different concentrations of 2,3,4,5-tetrafluoroBBA .....	73
<b>Figure 30:</b> The hydrolysis of (a) salicylidene-o-hydroxytyrosine (b) salicylidene-2-hydroxybenzylamine with different concentrations of 2,3,4,5-tetrafluoroBBA .....	74
<b>Figure 31:</b> The hydrolysis of a) salicylidene-o-hydroxytyrosine b) salicylidene-2-hydroxybenzylamine with different concentrations of 2,3,5-trifluoroBBA.....	77

<b>Figure 32:</b> Bar graph depicting catalytic constants.....	81
<b>Figure 33:</b> A Hammett plot relating $\text{Log}_{10}(k_{\text{cat}})$ values and $\sigma$ for the hydrolysis of salicylidene-3-hydroxyaniline by different substituted benzenboronic acids.....	85
<b>Figure 34:</b> A Hammett plot relating $\text{Log}_{10}(K_M)$ values and $\sigma$ for the hydrolysis of salicylidene-3-hydroxyaniline by different substituted benzenboronic acids.....	86
<b>Figure 35:</b> A Hammett plot relating $\text{Log}_{10}(k_{\text{cat}} / K_M)$ values and $\sigma$ for the hydrolysis of salicylidene-3-hydroxyaniline by different substituted benzenboronic acids .....	87
<b>Figure 36:</b> SCUPLT modelling of (a,b)2,3,4,5-tetrafluoroBBA (c,d)2,3,5-trifluoroBBA and salicylidene-3-hydroxyaniline.....	90
<b>Figure 37:</b> pH-dependent hydrolysis of salicylidene-3-hydroxyaniline with a) 2,3,4,5-tetrafluoroBBA, b) 3,5-bistrifluoromethylBBA, c) 3,5-dinitro-2-methylBBA, d) 2,3,5-trifluoroBBA, e) 3,4,5-trifluoroBBA, .....	92
<b>Figure 38:</b> $^1\text{H-NMR}$ spectra corresponds to the a) salicylidene-3-hydroxyaniline and b) salicylaldehyde in DMSO-d.....	95

**List of Scheme:**

<b>Scheme I:</b> Mechanistic scheme for the hydrolysis of the imine by BBA.....	105
---------------------------------------------------------------------------------	-----

## 1. Introduction

### 1.1.1 Enzyme models

Enzyme catalyzed reactions are important and mechanisms of these reactions are exploited with various new systems. These systems are collectively called enzyme models. Naturally occurring molecules are involved in some of these systems and in others are involved artificially-made molecules. In all the system attempts are taken to mimic the enzyme activity for an efficient reaction product. The mathematical model used to explain the enzyme catalyzed reaction such is Michaelis-Menten *et al.*<sup>1</sup> Polymers, micelles, cyclodextrins, macrocyclic molecules, RNA & DNA are different model systems that monitor and study different catalysis and inhibition of reactions and reveal the mechanisms.

#### 1.1.1a. Polymers as enzyme models

Steinhardt and Fugitt<sup>2</sup> found that the rate of hydrolysis of proteins increases with an increase in the chain length of the catalyst, the n-alkylsulfonate anion. Ladenheim *et al.*<sup>3,4</sup> showed that poly(methacrylic acid) and poly(vinylpyridine betaine) catalyze the nucleophilic displacement of bromide ion from bromoacetamide. They suggested that the polymer is hydrogen bonded to the amide through unionized carboxyl, whereas the carboxyl anions function as nucleophiles to displace bromide ion.

Letsinger and Klæ<sup>5</sup> studied the catalysis of hydrolysis of polymeric anionic substrates by cationic polymers. The reaction of partially protonated poly-(N-vinylimidazole) with copoly-(acrylic acid-2,4-dinitrophenyl-p-vinyl benzoate) follows Michaelis-Menten kinetics by forming a complex between the substrate and the polymer due to cationic and anionic charges on them. It is an interesting model for the enzyme-substrate interaction which provides the catalytic constant.

Overberger<sup>6</sup> showed that vinyl polymers, containing imidazole and benzimidazole, enhance the hydrolysis of p-nitrophenyl-acetate. Another polymer, poly(vinylimidazole)-co-poly(vinyl alcohol), which contains imidazole and hydroxyl groups has been prepared to mimic

chymotrypsin. However, this polymer is only slightly more active than poly(vinylimidazole) in esterolytic reaction.

Klotz and his group<sup>7</sup> developed a very good enzyme model system by attaching dodecyl chains to a small cross-linked water soluble poly(ethylenimine) matrix and introducing imidazole on the polymer by reacting polymer with methylene-imidazole. This system accelerates the hydrolysis of phenolic sulfate esters by about tenfold, compared to unbound imidazole, a rate which is comparable to many enzymes.

There are bifunctional enzymes, which have two active domains and thus two different enzymatically active sites. There are also enzyme complexes where the substrate is transferred from one to the next, which can be seen as having multiple binding sites. Recently, a review by Wulf *et al.* shows the principals of enzymatic catalysis based on polymers for the designs of other catalytic materials.<sup>8</sup>

The main disadvantages with polymer systems are their limited solubility in water and the random arrangement of the polymer chains. Polymers possess many binding sites and make the kinetic profile more complex as compared to enzymes which have only one active site region.

### **1.1.1b. Micelles as enzyme models**

Micelles are also used like polymers as enzyme models. Micelles are aggregates of a large number of soap or detergent molecules and are loosely bound mainly through hydrophobic interactions. They have polar groups on the outside surface and apolar groups in the inside of micelles. Many different organic molecules can bind into the apolar groups of the micelles. Chiral molecules are also used for micelle formation and where stereospecific reactants and products were monitored.

Cationic detergent, cetyltrimethylammonium bromide (CTAB) was used by Duynstee and Grunwald<sup>9</sup>. CTAB made it possible for the hydrolysis of p-nitrophenyl acetate through proximity and the electrostatic interaction.

Sodium lauryl sulfate or sodium oleyl sulfate was used for the hydrolysis of methyl*ortho*benzoate which accelerated the reaction up to 80-fold for Fullington and Cordes.<sup>10</sup>

Shorenstein *et al.*<sup>11</sup> made micelles better catalysts by attaching catalytic groups namely acetyl. The micelle with N-acetyl histidine hydrolyzes the ester, N-dodecyl-N-N'-dimethyl aminoethyl carbonate ion, 2240 times faster than the micelle without N-acetyl histidine.

Bunton *et al.*<sup>12</sup> demonstrated that D(-)-ephedrine-cationic micelle shows more stereoselectivity in the hydrolysis of D(-)-mandelic ester over L(+)-mandelic ester. In 1974, they made a better chiral micelle for the hydrolysis of n-acetyl-phenylalanine ester. For his reaction the S-isomer deacylates three times faster than the R-isomer.

Another group developed a micelle which mimics papain and that micelle had a cysteine group attached<sup>13</sup>. With that functional group present that micelle hydrolyzed p-nitrophenyl acetate 180 times faster than without the functional group in the micelle system.

Recently another group developed a micellar system in which they studied hydrolysis of imines.<sup>14</sup>

All the above studies with micellar system show that they exhibit enzyme-like features such as Michaelis-Menten type of kinetics and stereospecificity. There are some disadvantages with micellar systems, their structure is not well defined and depends on surfactant concentrations the orientation of reactive groups are not known.

### 1.1.1c. Cyclodextrins as enzyme models

Cyclodextrins are large molecular aggregates composed of glucose units. It gets a donut like molecular shape and its size depends on the number of glucose units. Hydroxyl groups of glucose make up the rim of the cavity and so the cyclodextrins are water soluble but the cavities interact as hydrophobic. This hydrophobic character enables cyclodextrins to bind certain molecules that have the correct shape and have hydrophobic character.

For the hydrolysis of the diaryl pyrophosphate in the presence of calcium ions the cyclodextrin chemistry was used<sup>15</sup> and it produced a 200 fold acceleration.

Bender and his group was able to show stereoselective activity of cyclodextrins in the hydrolysis of substituted phenyl acetates<sup>16,17</sup> and *meta* isomer was accelerated over 200 times faster than the *para* isomer.

Breslow<sup>18</sup> first showed a selective aromatic substitution reaction with the cyclodextrin system. Anisole in the presence of hypochlorous acid yields 60% *ortho*-chloroanisole and 40%

*para*-chloroanisole. But in the presence of cyclodextrin, 96% of *para* and only 4% of *ortho* products are obtained. The enzyme chlorinase produces 60/40 distribution of *para*- and *ortho*-chloroanisoles. In this reaction, the cyclodextrin shows more typical enzyme-like selectivity than does the enzyme itself.

Kaiser and his group<sup>19</sup> demonstrated that cyclodextrins exhibit D,L specificity with respect to substrates. Cyclodextrin shows specificity in the hydrolysis of 3-carboxy-2,2,5,5,-tetramethyl-pyrrolidine-1-oxy-m-nitrophenylester. The rate constant for the (+) enantiomer is 6-9 times larger than for the (-) enantiomer. The enantiomeric specificity shown by the cyclodextrin is close to that shown by chymotrypsin (9 times) in the hydrolysis of the closely related ester, 3-carboxy-2,2,5,5-tetramethylpyrrolidinyl-1-oxy-p-nitrophenyl ester.

Breslow's group made good progress in this field by designing artificial enzymes using cyclodextrins to mimic natural enzymes like transaminase<sup>20</sup> and ribonuclease<sup>21</sup>. Transaminase with a coenzyme converts ketoacids to amino acids. The pyridoxamine-cyclodextrin system where the coenzyme pyridoxamine is attached to the cyclodextrin is selective for the transamination process. This system accelerates the reaction by about 200-fold and also produces the natural L-enantiomer five times more abundantly than the unnatural D-enantiomer. Ribonuclease catalyzes the hydrolytic cleavage of RNA. In the model system for ribonuclease, two imidazole rings, the principle catalytic groups of ribonuclease are attached to the cyclodextrin. Such a system is an effective catalyst for the hydrolysis of a cyclic phosphodiester, which resembles the RNA cleavage intermediate. This catalyst shows a rate optimum near pH 6 similar to an enzyme. The cyclic phosphate without the cyclodextrin undergoes hydrolysis and gives two products. But in the presence of cyclodextrin, only a single product is obtained. This selectivity is caused by the geometry of the catalyst-substrate complex.

Tabushi *et al.*<sup>22</sup> successfully mimicked a carbonic anhydrase enzyme with the cyclodextrin. Bis (2-histamino)-cyclodextrin and bis (N-imidazole) cyclodextrin with zinc ion show larger rates of hydration of carbon dioxide than the compounds without the cyclodextrin derivative. But the catalytic rate constants are lower than the enzyme by many orders of magnitude.

#### 1.1.1d. Macrocyclic molecules as enzyme models

Paderson<sup>23</sup> first demonstrated the feasibility of synthesizing large cyclic polyethers composed of ethyleneoxy units and its ability to complex with various metal ions. This property has led organic chemists to use crown ethers as enzyme models. The size of crown ethers can be varied and also modified to bind ligands of different size.

Donald Cram named this chemistry as host-guest complexation chemistry. Chao and Cram<sup>24</sup> synthesized a chiral macrocyclic polyether with sulfhydryl group as a host, and L- and D-amino acid p-nitrophenyl esters as guests. The cyclic host produced a result of  $10^2$  - $10^3$  times faster for the hydrolyses of amino esters  $10^2$  - $10^3$  times faster than the open-chain host analogue. The cyclic host also shows stereospecificity in the hydrolysis.

Lehn and Sirlin<sup>25</sup> synthesized a chiral macrocyclic molecule bearing cysteinyl residue. This host enhances the hydrolysis of p-nitrophenyl esters of amino acids and dipeptides. It accelerates the hydrolysis of Gly-Gly-OPNP by a factor of  $10^4$ . It shows structural selectivity among the various amino esters and best substrates are dipeptide esters. The host also shows enantiomeric selectivity in the hydrolysis of dipeptide esters. It enhances the hydrolysis of glycyl-L-phenylalanine ester by nearly 70-fold greater than glycyl-D-phenylalanine ester.

Murakami *et al.*<sup>26</sup> developed a different macrocyclic system, 11-amino-[20]-paracyclophan-10-ol. It accelerates the hydrolysis of p-nitrophenylhexadecanoate with a rate 1000-fold greater than 2-aminocyclodecanol.

All the above studies with macrocyclic systems show many enzyme-like properties, saturation, structural recognition, enantiometric selectivity and inhibition by metal ions.

#### 1.1.1e. RNA & DNA as enzyme models

RNA as Enzyme model:

Over the past 30 years RNA research has centered on RNA's more central role in biology and specifically RNA as catalyst. RNA often controls the expression of genes, for example splicing is a modification of RNA after transcription, in which introns are removed and exons are joined. For many eukaryotes introns splicing is done by small nuclear ribonucleic proteins (snRNPs), but there are also self-splicing introns. Self-splicing occurs for introns that form a ribozyme. A ribozymes is an RNA molecule that has a well defined tertiary structure that

enables it to catalyze either the hydrolysis of its own phosphodiester bonds or the hydrolysis of bonds in other RNAs thereby performing the function of a spliceosome by RNA alone. They also have been found to catalyze the amino transferase activity of the ribosome.<sup>27,28,29,30</sup>

Ribonuclease P cleaves RNA, it is a ribozyme that acts as a catalyst in exactly the same way a protein based enzyme would. Ribonuclease P purified from both *E.coli* and *B. subtilis* was found to cleave off a precursor sequence on tRNA precursor molecules whereas the protein moieties of the enzymes alone show no catalytic activity. This discovery earned Sidney Altman and Thomas Cech the 1989 Nobel Prize in Chemistry.

When *Tetrahymena thermophila* ribosomal RNA is transcribed it contains an intron (a sequence not present in the mature RNA). Tom Cech *et al.*<sup>27</sup> showed that the intron excises itself, in a two-step *trans*-esterification reaction in the presence of a guanosine nucleotide and in the absence of any protein cofactors. It is now accepted that this class of self-splicing intron is distributed widely in nature and members are known as group I introns<sup>31</sup>. The discovery of group I self-splicing introns and other catalytic RNAs marked a shift in biology. Previously it was believed that protein was the only biological catalyst.

Zaug and Cech<sup>32</sup> described a system in which a 395-nucleotide form of the *Tetrahymena thermophila* ribosomal RNA intervening sequence (IVS) acts as an RNA cleavage-ligation enzyme. Using the same activity of the self-splicing reaction the RNA converts pentacytidylic acid to polycytidylic acids, acting as a polycytidylic polymerase synthesizing RNA in a 5'-to-3' direction.

This IVS RNA catalyzed reaction exhibits many similarities to protein enzyme catalyzed reactions. The reaction follows classic Michaelis-Menten kinetics; kinetic parameters can be obtained and are close to those of protein enzymes.

DNA as Enzyme Model:

Shimizu and Letsinger<sup>33,34</sup> used modified DNA as a catalyst in the hydrolysis of esters. They demonstrated that a modified OligoDNA can react with a PolyDNA to condense the oligonucleotide on the polynucleotide. The hydrolysis of p-nitrophenyl (oligoDNA) proceeds by means of a nucleophilic for the hydrolysis of esters. The reaction that they undertook was to prepare an oligoribonucleotide with attached N-acetylhistidates and used it in the hydrolysis of p-nitrophenyl-oligoDNA succinate in the presence of polycytidylic acid. Deoxyguanylyldeoxyguanosine n-acetylhistidate hydrolyzes p-nitrophenyldeoxyguanosine

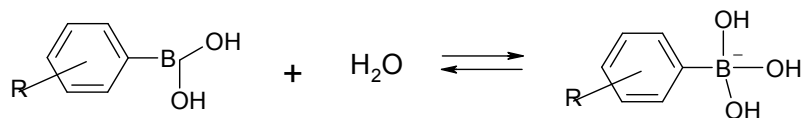
succinate four times faster than without to polycytidylic acid. In this reaction the polycytidylic acid acts as a template and the imidazole group acts as the nucleophile for the ester hydrolysis.

To further demonstrate that DNA can also act as an enzyme Zhuo Tang and Andreas Marx<sup>35</sup> used DNA-template synthesis to show that proline tethered to a DNA strand can efficiently catalyze the cross-aldol reaction of a complementary DNA-aldehyde. These findings not only serve to extend the collection of DNA-template reactions but demonstrate how nucleic acids can catalyze reactions and implicate them as catalysts in the early history of life. In recent years many examples demonstrate that nucleotide bases can and do act as enzymes.<sup>36,37,38,39</sup>

All the above studies show that non-enzymes exhibit enzymatic properties and the enzymatic activity can be created in non-enzymatic systems. In this project various boronic acid were selected to mimic enzyme catalyzed reaction to establish a model system.

### 1.1.2. Boric, boronic and arylboronic acid as enzyme model

The chemistry of boric and boronic acids has long been of interest to chemists due to the Lewis acid character of these compounds (as electron pair acceptors). Boron in trivalent compounds has one vacant orbital which is available for the formation of a fourth covalent bond with electron donor atoms. Boric and boronic acids are trigonal compounds and ionize to tetrahedral,  $B(OH)_4^-$  in aqueous solution by accepting an electron pair from hydroxy as shown in the following equation. Edwards *et al.*<sup>40</sup> investigated the structure of borate ion in aqueous solution by Raman spectroscopy. They indicated that it has a tetrahedral symmetry and is  $B(OH)_4^-$ .



It was observed that by adding glycerol and other various compounds to boric acid the solution acidity is raised.<sup>41</sup> Later, in the early part of the past century, several investigators studied the formation of boric acid complexes with polyols (carbohydrates), phenols, cyclic glycols and hydroxyl acids.<sup>37</sup> They determined the extent of complex formation by measuring the enhancement of the conductivity of boric acid with the above alcoholic compounds. Boeseken<sup>37</sup> applied this method to determine the configuration of carbohydrates. Boric and boronic acids prove to form esters with simple alcohols and these esters of simple primary alcohols undergo hydrolysis in water to regenerate the boron acids.<sup>42</sup>

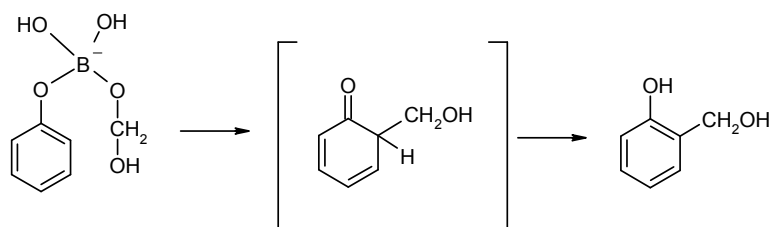
The reaction of boric acid, benzenboronic acid and substituted benzenboronic acid acids with polyols, dicarboxylic acids and hydroxyl acids are studied by Pizer and his group<sup>43,44,45,46,47,48</sup> by temperature jump method. They showed that the complex formation is very rapid and they found that the dissociation constants are in the millimolar to micromolar range, and depend upon the acidities of the boronic acids and the ligands.

The complex formation of boric and boronic acids with various ligands has several applications. The first application has been in chromatography. The boronic acid is attached to cellulose derivatives and it is then used to separate various sugars.<sup>49</sup>

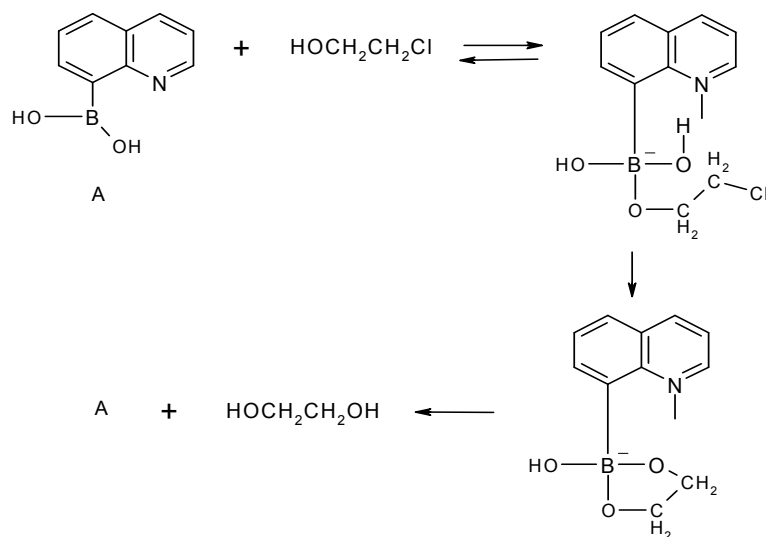
Transition state analog inhibitors for serine proteases have been another application of boronic acid. Torssel<sup>50</sup> found out the inhibition of cholinesterase by benzenboronic acid. Philipp and Bender<sup>51</sup> used several substituted benzenboronic acids to inhibit chymotrypsin and *subtilisin*. Peptideboronic acids are also used as inhibitors and are found to inhibit enzymes in nanomolar concentration range.<sup>52,53</sup> Koehler and Lienhard<sup>54</sup> proposed that boronic acids are transition state analogs. Boronic acid esterifies the alcoholic group of serine amino acid present in the active site of an enzyme. As a result, the boronic acid becomes tetrahedral and mimics the tetrahedral transition state of the enzyme-catalyzed ester hydrolysis.

The third application is to use boronic acids as enzyme models. The first step in enzymatic catalysis is usually the formation of an enzyme-substrate complex. The complexation can juxtapose substrate and catalyst and this leads to an intramolecular reaction. Boric and boronic acids have hydroxyl groups and can act as general bases. They complex with various ligands and this complexation can lead to hydrolysis of ligand of interest.

Peer<sup>55</sup> first found that phenol reacts with formaldehyde and gives exclusively *o*-hydroxymethylphenol in the presence of boric acid. There is no formation of *ortho*-product in the absence of boric acid under the same conditions. This may be due to the rapid and reversible formation of a complex of phenol, borate and formaldehyde.<sup>56</sup>



Letsinger *et al.*<sup>57</sup> used 8-quinolineboronic acid as a catalyst in the hydrolysis of chloroethanol to ethyleneglycol. It catalyzes the hydrolysis at least 80 times faster than a mixture of quinoline and benzenboronic acid. This shows the advantage of intramolecular catalysis over intermolecular catalysis.



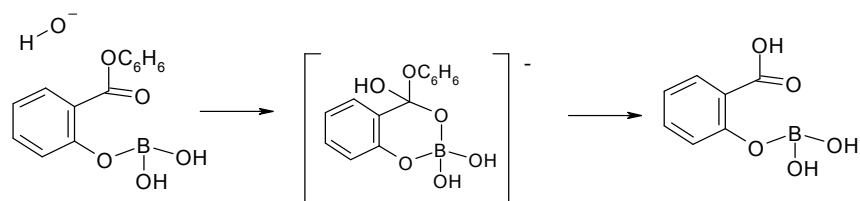
The boronic group in 8-quinolineboronic acid forms a complex with chloroethanol and the nitrogen particulates in the reaction by increasing the nucleophilicity of the oxygen atom joined to boron, which in turn displaces chloride ion.<sup>53</sup> The hydrolysis is inhibited in the presence of diol compounds, as the latter form a complex with the boronic acid.

8-Quinolineboronic acid also shows stereoselectivity in the hydrolysis of chloroalcohols.<sup>58</sup> It hydrolyzes the *trans*-2-chloro-1-indanol to the product and not the *cis* isomer, in a certain period of time. This was explained as being due to geometry of the complex formed between the catalyst and the substrate. The complex formed with the *cis* isomer may not be favorable for an attack on the carbon of chloroalcohol by the oxygen joined to boron.

In another study, Letsinger *et al.*<sup>59</sup> used boronoarylbenzimidazole as a catalyst in the formation of ethers from chloroethanol in butanol solution. Here also the boron group in boronoarylbenzimidazole binds the alcoholic substrates and holds them in a position favorable for the reaction.

Capon and Ghosh<sup>60</sup> found that borate catalyzes the hydrolysis of phenyl salicylate more than 100-fold more rapidly than the hydrolysis of phenyl salicylate more than 100-fold more rapidly than the hydrolysis of phenyl-*o*-methoxybenzoate and phenyl benzoate. Borate may increase the rate of ester hydrolysis by stabilizing the transition state involved in that hydrolysis,

resulting in a lowering of the activation energy. In the borate-catalyzed hydrolysis of phenyl salicylate, borate forms a complex with the ester and then boron acts as a Lewis acid to accept lone pair of electrons from oxygen, which leads to the formation of an intermediate. This intermediate resembles the transition state of ester hydrolysis.<sup>52</sup>



Okuyama *et al.*<sup>61</sup> showed that borate catalyzes the hydrolysis of S-butyl 2-hydroxy-2-phenylthioacetates by a factor of about 80 at pH 9. Butylthioacetate is not hydrolyzed by borate since there is no hydroxyl group in this ester to form a complex with borate. This may be a good model to show that the catalyst and the substrate should form a complex before the catalysis.

Boric acid catalyzes the hydrolysis of hydroxyl and salicylaldehyde Schiff base.<sup>62,63,64</sup> The hydrolysis rate as a function of boric acid concentration follows a saturation curve. The same type of curve is observed in the case of an enzyme-catalyzed reaction as a function of enzyme concentration. It suggests that there is formation of a borate-Schiff base complex. They suggested the possible mechanism for the catalysis of this hydrolysis to be an intramolecular transfer of a boron-coordinated hydroxide ion within a borate-substrate complex. The most obvious reason by which an enzyme increases the rate of a reaction is by binding to the substrate molecule and holding it close to the reactive groups. Borate also acts in the same way.

In another study, it has been shown that boric acid catalyzes the formation of a Schiff's base.<sup>65</sup> A true catalyst is the one that catalyzes the reaction in both directions. Boric acid also catalyzes the reaction in both directions i.e. in the formation of a Schiff's base and in its hydrolysis. All these examples suggest that boric acid has some enzyme-like properties.

Boronic acids have been used as catalysts in one study by Letsinger *et al.*<sup>53,54,55</sup> Boronic acids proved to be better catalysts than boric acid since it has been found that boronic acids are better inhibitors of serine proteases than boric acid. As inhibitor boronic acids form a strong complex with the hydroxyl group of serine amino acid present in the active site of an enzyme.<sup>66</sup> It is also known that the stability constants for phenylboronic acid with diols are greater than those for boric complexes by factors of 4-6.<sup>43</sup> The binding constant is an important factor in the catalyzed reactions, since the observed catalytic rate constant increases with better binding

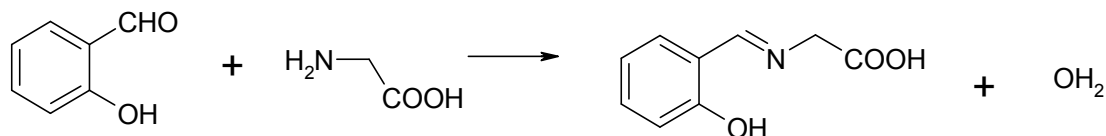
constant. It is found that boronic acids are proving to be increasingly valuable catalyst.<sup>67</sup> Recently and most significantly 3,4,5-trifluorobenzeneboronic acid is found to act as an extremely active catalyst for an amidation reaction.<sup>68</sup>

Boronic acid mimics enzymes in biological system and one of the functions of boronic acid in organic chemistry and biological system can be recognized by the hydrolysis reaction of imines. Ideally, model reactions for enzymatic processes should include an association through weak binding forces of substrate and catalyst or other reactant leading to facilitations of bond-changing reaction (e.g. hydrolysis) and conferring specificity on the reaction. Such a binding force was investigated for the hydrolysis of an imine namely salicylaldehyde-L-isoleucine catalyzed by boric acid and boronic by Rao and Philipp.<sup>69</sup> Catalytic efficiencies are accounted with the kinetic constants such as  $k_{cat}$  (turnover number or first order rate constant),  $K_M$  (Michealis constant, and is expressed in units of substrate concentration, concentration of substrate where rate of reaction is half of maximum rate),  $k_{cat}/K_M$  (second order rate constant).

In these studies, I investigated the ability of various arylboronic /benzeneboronic acids to act as enzyme like catalyst for the hydrolysis of different imines.

### 1.1.3. Imines (Schiff's bases) as model hydrolysis substrates

A Schiff base is a nitrogen analog of an aldehyde or ketone in which the C=N replaces the C=O bond. It is usually formed by condensation reaction of an aldehyde or ketone with a primary amine. Another common name of them is imines. Chemistry of imines is important both in organic and biological chemistry.<sup>70</sup> Imines made of salicylaldehyde and primary amines are the substrates of this study. Schiff bases of aliphatic aldehydes are relatively unstable and readily polymerizable whereas those of aromatic aldehydes having effective conjugation are more stable. The formation of an imine from an aldehyde or ketone is a reversible reaction and it generally takes place under acid or base catalysis. Following is an example of imine formation reaction.



One of the usages of imine is formation of a secondary amine and that is produced by reducing the imine. Among other derivatives of imines are oxime, hydrazone, semicarbazone which comes from hydroxylamine ( $\text{NH}_2\text{OH}$ ), Hydrazine ( $\text{NH}_2\text{NH}_2$ ) and semicarbazide ( $\text{NH}_2\text{NHCONH}_2$ ) respectively.

Some imines acts as coenzymes in biological catalysis such as imines of pyridoxal 5'-phosphate with amines and amino acids and familiarity with the properties this is important for understanding the function of this coenzyme.<sup>71</sup>

Use of amino acid derived Schiff bases is important. And one example of their use is in metal coordinated complexes.<sup>72</sup> In another study they undertake redox and amphiphilic properties of a salicylaldimine-copper complex.<sup>73</sup> Schiff base intermediates are the concept of many enzyme derived reactions.<sup>74</sup>

The hydrolysis of imine has been reported in recent work.<sup>75</sup> Imine hydrolysis and the role of imine complex have been useful in imine hydrogenation reaction.<sup>76</sup> Acidic hydrolysis of an imine such as bis(salicylidenamino)diimine,  $\text{CH}_2[4\text{-C}_6\text{H}_4\text{N}=\text{CHC}_6\text{H}_4\text{-2-hydroxy}]_2$  has been studied and the metallic catalysts on the hydrolysis are monitored.<sup>77</sup> Rate constants for the formation and hydrolysis of Schiff bases derived from pyridoxal 5-phosphate and co-polypeptides have been determined in the pH range 4–11 where the co-polypeptides contained L-lysine, and aromatic L-amino acids.<sup>78</sup>

## **1.2. Working model for the kinetics of imine hydrolysis by arylboronic/benzeneboronic acids**

In order to determine the efficiency of benzeneboronic acids (BBAs) as catalysts, the general chemical kinetics will be reviewed. Chemical kinetics studies the rates of reactions, reaction mechanisms and the various factors that influence them.

The kinetic parameters  $k_{\text{cat}}$  (rate constant) and  $K_M$  (binding constant) are generally useful for the studies and comparison of different enzymes catalysts.  $k_{\text{cat}}$  is the first-order rate constant with units of reciprocal time. The most useful parameter for assessing the catalytic efficiency is the one that includes both  $k_{\text{cat}}$  and  $K_M$  when  $[\text{S}]$  is less than  $K_M$ , i.e. the ratio  $k_{\text{cat}}/K_M$ .

This thesis project focuses on the ability of BBAs to catalyze the hydrolysis of different imines, most of them derived from salicylaldehyde. The classic kinetic treatment of an enzyme-

catalyzed reaction, following Michaelis-Menten hyperbolic model is applied in this case to the hydrolysis of imines by different BBA. The first order rate constant for the hydrolysis of the imine is determined at various concentrations of BBA and at constant concentration of the substrate imine. When the catalyst concentration is greater than the substrate concentration then a condition exists that is opposite to a normal enzymatic reaction ( $S_o > E_o$ ) ( $S_o$  = observed substrate concentration,  $E_o$  = observed enzyme concentration). According to the Michaelis-Menten equation, the first order rate constant under the normal enzymatic reaction conditions of  $S_o > E_o$ , is given by

$$k_o = \frac{k_{cat} S_o}{(K_M + S_o)}$$

Whereas, the first order rate constant under the conditions of  $E > S$ , is given by

$$k_o = \frac{k_{cat} E_o}{(K_M + E_o)}$$

and are used for the reaction analysis of this research on BBA catalyzed hydrolysis of different imines.

The next sections of this thesis present the structural features of both the boronic acids, as catalysts, and of their substrates, imines.

### **1.3. Arylboronic/benzenboronic acids (BBA) as catalyst for the hydrolysis of imine**

A number of benzenboronic acids (BBA) are available commercially and many have been plausible candidates for this study. Their structures are very diverse, from relatively chemically simple boronic acids to very complex ones. The goal of this research was to find the best BBAs catalysts that will ultimately reveal the structure-reactivity relationship underlying the mechanism of imines hydrolyses.

Previous research studies were performed on different available boric, boronic and benzenboronic acids (BBAs) using only one imine compound as substrate, namely salicylidene-L-isoleucine. The values for  $k_{cat}/K_M$  for the hydrolysis of salicylidene-L-isoleucine by different boronic acids and BBAs are presented in the Table I.<sup>69</sup>

**Table I:** Catalytic constants for the hydrolysis of salicylidene-L-isoleucine by different boronic acid related catalysts

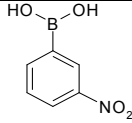
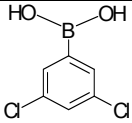
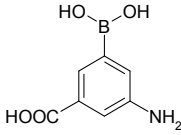
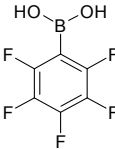
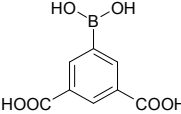
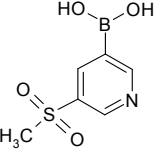
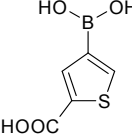
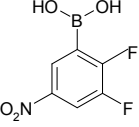
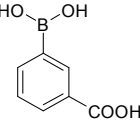
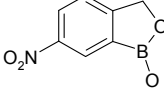
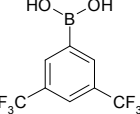
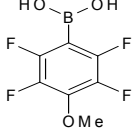
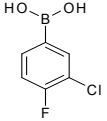
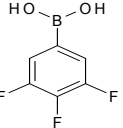
Boronic acid	$K_M$ (M)	$k_{cat}$ ( $sec^{-1}$ )	$k_{cat} / K_M$ ( $sec^{-1}M^{-1}$ )
3-aminobenzeneboronic acid	$19.5 \times 10^{-2}$	$21.7 \times 10^{-2}$	1.11
benzeneboronic acid	$17.0 \times 10^{-2}$	$2.50 \times 10^{-2}$	0.15
3-carboxybenzeneboronic acid	$21.7 \times 10^{-2}$	$4.34 \times 10^{-2}$	0.20
4-tolueneboronic acid	$15.0 \times 10^{-2}$	$1.47 \times 10^{-2}$	0.09
4-bromobenzeneboronic acid	$3.1 \times 10^{-2}$	$1.16 \times 10^{-2}$	0.37
3-nitrobenzeneboronic acid	$1.3 \times 10^{-2}$	$1.81 \times 10^{-2}$	1.39
3,5-bis(trifluoromethyl)benzeneboronic acid	$5.6 \times 10^{-2}$	$1.35 \times 10^{-2}$	2.38
diphenylborinic acid	$1.0 \times 10^{-3}$	$7.7 \times 10^{-2}$	77
boric acid	4.35	$12.8 \times 10^{-2}$	0.029

As other boronic acids became available during last two decades, attention has been given to these compounds and their efficiency as catalysts for the hydrolysis of different imine substrates in this work. The results for these BBA catalyzed reactions are the main subject of this thesis and are further presented and discussed in the next sections.

The physical-chemical properties of some new available BBAs were further analyzed to generate a scaffolding structure based on which the catalytic properties could be determined. New proposed structure deliver physico-chemical basis to function as a catalyst. And from that prospective following boronic acids are found to be the candidates of the study.

One common structural feature of all boronic acids used in this research is their aromatic character. Derived from the benzeneboronic acid are other compounds, which have different chemical groups substituted to the benzene ring.

**Table II:** Substituted arylboronic acids used in this dissertation

Name of the Boronic acids	Structure	Name of the Boronic acids	Structure
3-nitroBBA		3,5-dichloroBBA	
3-amino-5-carboxylBBA		2,3,4,5,6-pentafluoroBBA	
3,5-dicarboxyBBA		5-(methylsulfonyl)pyridine-3-BBA	
2-carboxythiophene-4-boronic acid		2,3-difluoro-5-nitroBBA	
m-carboxyBBA		2-hydroxymethyl-5-nitroBBA, dehydrate	
3,5-bis(trifluoromethyl)BBA		4-methoxy-2,3,5,6-tetrafluoroBBA	
3-chloro-4-fluoroBBA		3,4,5-trifluoroBBA	

**Table II:** Substituted Benzenboronic Acids Used in this Dissertation continues

Name of the Boronic acids	Structure	Name of the Boronic acids	Structure
3-carboxy-5-nitroBBA		2,3,4,5-tetrafluoroBBA	
3-aminoBBA		2,3,4,6-tetrafluoroBBA	
3-carboxy-4-fluoroBBA		2,4,6-trifluoroBBA	
3,5-dinitro-2-methylBBA		diphenylboronic acid	
5-trifluoromethyl-1,3-phenylenediboronic acid		2,3,5-trifluoroBBA	
3-fluoro-5-trifluoromethyl			

#### 1.4. The imines as substrates for the hydrolysis with boronic acids

In this research I have used different types of imines which were prepared in general by the reaction of aliphatic and aromatic primary amines with the salicylaldehyde (2-hydroxybenzaldehyde). The next sections present the major imines used in the BBA catalyzed hydrolysis studies and their structural features that enabled them to be suitable substrates.



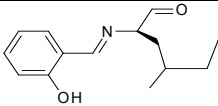
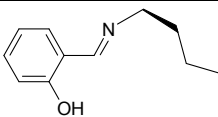
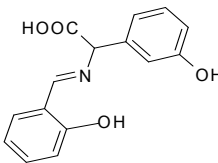
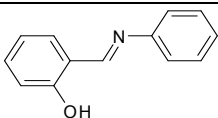
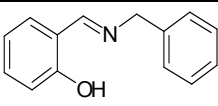
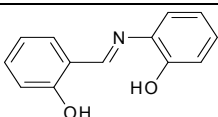
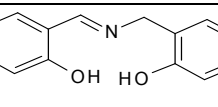
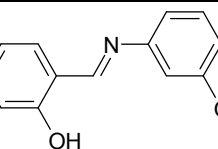
Based on minimal autohydrolysis data, amino acids that were selected for initial imine formation had been phenylalanine, threonine, leucine, lysine, valine, alanyl-valine.

As I selected the amino acids based imines based on their minimal autohydrolysis, the same criteria were applied in the selection of other imines substrates which are presented in the next sections. All the imines presented next have different primary amino group than those found in the amino acids structure.

#### **1.4.2. Imines with non amino acid amine**

Other primary amines were further investigated; some of them related to the aliphatic amino-acids, such as n-butyl amine which was reacted with the salicylaldehyde to produce the imine. The next arrays of imines were derived from unnatural amino acids, such as the m-hydroxyphenylglycine, which gave enhanced hydrolysis results as compared to other amino acids derived imines. I hypothesized based on this result that the hydroxyl group could be a major structural determinant that would increase the rates of imine hydrolyses. To this point I further considered for the investigation, the primary amines with hydroxy-substituents on the amine side. In addition, the aromatic character of the m-hydroxyphenylglycine was also exploited in the development of the next generation of aromatic primary amines based imines. Thus, imines derived from aniline and benzylamine were used containing a hydroxy group substituted at different position on the benzene ring, such as hydroxy aniline and hydroxy benzylamine based imines. The structurally related imines that are synthesized and used in the presented research are shown in the Table III in their *trans* isomer state. Synthesis step produced both *cis* and *trans* isomers of the substrates where possible.<sup>79</sup>

**Table III:** Names and structures of the imines used for the hydrolyses

Imines	Structure
Salicylidene-L-isoleucine	
Salicylidene-n-butylamine	
Salicylidene-D(-) m-hydroxyphenylglycine	
Salicylidene-aniline	
Salicylidene-benzylamine	
Salicylidene-2-hydroxyaniline	
Salicylidene-2-hydroxybenzylamine	
Salicylidene-3-hydroxyaniline	

### 1.4.3. The spectral characteristics of the imines

As an important step in defining the major requirements for developing a reliable assay for the imine hydrolysis, which in turn would have helped to derive the catalytic constants  $k_{\text{cat}}$  and  $K_M$  for assessing the catalytic efficiency of each BBA catalyst, the maximum absorption is determined for each of the studied imines substrates. The Schiff bases of salicylaldehyde and primary amino acids have very well known absorption band at 395nm.<sup>80</sup> However, other imines differ in their characteristic absorption band in the UV region, some due to the effect of the solution used in the reaction.<sup>81</sup> Therefore, other prominent absorption band in the visible region for each of the imines of interest can be used to monitor the imine hydrolysis.<sup>82</sup>

Many measurements in the UV-Vis region using different buffer solutions for the imines were made and it was found that each imine had its own maximum absorption which were used to monitor their hydrolyses by BBAs.<sup>83</sup>

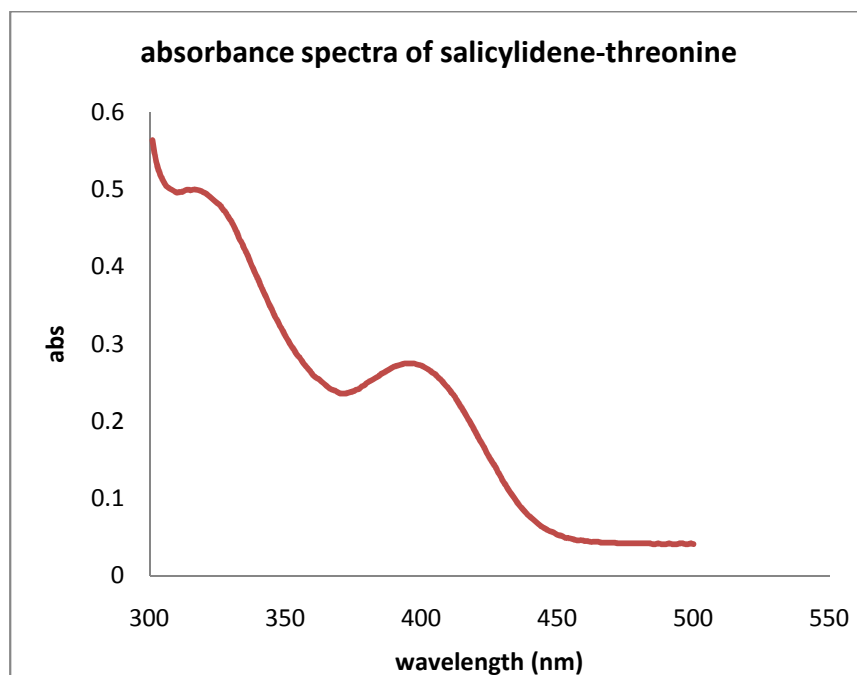


**Figure 2:** UV-Vis spectrum of 0.5 mM salicylidene-threonine. The solvent was 0.10 M phosphate buffer at pH 6.0.

**Table IV:** Maximum absorption band for different imines used to monitor the hydrolysis

Imines	Absorbance band (nm)
salicylidene-L-isoleucine	395
salicylidene-n-butylamine	395
salicylidene-threonine	395
salicylidene-D(-) m-hydroxyphenylglycine	404
salicylidene-aniline	440
salicylidene-benzylamine	397
salicylidene-2-hydroxyaniline	440
salicylidene-2-hydroxybenzylamine	400
salicylidene-3-hydroxyaniline	430

### 1.5. Effect of benzenboronic acids (BBA) as catalyst for the hydrolysis of imine

An important property of BBAs was that during binding to the imine substrates their boron come in close proximity to the nitrogen side of the imine, enabling the formation of a new boron-nitrogen bond which stabilizes the complex BBAs-imine, similar to an enzyme-substrate complex. Moreover, the hydroxyl groups of BBAs form ester bond to the benzene rings of the salicylaldehyde part of the imines; that bond further strengthen the stability of the complex between BBA and the imines.

This research focused on finding functional groups substituted to the aromatic ring of BBA which had electronic withdrawing properties. It was thought that these electronic withdrawing groups were the main structural feature that enhanced the catalytic properties of the BBAs. The chemistry that supports this hypothesis relies on the properties of the electronic withdrawing groups which made the boron center more electrophilic, enhancing its ability to bind to the substrate through an electrophilic substitution reaction mediated by its hydroxy groups.

In addition, the side chain of the amine part was another focal point in this research. The side chain provided the H-bonds required to stabilize the complex between imine and the BBA, wherever these donor groups of hydrogen bonds were available. So, I have done an extensive experimental trial search. Different methods were applied to find various details of the imine hydrolyses by the boronic acids.

### **1.5.1. Modeling with Sculpt**

In docking software SCULPT by MDL, the force-field provides with potential energies that are used to model: explicit hydrogen bonds; variable dihedral angles; van der Waals interactions; electrostatic interactions; user-applied tugs (springs). The free energy of interaction were assessed between the boronic acids and the imines using the built-in advanced molecular mechanics force-field (MMFF)

Van der Waals interactions in SCULPT are modeled with a modified Lennard-Jones function between atoms within 6Å of each other. The electrostatic interactions are modeled with a Coulomb model. These interactions were used in the docking experiments when refined structure between boronic acids and the imine were generated.

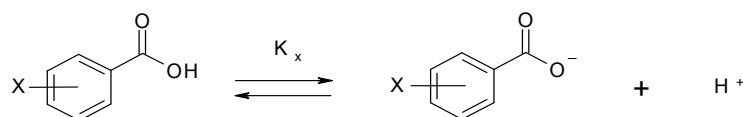
One of the most important questions raised during molecular docking is related to the conformation of the boronic acid and imines. Originally, I focused on those complexes that were characterized by a negative free energy of interaction (both based on van der Waals and electrostatic forces). Thus, I considered as leading group compounds were those with low free energy and these free energy of interaction might qualitatively represent a very stable complex between boronic acid and the imine.

After each round of minimization of the structure of the complex between BBA and the imine, new categories of the boronic acid and the imines were tried simultaneously with the performance of their hydrolyses for the validation of the predicted favorable complex. The structural basis for those favorable complexes were further investigated and confirmed through molecular docking and modeling.

### 1.5.2. Effect of different substituents of benzenboronic acids on the hydrolysis of selected imine substrates

This thesis describes the original structure-activity relationship performed on some major classes of very well known electron withdrawing groups substituted to the BBA benzene ring<sup>84</sup> with respect to their effectiveness in increasing the binding affinity of BBA catalyst to the imine substrates. The limitations imposed by the pH and the solubility of some imines substrates in combination with different BBAs restrained the original wide group of chosen electronic withdrawing group associated compound to a number of BBA compounds which are described in detail in this project.

In order to gain insight into the mechanisms that regulate the effect of the electronic withdrawing groups on the rate of imine hydrolysis were studied. The study revelation comprised chemical activities such as electronic, steric, hydrophobic, hydrophilic, and hydrogen-bonding. All these activities were accounted in driving the conclusion for the quantitative structure-activity relationship for the imine hydrolysis. One established method to determine all the effect of different substituents of the BBA on the rate of the reaction relied on finding Hammett  $\rho$  value for the different benzenboronic acids. This structure-reactivity relationship was originally described by L.P. Hammett in 1937<sup>85</sup> for benzoic acids and focuses on the linear Gibbs energy relationship included in the Hammett equation below.



In the Hammett equation the ionization of benzoic acids in water at 25<sup>0</sup>C is presented and it is expressed as  $\log\left(\frac{K_X}{K_H}\right) = \sigma\rho$  where  $K_X$  and  $K_H$  are the equilibrium acid constants of *meta*- or *para*-substituted and unsubstituted aromatic compounds respectively,  $\sigma$  is the substituent constant, and  $\rho$  is the reaction constant. By the  $\sigma$  value, electronic effect of the substituent group X on the ionization of benzoic acid is presented. So it can be written as  $\log\left(\frac{K_{ben,x}}{K_{ben,H}}\right) = \sigma$  where  $K_{ben,x}$  and  $K_{ben,H}$  are the equilibrium acid constants of *meta*- or *para*-substituted and unsubstituted benzoic acid, respectively.

In the ionization reaction of benzoic acid a substituent that is predominantly electron-withdrawing at a given position will stabilize the benzoate anion and expected to give a positive  $\sigma$  value. Whereas, a substituent that is predominantly an electron-donating group at a given position is expected to destabilize the benzoate anion and will give a negative  $\sigma$  value. When rate constants are involved the Hammett equation takes the form of  $\log\left(\frac{k_x}{k_H}\right) = \sigma\rho$ , where  $k_x$  and  $k_H$  are rate constants for a reaction of a *meta*- or *para*-substituted and unsubstituted aromatic compound, respectively.

The  $\rho$  value will be positive if the substituent, X, increases the rate of the reaction and decreases the acid constant of benzoic acid. The  $\rho$  value also indicates the magnitude of this substituent effect in the reaction under study as compared to its effect on the acid dissociation of benzoic acid where  $\rho$  value is one. Following the established results from hydrolysis study of benzoic acid, other organic reactions and their mechanism are studied. For example, *p*-nitrophenyl benzoate ester hydrolysis is studied by Keenan *et al.*<sup>86</sup>

And in this research project, the experimental data were collected with different substituted benzenboronic acids (BBA) and the hydrolysis rates of the imines were recorded at pH 6.0. The kinetic constants,  $k_{cat}$  and  $K_M$  were determined for all investigated boronic acids using Lineweaver-Burk plots.

The second-order rate constants,  $k_{cat}/K_M$  ( $M^{-1}sec^{-1}$ ), first order rate constant,  $k_{cat}$  ( $sec^{-1}$ ) and the relative binding constant,  $K_M$  (mM), are then plotted against the total  $\sigma$  values for each BBA as a linearized plot, i.e.  $\text{Log}(k_{cat}/K_M) = f(\sigma)$ ,  $\text{Log}(K_M) = f(\sigma)$  and  $\text{Log}(k_{cat}) = f(\sigma)$ . The plots were then analyzed and were compared for different substituents at different positions of the benzene ring in the BBA to highlight the electron-withdrawing effect on the hydrolysis rate.

### 1.5.3. pH profile of the benzenboronic acid on the hydrolysis of imine

Hydrolyses were also analyzed with pH profiling and the effect of pH on  $k_{cat}$  and  $K_M$  were tabulated and analyzed in detail. pH dependency is important for the enzyme related study.  $pK$  value is the property normally used to study proton transfer reaction in solution. It can be experimentally determined with very well established method.<sup>87</sup>  $pK$  can tell much about the level of protonation of a predominating species in a range of pH.

## 2. Materials & Methods

All the boronic acids were obtained from Boron Molecular, and Combi-Blocks. They were used without further purification. Amino acids and Salicylaldehyde were obtained from Sigma Aldrich. Salicylaldehyde was distilled before it was used in experiments. n-butyl amine and aniline were obtained from Fischer Scientific. 2-hydroxy aniline, 3-hydroxyl aniline, benzylamine, 2-hydroxybenzylamine, O-methoxyanisaldehyde, p-methoxyanisaldehyde were purchased from Acros Organics. 2,2'-dihydroxy benzophenone were purchased from Aldrich. Buffers of different pH were made from reagent grade chemicals and following Biochemical handbook.<sup>88</sup> Boronic acid solutions were prepared in 95% ethanol.

### 2.1.1. Synthesis of the imines

The majority of the imines were prepared from the distilled salicylaldehyde and the selected primary amines. When the primary amines were selected from different amino acids, then a buffer of pH 10 was used to dissolve the amino acids. In one representative synthetic route, a 1:1 stoichiometric mole ratio of salicylaldehyde and amine were mixed for half an hour at room temperature and kept overnight at 4°C. Other imines, such as 2-hydroxyaniline, 3-hydroxyaniline, benzylamine and 2-hydroxybenzylamine formed precipitates in the pH 10 buffer. For the synthesis of these imines, the primary amines were dissolved in 95% ethanol and then mixed with salicylaldehyde in one to one mole ratio. The synthesized imine samples and the BBA solutions were filtered using Whatman syringe filter (0.25µm) before running the hydrolysis assay.

### 2.1.2. Hydrolyses conditions of imines by different BBAs

Hydrolyses of the imine substrates were studied by varying the concentration of boronic acids while keeping constant the imine concentration. The concentrations of the imines were selected such that absorption of less than 1.0 at their maximum absorption wavelength was achieved for each of the specifically chosen buffer and pH. All the reactions were monitored at a constant temperature of 30°C. Different buffered pH solutions were pre-equilibrated at 30°C before performing each hydrolysis assay. It was observed that the autohydrolysis of the imine generally occurred at acidic pH. All hydrolyses reactions were corrected for the spontaneous hydrolysis effect, even though they were monitored also at higher pH conditions, such that an accurate effect of pH upon the catalytic efficiency could be determined.

### **2.1.3. Instrumental discussion of the imines hydrolyses by BBA**

A Perkin Elmer UV-Vis spectrophotometer was used for an initial hydrolysis. The assay was further translated in a microplate format and the kinetics constants were determined using the hydrolysis microassay monitored on a BioTek plate reader spectrophotometer. The output changes in the absorbance were recorded and analyzed using the built-in software Gen 5. The 96 wells format microassay protocol included the readings of the absorbance at every 3 seconds for the use of simultaneous eight well readings at the maximum absorption wavelength determined for each imine. The total runtime ensured that the hydrolysis reaction runs to completion. In most cases this was recorded to be 15-25 minutes).

Structures of the imines have been monitored by  $^1\text{H}$  NMR spectroscopy experiments with FT-300MHz Bruker Aspect 3000 spectrometer.

### **2.2. Experimental steps for the hydrolysis assay**

The hydrolyses of the imines were monitored by recording the changes in absorbance at a specific absorption band (maximum absorption wavelength) determined for each imine, immediately following the mixing of the imines with the BBAs solution or the buffer itself (control measurement for the spontaneous hydrolysis).

In a first step BBA are added in a buffer solution of specific pH in the eight well section of the 96-well plate. In the next step imine solution were added which was maintained at constant concentration in all eight wells. Each set of kinetic reactions was run to completion for about 15-25 minutes, at  $30\pm 1^\circ\text{C}$  constant temperature (provided by the thermostat associated with the microplate reader). So, there were eight hydrolysis reactions by one run of the Biotek plate reader. The concentrations of the imine substrates and of the BBAs catalysts were selected such that the completion of the reaction was achieved in less than one hour, thus inherent spontaneous hydrolysis was at its minimum.

The Figure 3 presents one representative imine hydrolysis experiment in which the changes in the absorption at 395 nm are monitored with the BioTek plate reader.

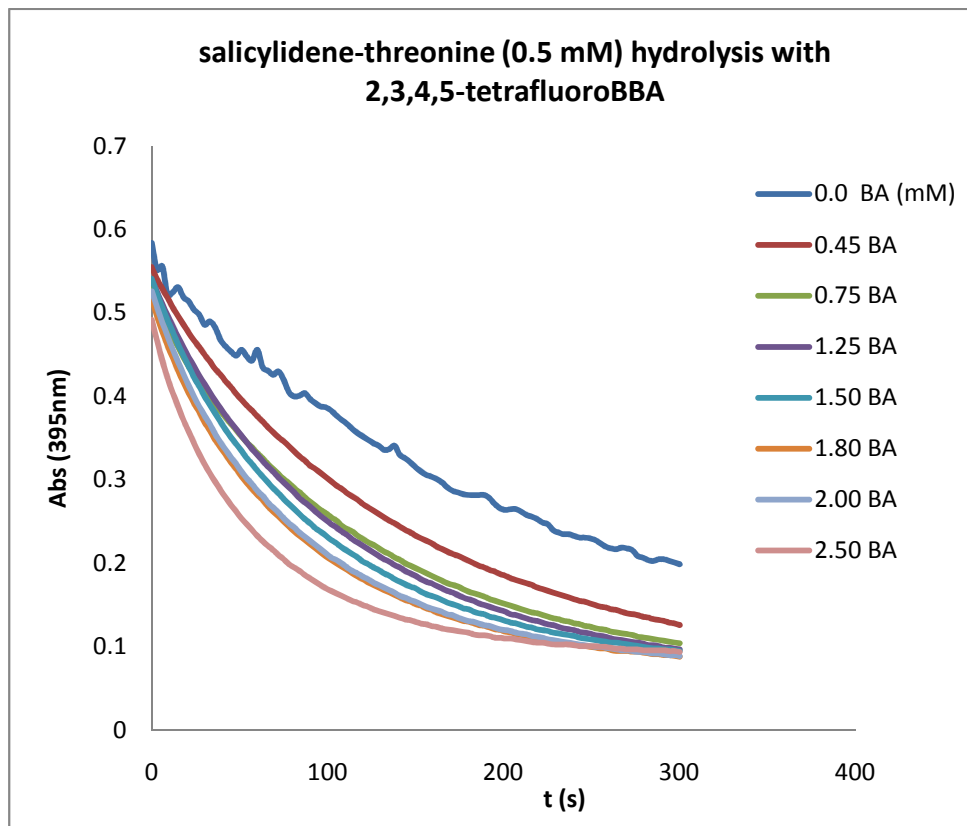


**Figure 3:** Hydrolysis of salicylidene-threonine with different concentration of 2,3,4,5-tetrafluoroBBA at 0.1 M pH 6.0 phosphate buffer.

### 2.2.1. Progress curve analysis of imine hydrolysis by BBA

A progress curve analysis was done for each hydrolysis reaction, such that the first order rates of imine hydrolysis could be extrapolated for each concentration of BBA. The observed first order rate constants are determined from the plots of  $\text{Log}(A_t - A_\infty)$  vs. time.  $A_t$  is the absorbance at any time,  $t$ .  $A_\infty$  is the absorbance at infinite time, in other words, is the final absorbance corresponding to a time when all the imine substrate is fully hydrolyzed, as the reaction went to completion.

### Determination of absorbance infinity value ( $A_{\infty}$ )

The hydrolysis reactions were run to completion in order to obtain  $A_{\infty}$ , i.e. they were monitored until no more changes were observed in the absorption. For the most imines hydrolysis the completion of the reactions were achieved after 10-20 min. Figure 4 presents a typical example for imine hydrolyses run to completion, where salicylidene-threonine was hydrolyzed with different concentrations of 2,3,4,5-tetrafluoroBBA at pH 6.0. The spectra show hydrolyses for 1200 seconds until there were no changes of absorption. So there was one  $A_{\infty}$  values for each kinetic run with one specific concentration of imine and one specific concentration of boronic acid.

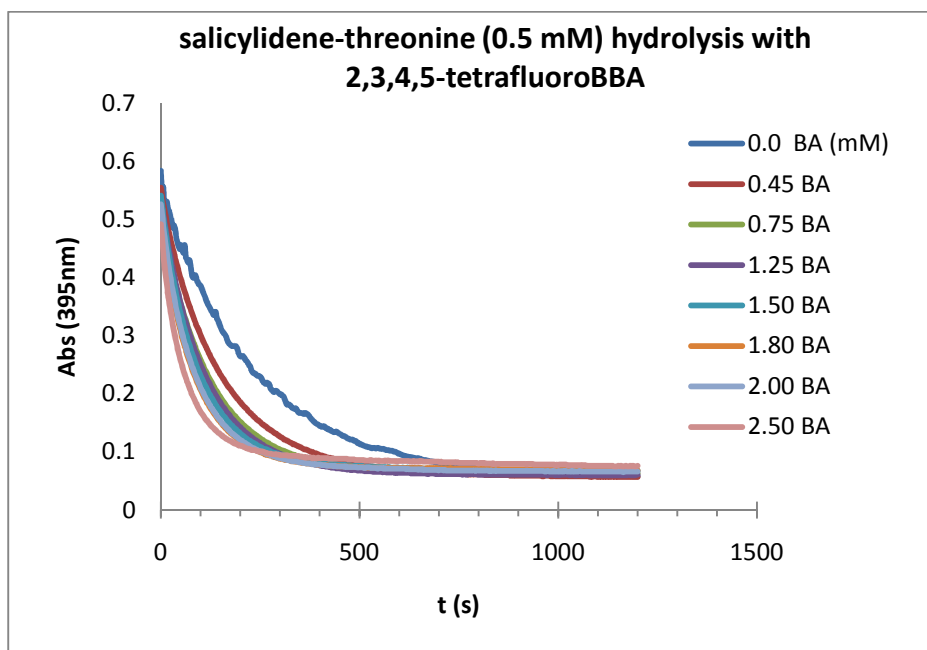


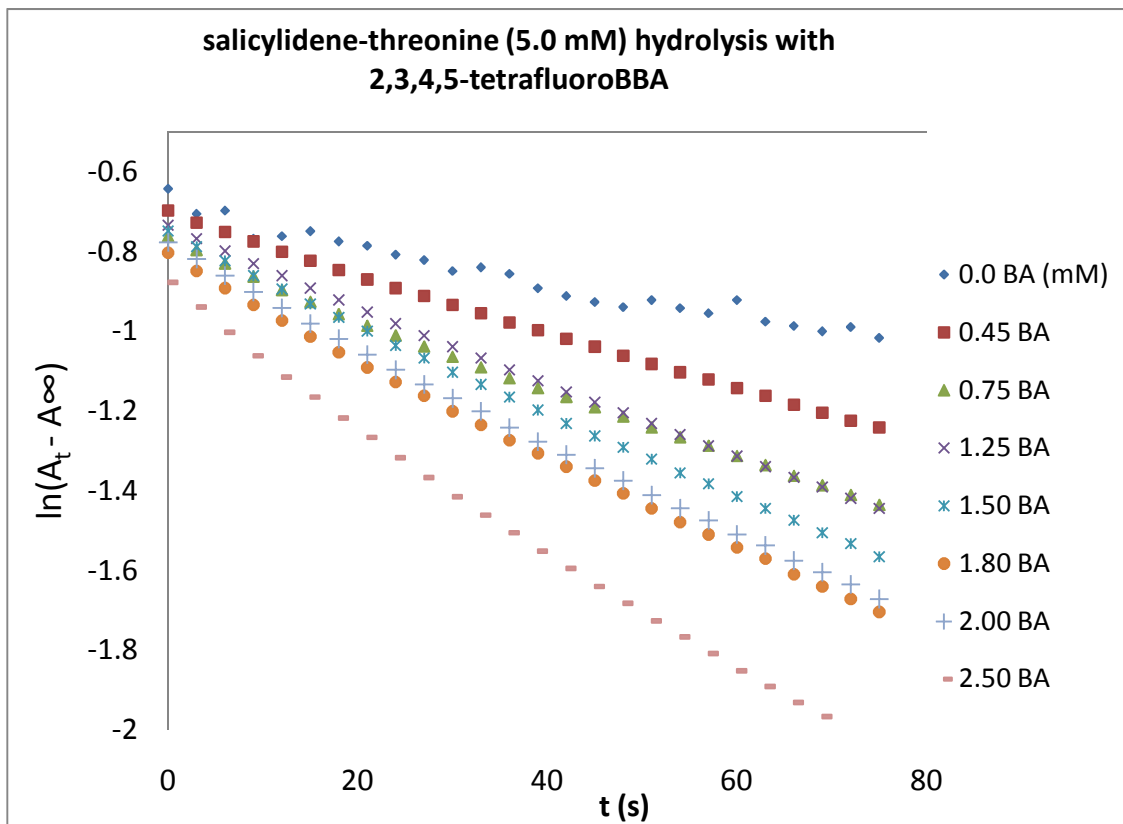
**Figure 4:** Hydrolysis progress curves for salicylidene-threonine with different concentration of 2,3,4,5-tetrafluoroBBA at 0.1 M pH 6.0 phosphate buffer.

### **Determination of absorbance at time, A(t)**

From the graph of the imine hydrolysis shown in Figure 4 it was possible to extract the absorption at each recorded time,  $t$ . Thus, for a recorded values of  $A(t)$  for each kinetic run with different concentrations of BBAs there was one specific concentration of imine and one concentration of BBA.

### **Plot of Log ( $A_t - A_\infty$ ) vs. time**

After  $A_\infty$  and  $A(t)$  were determined for each set of kinetics curves (i.e. one imine substrate kept at constant concentration and different concentrations of BBA catalyst), the Log ( $A_t - A_\infty$ ) vs. time was plotted and fitted to a first order equation ( $y=mx+y_0$ ) from which the slope  $m$  was calculated and reported to be  $k_{obs}$  ( $\text{sec}^{-1}$ ), i.e. the first order rate constant for the imine hydrolysis. The fit to a linear equation was executed so that the initial rate for the hydrolysis was determined (i.e. only the first one to two half lives or the steady state portion of the reaction time was taken into account). The following graph presented in Figure 5 shows an example of such linearized plot of Ln ( $A_t - A_\infty$ ) vs. time used to determine the  $k_{obs}$  ( $\text{sec}^{-1}$ ) for the imine hydrolysis. The data presented in Figure 5 were normalized for the effect of the imine auto-hydrolysis.



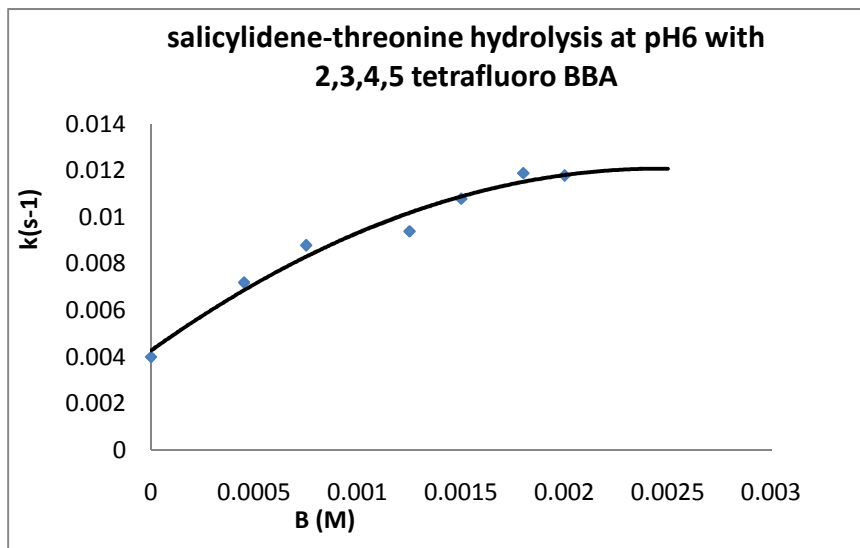
**Figure 5:** Steady state portion of the hydrolysis of 5.0 mM salicylidene-threonine with different concentrations of 2,3,4,5-tetrafluorobenzamide at 0.1 M pH 6.0 phosphate buffer and 30<sup>0</sup>C.

Table V presents the rate constants determined from that graph of  $\text{Log}(A_t - A_\infty)$  vs. time. Initial slopes were determined as the observed first order rate constants and were designated as  $k_0$ . The very first rate constant for the autohydrolysis of imine (the hydrolysis without BBA in the reaction mixture) was designated as  $k_{\text{auto}}$ .

**Table V:** Rate constants for the hydrolysis of salicylidene-threonine with 2,3,4,5-tetrafluoroBBA

Imine concentration =0.50 mM					
<b>B (M)</b>	<b>1/B (M<sup>-1</sup>)</b>	<b>k<sub>o</sub> (s<sup>-1</sup>)</b>	<b>1/k<sub>o</sub> (s)</b>	<b>k(s<sup>-1</sup>)</b>	<b>1/k (s)</b>
0		k <sub>auto</sub> =0.004	250		
4.50E-04	2220	7.20E-03	139	5.40E-03	185
7.50E-04	1330	8.80E-03	114	7.00E-03	143
1.25E-03	800	9.40E-03	106	7.60E-03	132
1.50E-03	667	1.08E-02	93	9.00E-03	111
1.80E-03	556	1.19E-02	84	1.01E-02	99
2.00E-03	500	1.18E-02	85	1.00E-02	100
2.50E-03	400	1.40E-02	71	1.22E-02	82

Table V also shows the initial rate constants which were corrected for the auto hydrolysis using the formula:  $k = k_o - k_{\text{auto}}$ . These rate constants analyses were performed for each of the hydrolysis reaction. Using the information presented in the Table V, next graph,  $k$  vs.  $B$  was plotted as it is shown in Figure 6. In that graph,  $k$  vs.  $B$  was plotted for the hydrolysis salicylidene-threonine with 2,3,4,5-tetrafluoroBBA at 0.1 M pH 6.0. This graph is further linearized by plotting  $1/k = f(1/B)$  from which the  $K_M$  and  $k_{\text{cat}}$  values were calculated as described in the next following section.



**Figure 6:** Graph depicting first order rate constants at different concentration of 2,3,4,5-tetrafluoroBBA.

### 2.2.2. Determination of $K_M$ & $k_{cat}$

In order to determine  $k_{cat}$  and  $K_M$  a plot of  $1/k$  as a function of  $1/B$  was used, this is a modified Lineweaver Burk plot.<sup>89</sup> In these plots the inverse of the y axis intercept gave the value of  $k_{cat}$ . The slope multiplied with  $k_{cat}$  gave the value of  $K_M$ . These  $k_{cat}$  and  $K_M$  determinations allowed the calculation of the catalytic efficiency,  $k_{cat}/K_M$ .

Figure 7 shows a representative plot of  $1/k$  vs.  $1/B$  for the hydrolysis of salicylidene-threonine with 2,3,4,5-tetrafluoroBBA. The data points were fit to the linear least square equation which gave the slope (0.034) and the intercept with the y axis, of 67.14. The calculated  $k_{cat}$ ,  $K_M$  and  $k_{cat}/K_M$  values are presented in the adjacent table.

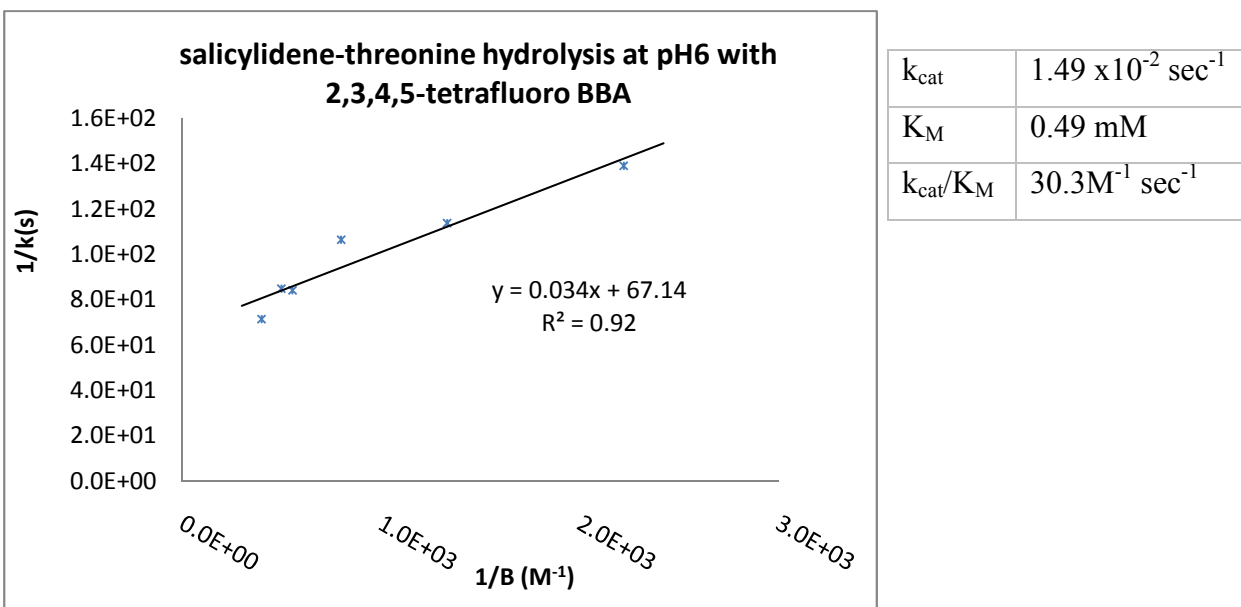


**Figure 7:** Lineweaver-Burk plot for the hydrolysis of salicylidene-threonine with different concentration of 2,3,4,5-tetrafluoroBBA. Catalytic constants are also tabulated next to the figure.

## 2.3. pH profiles for the imine hydrolysis

### 2.3.1. Description of pH profile

In a pH profile the Log of second order rate constants  $\text{Log}(k_{cat}/K_M)$  are plotted as a function of pH.<sup>90</sup> These plots show the pH dependency for the imine hydrolyses. The range of the pH was determined to be between 6.0 – 10 for the imines and BBA complexes investigated. All the points of the pH-rate profile were corrected for the auto-hydrolysis of the imine at the same buffer concentration. The protonation steps extrapolated from these pH profiles were noted for the pK values of the BBAs and compared with the pKs of the imine substrates such that mechanistic inferences about the imine hydrolysis could be proposed. In addition, the pK for some BBAs were further determined experimentally as it is described in the next following section.

### 2.3.2. pK determination for BBA

In order to determine the pK s of some BBAs used as catalysts, the UV spectrum of the selected compounds were collected at each different pH, in the region of 200-300 nm. The Figure 8 presents the UV scans collected at different pH for the 2,3,5-trifluoroBBA.

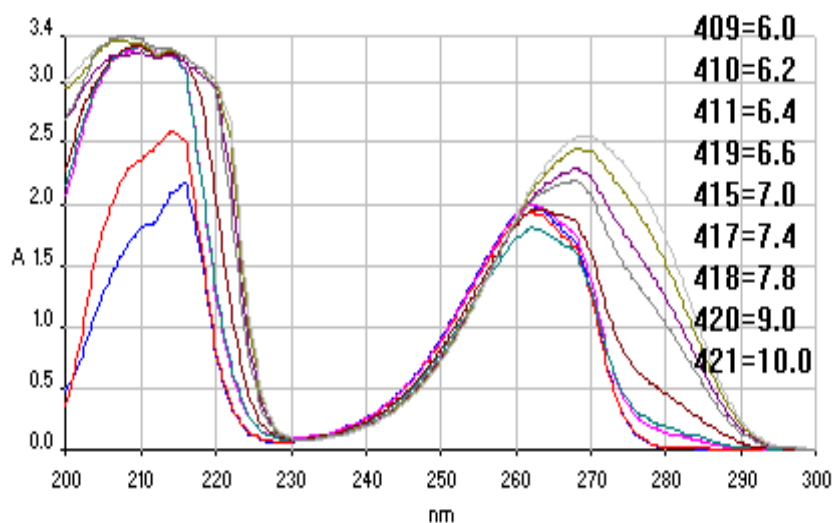


**Figure 8.** Absorbance vs. wavelength at different pH for 2,3,5-trifluoroBBA. The graph designates the experimental numbers from 409 to 421 for different pH from top to bottom on the figure looking at the wavelength of 278 nm. Temperature was 30°C. Buffers below pH 8.0 were 0.1 M phosphate and buffers above pH 9.0 were 0.1 M bicarbonate.

It can be seen from Figure 8 that the increase in the pH resulted in some spectral band changes for 2,3,5-trifluoroBBA. There is a decrease in the absorption at 278.5nm band, an appearance of a new change in the absorption at 218nm and a tight isobastic point remained at 230-232nm. These results suggest that the spectral changes as a function of pH could be due to the structural changes associated to the hydrogen ion transfer on the benzene boronic acid group. The change in the absorption at 278.5 nm is further analyzed to find the pK of this BBA as it is shown in the Table VI.

**Table VI:** Absorbance collected at 278.5 nm at different pHs (5.5-10.0) for 2,3,5-trifluoroBBA

pH	abs at 278.5 nm
5.5	1.97
6	1.92
6.2	1.70
6.4	1.39
6.6	1.16
7	0.52
7.4	0.23
7.8	0.17
9	0.05
10	0.04

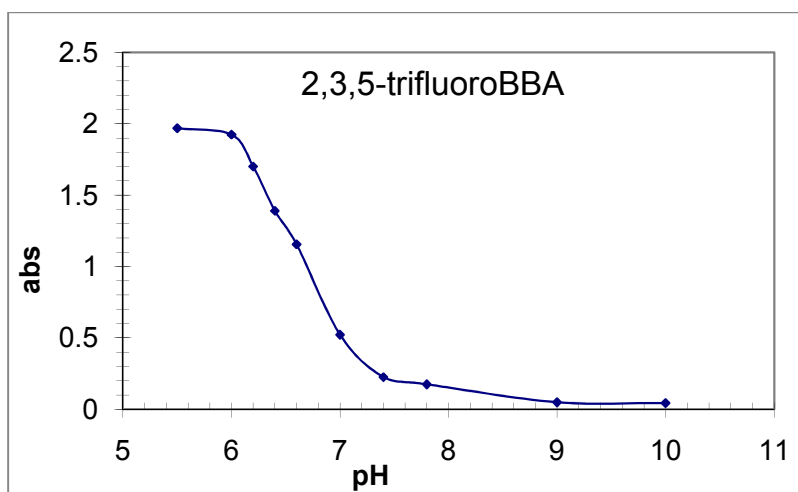


**Figure 9:** pH dependence (5.5-10) of the absorption spectra of 2,3,5-trifluoroBBA (0.002 M in ethanol); Temperature 30°C, Buffers below pH 8.0 are 0.1 M phosphate and above pH 9.0 are 0.1 M bicarbonate buffers.

From the analysis of the plot of absorbance at 278.5nm versus pH (6.0-10) the pK value of the 2,3,5-trifluoroBBA was estimated to be  $6.6 \pm 0.1$ .

### 2.3.3. pH profile example

A representative example of pH profile for the hydrolysis of salicylidene-3-hydroxyaniline with 2,3,5-trifluoroBBA shows the plot of  $\text{Log}(k_{\text{cat}}/K_M)$  at different pH in Figure 9. For the  $k_{\text{cat}}/K_M$  determination see Section 2.2.3.

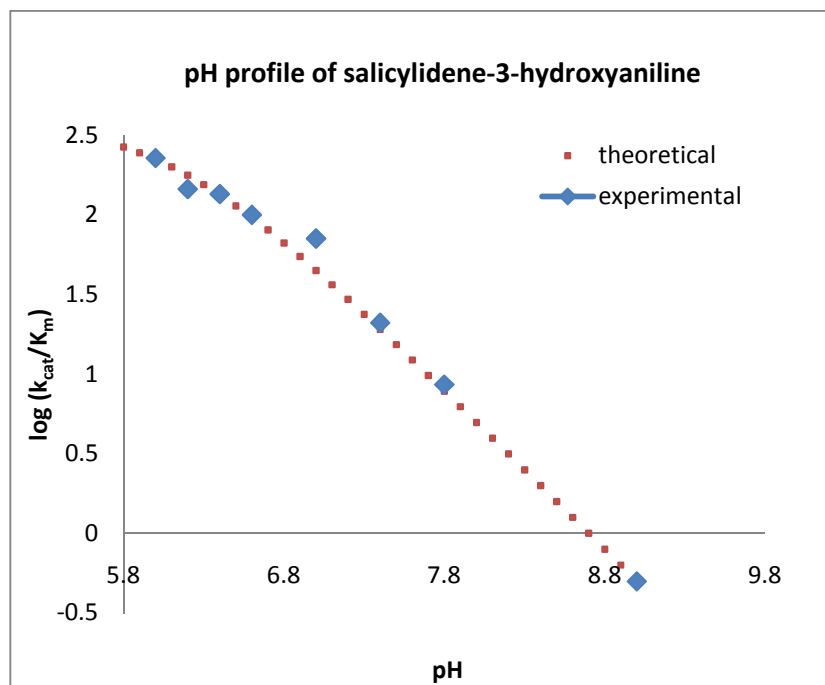


**Figure 10:** Red (■) denotes theoretical plot and blue (◆) denotes experimental data points for the graph showing  $\text{Log}$  of  $k_{\text{cat}}/K_M$  at different pH for the hydrolysis of salicylidene-3-hydroxyaniline with 2,3,5-trifluoroBBA at substoichiometric(1/10) ratio of BBA to imine.

## **2.4. Modeling with a SCULPT of different complexes between benzeneboronic acids and imines**

The relative stability of different complexes between BBAs and imines was predicted through docking experiments. I used the docking software (SCULPT) provided by MDL to perform all the docking experiments and I assessed the free energy of interaction between the boronic acids and the imines using the built-in advanced molecular mechanics force-field (MMFF). The software allows the prediction of the van der Waals steric fitness of the two target components in the complex. In addition, SCULPT provides the Coulombic electrostatic force field to assess the contribution of the electrostatic interactions for the stability of the complex. The relationship between the structures of imines and their affinity for the benzene-boronic acid catalysts was predicted using both the van der Waals and the electrostatic terms of the MMFF built-in the software SCULPT. A technical limit of the Sculpt was imposed to use the carbon atom instead of boron in all modeling of the complexes. However, the tendency of boron to achieve an octet on its outermost valence shell through tetravalent bonds supports the replacement in the modeling studies (see also Section 1.1.2 describing the chemistry of boron as trivalent and tetravalent atom in different chemical combinations).

As an example for the experimental design of the docking procedure I refer Figure 11, which presents the complexes between the 2,3,5-trifluoroBBA and the imine salicylidene-3-hydroxyphenylglycine while Figure 12 shows one of the predicted models (performed with SCULPT) depicting the complex between the BBA and the imine, in which the hydroxy groups of the BBA are substituted to the aromatic rings of the imine.

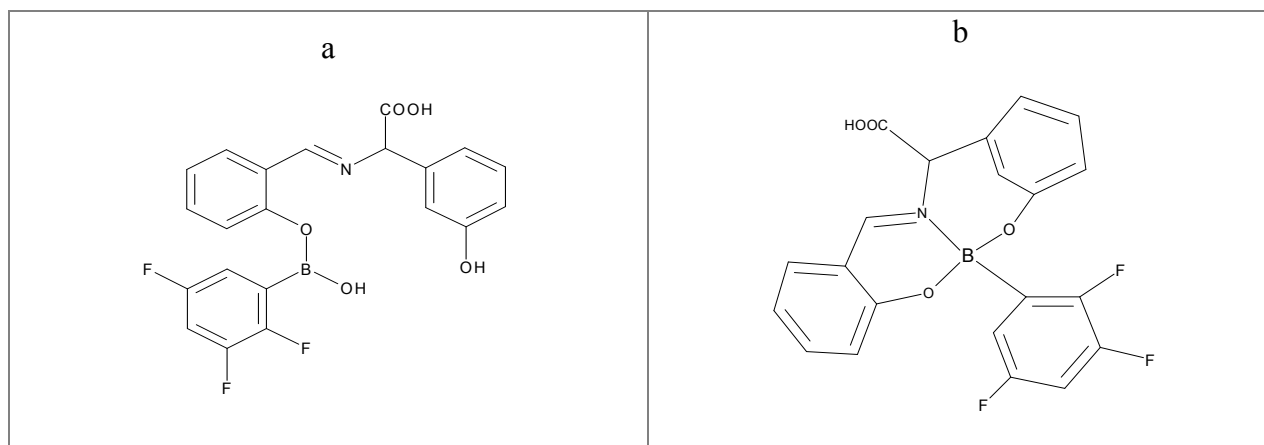


**Figure 11:** (a) Initial ester formation between the 2,3,5-trifluoroBBA and the salicylidene-3-hydroxyphenylglycine. b) Further ester bond and a new boron-nitrogen covalent bond between the BBA and the imine are shown to be engaged in the complex.

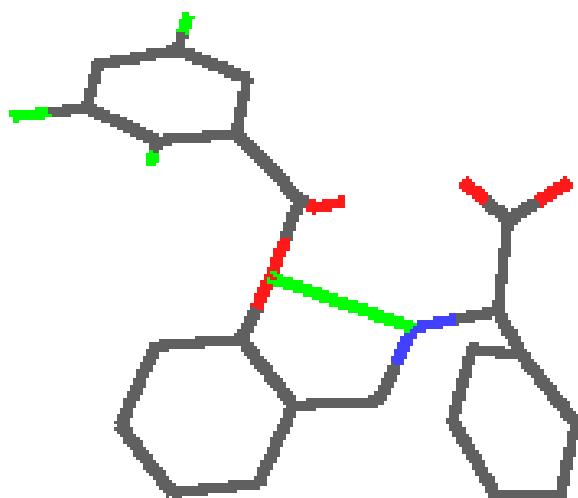


**Figure 12:** An example of a complex between salicylidene-*meta*-hydroxyphenylglycine and 2,3,5-trifluoroboronic acid.

### 3. Results and Discussions

Studies previously proposed that the aromatic boronic acids could be very good catalysts for the hydrolysis of different types of imines by Rao *et al.*<sup>69</sup> However, the investigation used limited number of substituted benzeneboronic acids and imines substrates. To further investigate the mechanisms underlying the benzene based boronic acid mediated catalysis I developed as a first step some new assays for monitoring the hydrolysis of salicylidene-3-hydroxyaniline imine substrate by the 2,3,4,5-tetrafluoroBBA. I hypothesized that the highly electron withdrawing groups, such as the fluorine substituents, would allow a higher binding affinity between the benzeneboronic acid and the imine substrates, thus enabling a more stable transition state and a higher rate of hydrolyses of these substrates.

#### 3.1.1. The effect of different concentrations of 2,3,4,5-tetrafluoroBBA on the catalytic efficiency of salicylidene-3-hydroxyaniline hydrolysis

In order to acquire mechanistic insights for the catalytic properties of the benzeneboronic acids (BBA), I developed and optimized a spectrophotometric assay for monitoring the hydrolysis salicylidene-3-hydroxyaniline with different concentrations of 2,3,4,5-tetrafluoroBBA. The concentrations of 2,3,4,5-tetrafluoroBBA catalysts were varied such that substoichiometric (1/10 and 1/5, BBA: substrate), stoichiometric (1:1, BBA: substrate) and excess (4:1, BBA: substrate) molar ratios were achieved in a final 200-250  $\mu$ L volume of reaction mixture, in 0.1 M potassium phosphate buffer, pH 6.0.

The reaction were performed at 30°C and the decrease in the concentration of the starting substrate was recorded by monitoring the changes in the absorption at 430 nm, as described in detail in materials and methods (Section 2.2). The concentration of the imine substrate was maintained constant throughout all reactions trial sets. One set constituted 8 reactions of different boronic acid concentrations and one specific concentration of imine. The recorded changes in the absorption at 430 nm as a function of time (see Figure 14) showed that the reaction of imine hydrolysis (which has by itself a slow intrinsic rate of hydrolysis, as can be seen from the graph at 0.0 M BBA) is enhanced by the addition of the boronic acid catalyst (see the same Figure 14a and the graphs at different concentrations of BBA).

As already described in detail in the section of materials and methods (Section 2.2.1) these progress curves for the imine hydrolysis were used to extract the first order rate constants ( $k$ ). To further determine the catalytic parameters (i.e.  $k_{cat}$ ,  $K_M$  and  $k_{cat}/K_M$ ) for the imine hydrolysis by BBA at different molar ratios of catalyst : substrate I made the graph of  $1/k$  as a function of  $1/B$  (see Figure 14b). The data were fitted to a linear function of the type  $y = mx+b$ , where  $m$  = slope and  $b$  is the  $y$  intercept. The  $1/b$  is equal with  $k_{cat}$ , the slope  $\times k_{cat}$  is equal with  $K_M$  (for details of the mathematical analysis, see Section 2.2.2 from materials and methods). All the progress curves for the imine hydrolysis by BBAs were corrected by subtraction for the intrinsic hydrolysis of the imine before the extraction of the catalytic constants described in Table V and Section 2.2.1.

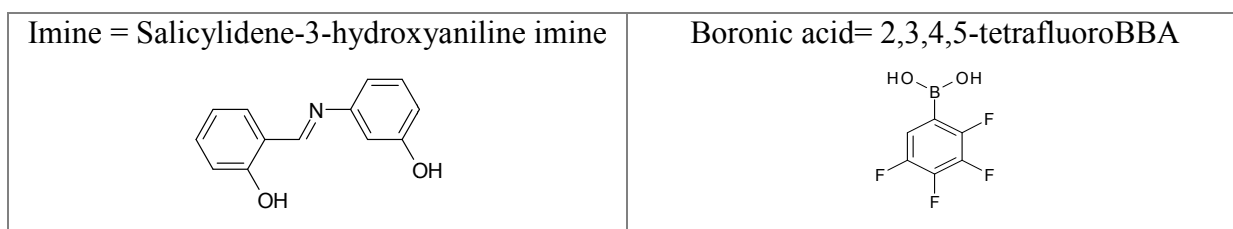


**Figure 13:** Structure and name of the substrate and the catalyst.

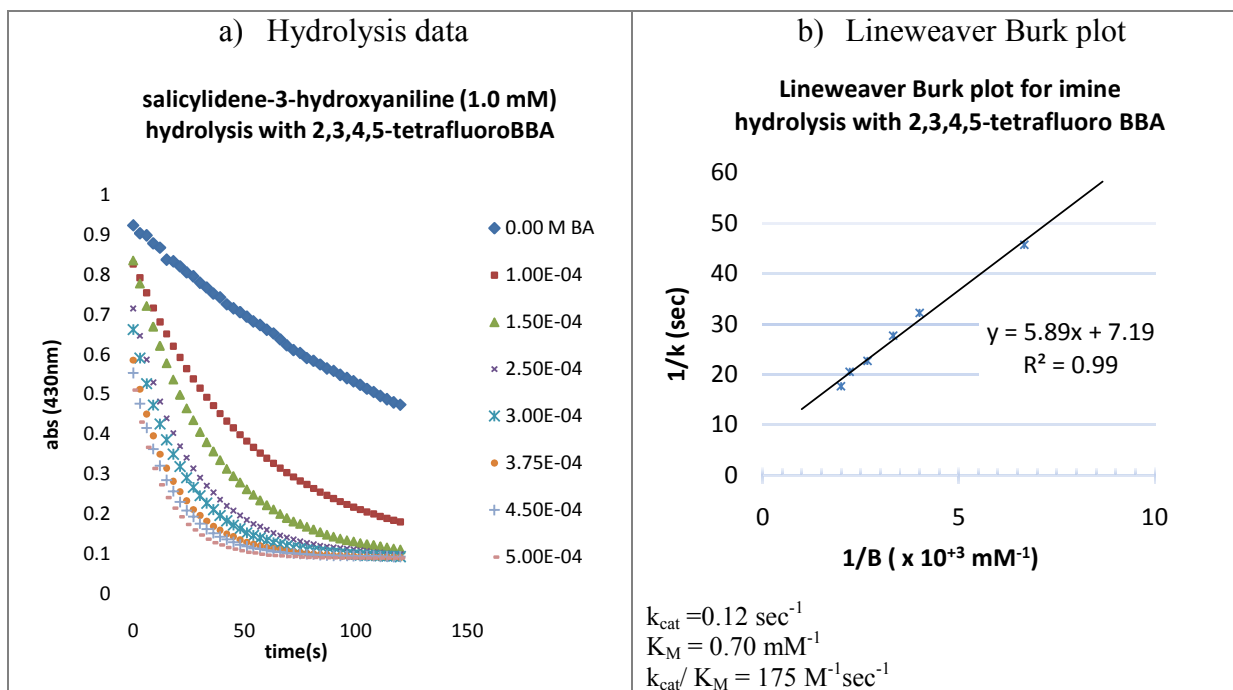


**Figure 14:** a) hydrolysis data plots and b) Lineweaver-Burk plot of salicylidene-3-hydroxyaniline hydrolysis with 2,3,4,5-tetrafluorobBA at substoichiometric (1/10) ratio of BBA to imine at 0.1 M phosphate buffer of pH 6.0. Calculated kinetic constant are also included.

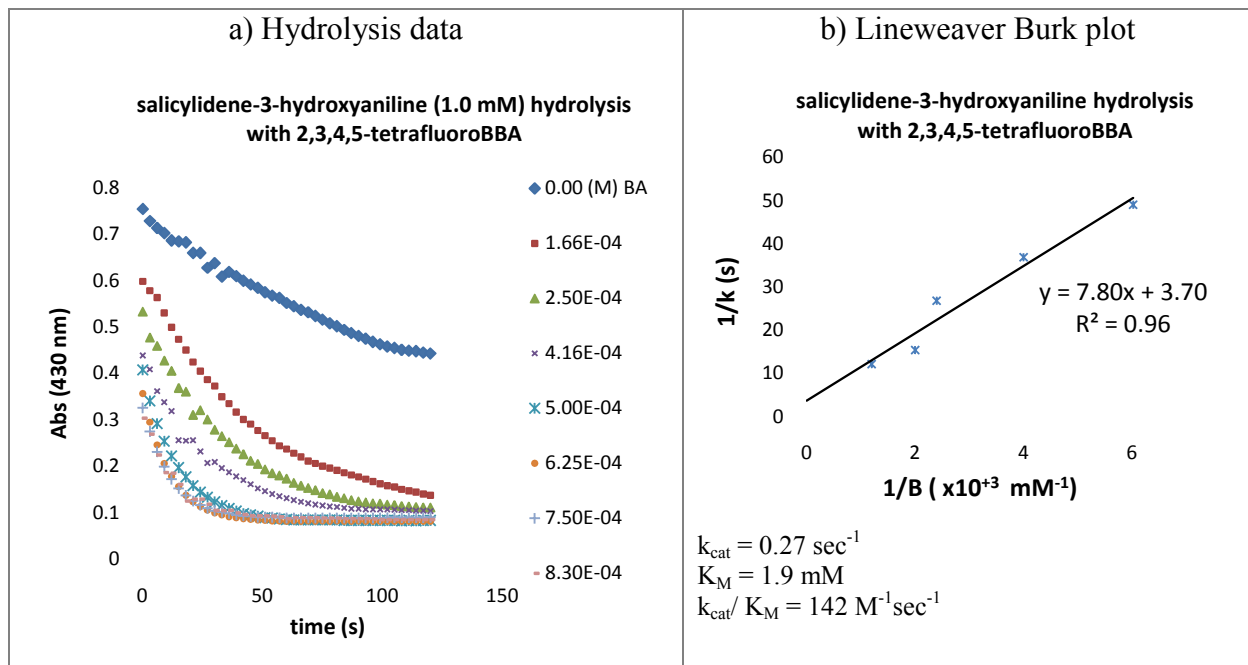


**Figure 15:** a) Hydrolysis data plots and b) Lineweaver-Burk plot of salicylidene-3-hydroxyaniline hydrolysis with 2,3,4,5-tetrafluoroBBA at substoichiometric (1/5) ratio of BBA to imine at 0.1 M phosphate buffer of pH 6.0. Calculated kinetic constant are also included.

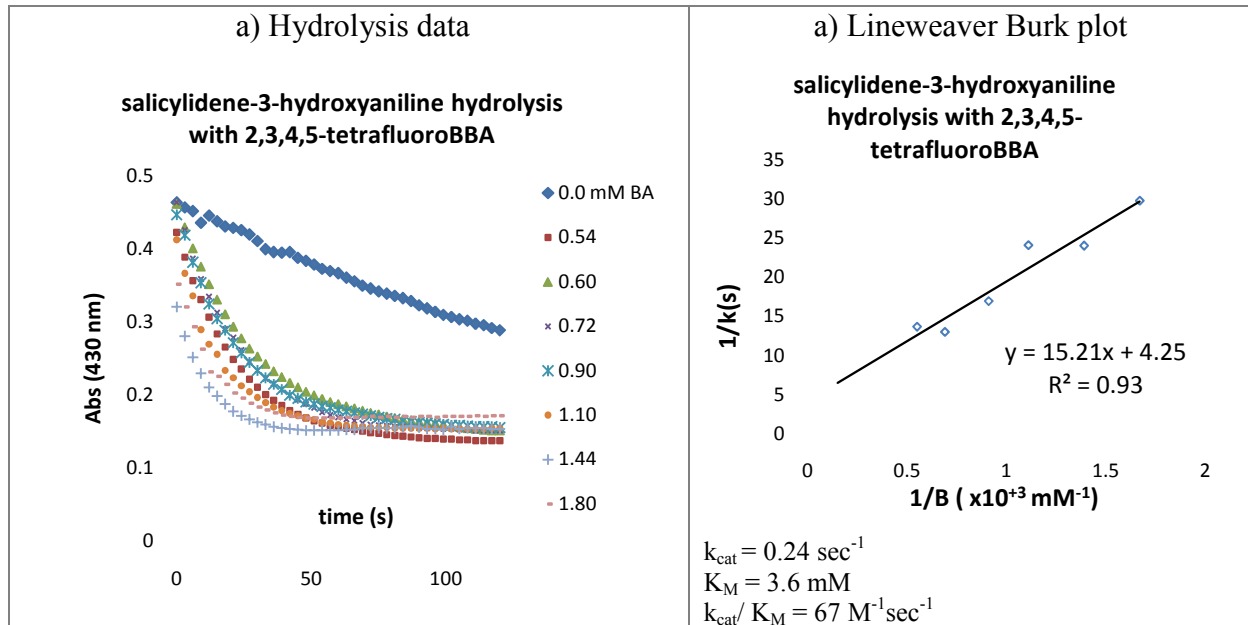


**Figure 16:** a) Hydrolysis data plots and b) Lineweaver-Burk plot of salicylidene-3-hydroxyaniline hydrolysis with 2,3,4,5-tetrafluoroBBA at stoichiometric (1/1) ratio of BBA to imine at 0.1 M phosphate buffer of pH 6.0. Calculated kinetic constant are also included.

**Table VII:** The catalytic constants for the hydrolysis of salicylidene-3-hydroxyaniline by 2,3,4,5-tetrafluoroBBA illustrated at different molar ratios of substrate and catalyst

<b>2,3,4,5-tetrafluoroBBA and salicylidene-3-hydroxyaniline imine</b>		<b><math>k_{cat}</math> (<math>sec^{-1}</math>)</b>	<b><math>K_M</math> (mM)</b>	<b><math>k_{cat}/ K_M</math> (<math>M^{-1}sec^{-1}</math>)</b>
<b>Imine (mM)</b>	<b>Boronic acid concentration range (mM)</b>			
<b>1.0</b>	<b>0.10 to 0.50</b>	<b>0.12</b>	<b>0.7</b>	<b>175</b>
<b>1.0</b>	<b>0.20 to 1.0</b>	<b>0.27</b>	<b>1.9</b>	<b>142</b>
<b>0.60</b>	<b>0.54 to 1.4</b>	<b>0.24</b>	<b>3.6</b>	<b>67</b>

It can be seen from Table VII that varying the molar ratios of catalyst: substrate had a significant effect on the catalytic efficiency ( $k_{cat}/ K_M$ ) for the imine hydrolysis by BBA. Sub-stoichiometric ratios of BBA: imine (i.e. 1/10 and 1/5 of BBA/imine) allowed the achievement of the lowest  $K_M$  values (0.7 mM) and an intermediate  $k_{cat}$  (0.12  $sec^{-1}$ ). Obtaining the lowest  $K_M$  value at sub-stoichiometric molar ratios of the catalyst : imine support the view that the BBA is more efficient in binding the imine substrate under these conditions. This is also a condition for a good catalyst. This was in turn translated in the achievement of the highest catalytic efficiency ( $k_{cat}/ K_M$ ) in the whole series of the molar ratios BBA: imine tested. Stoichiometric ratio of BBA : imine (1:1) and an excess of BBA (at least two fold higher molar concentration of BBA with respect to imine substrate) decreased significantly the  $K_M$  values (compare 3.6 mM for  $K_M$  at 1.4 : 0.6 mM ratio BBA: imine with 0.70 mM  $K_M$  at 0.10 : 1.0 mM ratio BBA:imine, almost five fold increase in the  $K_M$  value). The catalytic efficiency was in turn reduced at least 2.5 fold (175 vs. 67  $M^{-1}sec^{-1}$   $k_{cat}/ K_M$ ) when excess of BBA was used.

These results guided me to hypothesize that changes in the structural features of both the benzeneboronic acid catalysts and the imines substrates could determine the achievement of different catalytic efficiencies once the best molar ratios of BBA: imine are fixed. Whether the sub-stoichiometric amounts, equal molar ratios or excess of BBA with respect to the imine

substrate would enhance or decrease the catalytic efficiency could be directly related to the level of substitution of the benzenboronic acid with electron withdrawing groups (such as fluoro, chloro, nitro, carboxyl). These electron withdrawing groups would in turn increase the acidity of the BBA, making it more suitable to attack the Schiff base imine bond. A possible model for salicylidene-L-isoleucine hydrolysis by different BBAs is described by Rao *et al.*<sup>69</sup> and they suggest that additional hydrogen bonding network between the BBA and imine would enhance the stability of the complex, and thus would increase the rate of hydrolysis. Thus, electron withdrawing groups substituted to the benzene BA ring would enable the BBA to be more easily bonded in the active site of the imine that is in the C=N bond.

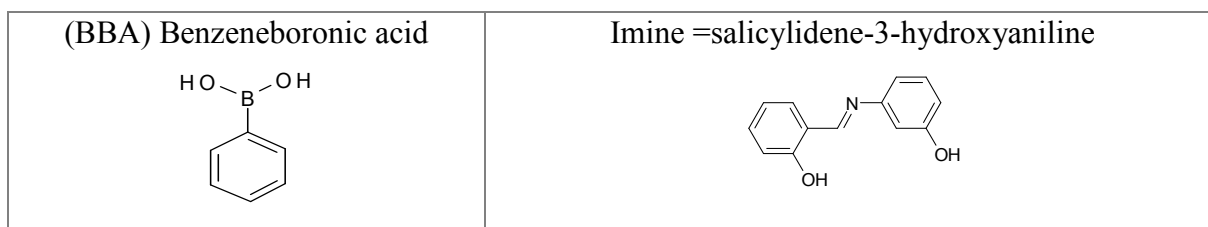
In order to test this working hypothesis I used the optimized assay for salicylidene-3-hydroxyaniline imine hydrolysis by BBA to determine the relationship between the structure of the electron withdrawing groups substituted to the benzene BA and their effect on the catalytic efficiency of the BBA derivatives. Section 3.2, presents the results for the hydrolysis of the above mentioned imine obtained with different BBA catalysts in which the benzene ring was substituted with fluoro, nitro, carboxy or mixed combination of these electronic withdrawing groups.

### **3.2. SAR of different substituted benzenboronic acids on the catalytic efficiency of imine hydrolysis**

The effect of various substituted benzenboronic acids on salicylidene-3-hydroxyaniline hydrolysis was studied as already described for the assay optimization at pH 6.0 using sub-stoichiometric ratios of BBA: imine, i.e. 1/5. The kinetic constants,  $k_{cat}$ ,  $K_M$ , and  $k_{cat}/K_M$  were determined as described in Section 2.2.

In order to obtain a reliable SAR for the effect of the electronic withdrawing group on the catalytic efficiency of different BBAs I first performed the assay for the imine hydrolysis using the unsubstituted BBA as a reference. The catalytic constants  $k_{cat}$ ,  $K_M$  and  $k_{cat}/K_M$  were  $0.0067 \text{ sec}^{-1}$ , 34 mM and  $0.19 \text{ M}^{-1}\text{sec}^{-1}$  respectively, all of them reflecting the hydrolysis of the salicylidene-3-hydroxyaniline imine by the unsubstituted BBA. These values are tabulated and discussed in the next sections by comparison with other substituted BBAs.

a)



b)

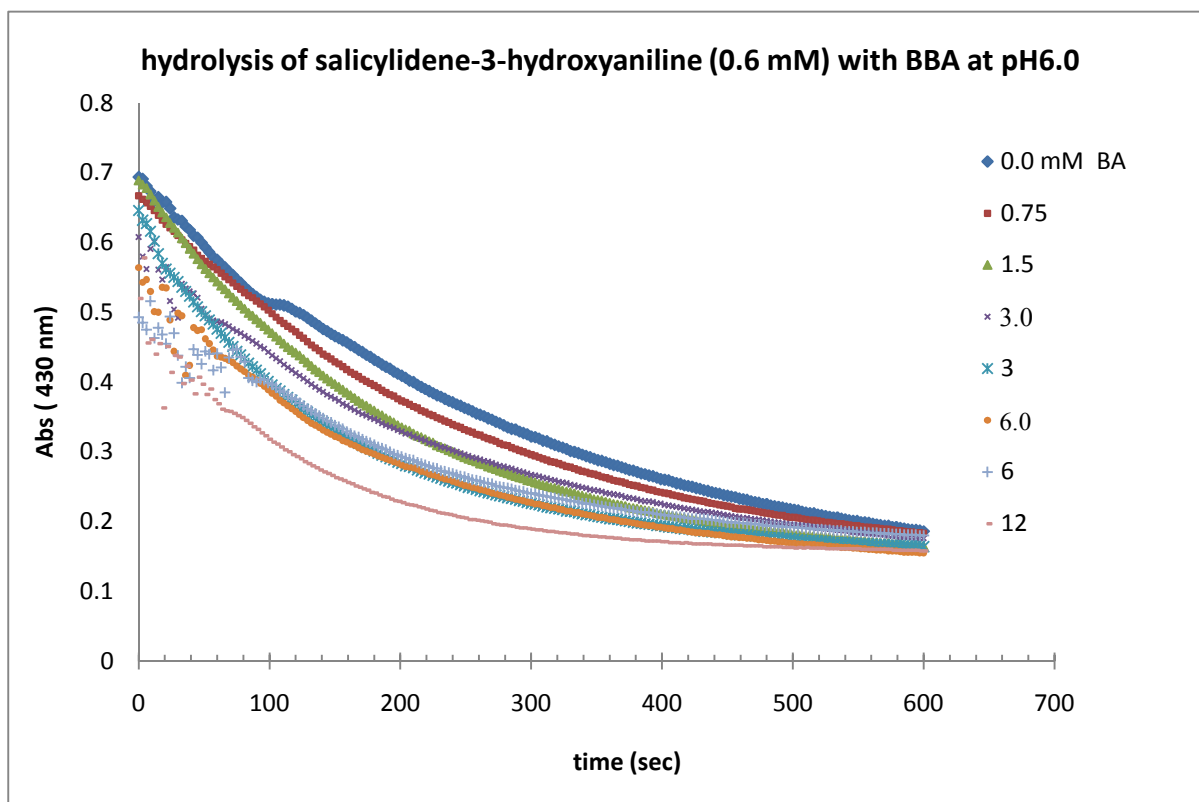
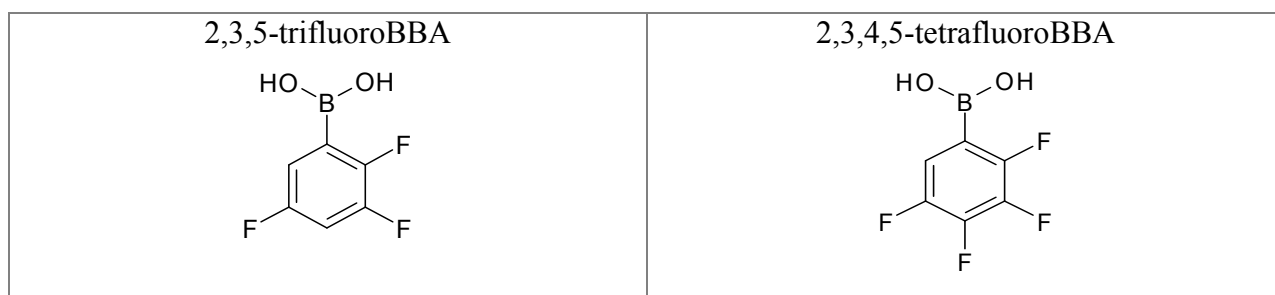


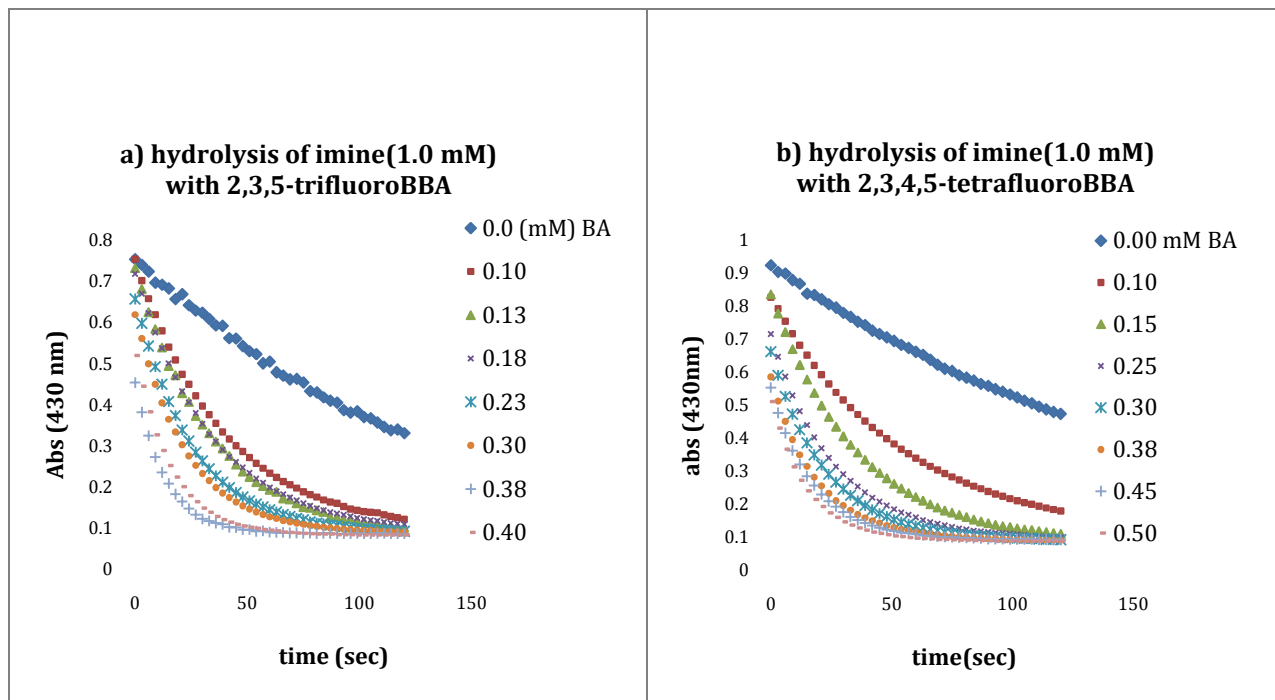
**Figure 17:** a) Structure and name of boronic acid catalyst and of imine substrate, b) Hydrolysis of salicylidene-3-hydroxyaniline with different concentrations of unsubstituted BBA at 0.1 M pH 6.0 phosphate buffer.

### 3.2.1. The fluoro-substituted BBAs have higher catalytic efficiency of imine hydrolysis than the unsubstituted BBA

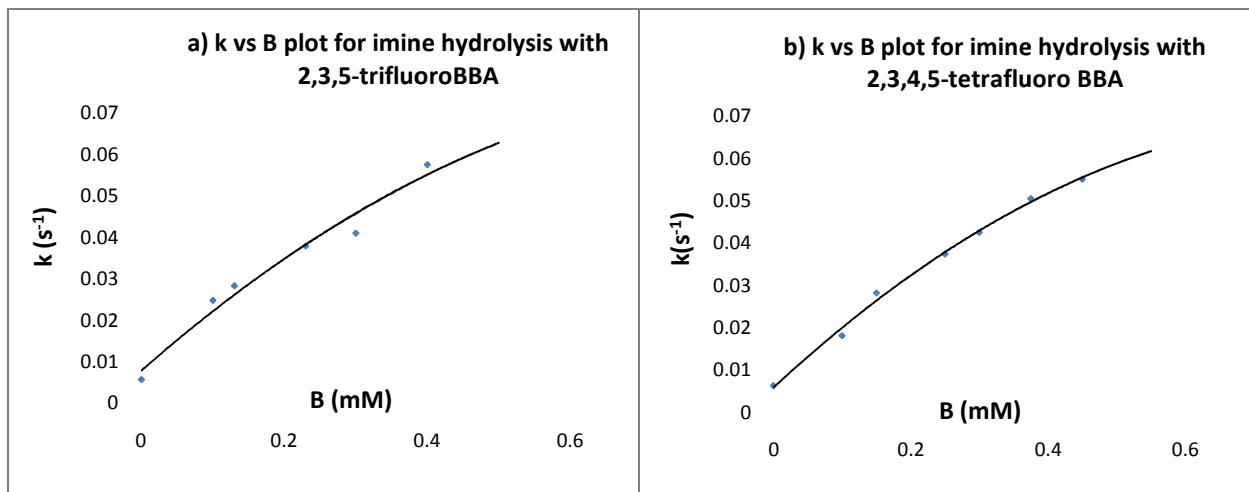
Since the fluorine is one of the best electronic withdrawing for the aromatic compounds I further investigated different fluoro-substituted BBA (main focus was on seven different substitution positions in the benzene ring). The catalytic constants for the imine hydrolysis by these fluoro-BBAs are presented in Table VIII and in the Figures 18, 19, 20. Most of the assays were performed at substoichiometric ratios of BBA/imine, such as 1/5 or 1/10 (depending on the best catalytic efficiency obtained with each fluoro BBA), (see Table VIII). These ratios were chosen based on the first trial for the assay optimization, where it is already proved that the hydrolysis was best performed with the highest efficiency under these conditions.

As it appears that better the catalyst lesser the catalyst amount needed. Figure 18 shows the raw hydrolysis run and Figure 19 shows  $k$  vs.  $B$  plots. The same data are used to draw Lineweaver Burk plots in Figure 20. From the linear fit from Lineweaver-Burk plot the  $y$  intercept gave the  $k_{cat}$ . And the  $k_{cat}$  value times the slope gave  $K_M$  value. These catalytic constant are shown together with the Lineweaver-Burk plot for a direct evaluation and comparison. All these figures include two important BBA namely 2,3,5-trifluoroBBA and 2,3,4,5-tetrafluoroBBA.

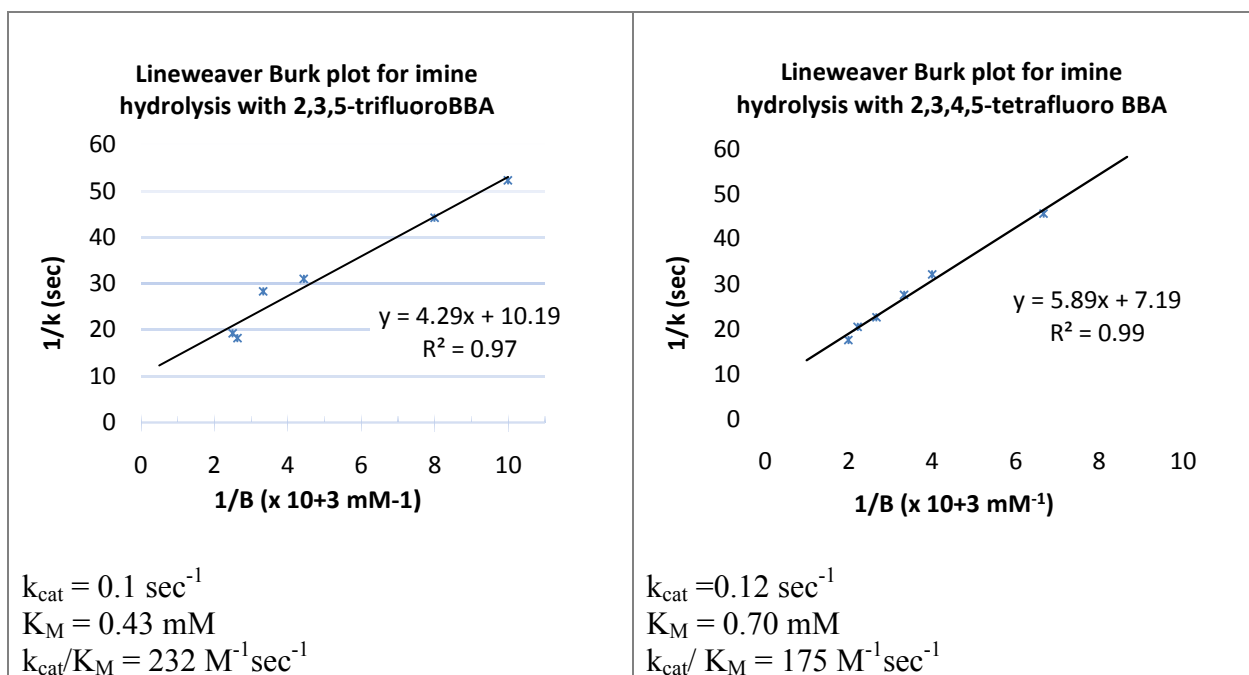




**Figure 18:** Hydrolysis of salicylidene-3-hydroxyaniline with different concentrations of a) 2,3,5-trifluorobBA and b) 2,3,4,5-tetrafluorobBA at 0.1 M pH 6.0 phosphate buffer.

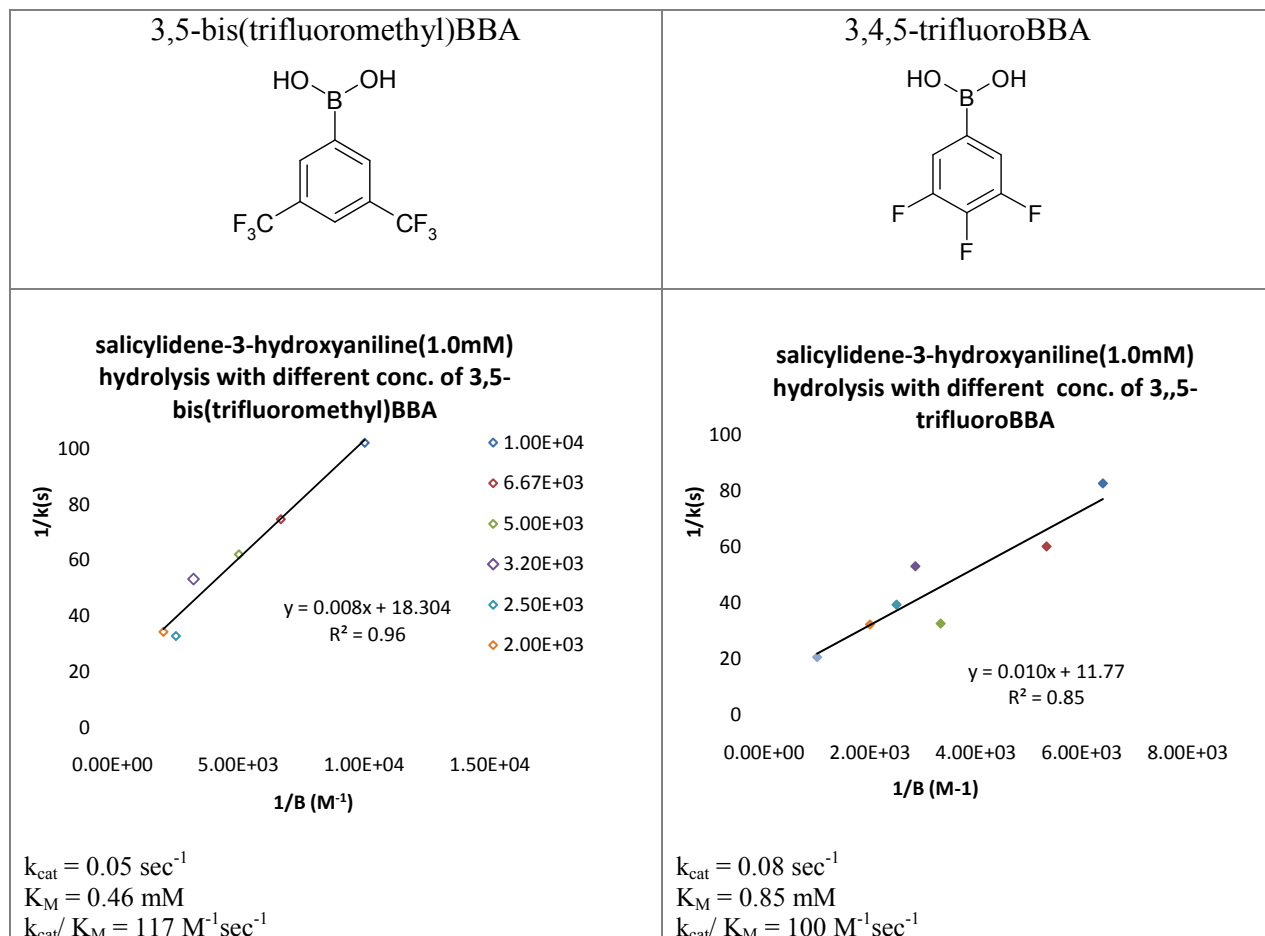


**Figure 19:** k vs. B plots for the hydrolysis of salicylidene-3-hydroxyaniline with different concentration of a) 2,3,5-trifluoroBBA and b) 2,3,4,5-tetrafluoro BBA at 0.1 M pH 6.0 phosphate buffer.



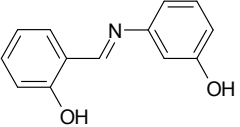
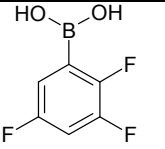
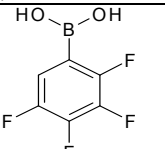
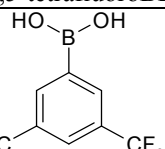
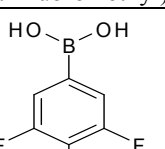
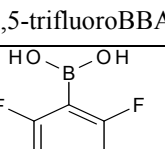
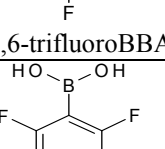
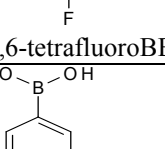
**Figure 20:** Lineweaver-Burk plots for the hydrolysis of salicylidene-3-hydroxyaniline with different concentration of a) 2,3,5-trifluoroBBA and b) 2,3,4,5-tetrafluoroBBA at 0.1 M pH 6.0 phosphate buffer.

The following figures show the data for two other important BBA that are 3,5-bis(trifluoromethyl)BBA and 3,4,5-trifluoroBBA. Only Lineweaver-Burk plots are shown here.



**Figure 21:** Lineweaver-Burk plots for the hydrolysis of salicylidene-3-hydroxyaniline with different concentration of (a) 3,5-bis(trifluoromethyl)BBA and (b) 3,4,5-trifluoroBBA at 0.1 M pH 6.0 phosphate buffer.

**Table VIII:** Catalytic constants for the hydrolysis of salicylidene-3-hydroxyaniline by BBA and different fluoro-substituted BBA illustrated at different molar ratios of substrate and catalyst

 salicylidene-3-hydroxyaniline imine		$k_{\text{cat}}$ ( $\text{sec}^{-1}$ )	$K_M$ (mM)	$k_{\text{cat}} / K_M$ ( $\text{M}^{-1}\text{sec}^{-1}$ )
Imine (mM)	Substituted benzeneboronic acid (BBA)			
1.0	 2,3,5-trifluoroBBA	0.10	0.43	232
1.0	 2,3,4,5-tetrafluoroBBA	0.12	0.70	175
1.0	 3,5-bis(trifluoromethyl)BBA	0.05	0.46	117
1.0	 3,4,5-trifluoroBBA	0.08	0.85	100
0.60	 2,4,6-trifluoroBBA	0.06	30	2
0.60	 2,3,4,6-tetrafluoroBBA	0.005	4	12
0.75	 BBA	0.0067	34	0.19

As can be seen from the Table VIII the most effective catalyst is 2,3,5-trifluoroBBA ( $k_{\text{cat}}/K_M$  232  $\text{M}^{-1}\text{sec}^{-1}$ ), followed by 2,3,4,5-tetrafluoroBBA ( $k_{\text{cat}}/K_M$  175  $\text{M}^{-1}\text{sec}^{-1}$ ), 3,5-bis(trifluoromethyl)BBA ( $k_{\text{cat}}/K_M$  117  $\text{M}^{-1}\text{sec}^{-1}$ ) and 3,4,5-trifluoroBBA ( $k_{\text{cat}}/K_M$  100  $\text{M}^{-1}\text{sec}^{-1}$ ). They are about 1200, 900, 600, 500 fold higher in the catalytic efficiency,  $k_{\text{cat}}/K_M$  respectively compared to the unsubstituted BBA. The first two fluoroBBAs are characterized by the presence of one single fluoro group in *ortho*- position with respect to the boron. The compounds which have two fluoro groups substituted in *ortho*- position with respect to the boron are having hundred fold less catalytic efficiency (see Table VIII), 2,4,6-trifluoroBBA ( $k_{\text{cat}}/K_M$  2  $\text{M}^{-1}\text{sec}^{-1}$ ) and 2,3,4,6-tetrafluoroBBA ( $k_{\text{cat}}/K_M$  12  $\text{M}^{-1}\text{sec}^{-1}$ ). The lost in the catalytic efficiency for the compounds 2,4,6-trifluoroBBA and 2,3,4,6-tetrafluoroBBA may be due to the steric hindrance generated by two fluoro groups in *ortho*-position to the boron atom. This steric hindrance could affect the orientation of the boronic acid hydroxy groups with respect to the plane of the Schiff base bond of the imine, and thus may affect in turn the rate of its hydrolysis. The substituent groups on 3,5-bistrifluoromethylBBA and 3,4,5-trifluoroBBA are in *meta* and *para* position and they are prompt to pose less steric hindrances. Discussed next are some selective pair comparisons between some fluoro-substituted BBA, highlighting the effect of the number and of the position of the fluoro substituents on the  $K_M$  and  $k_{\text{cat}}$ , and how those are in turn relates to the final effect observed on the catalytic efficiency ( $k_{\text{cat}}/K_M$ ).

**Comparison of 2,3,5-trifluoroBBA and 2,3,4,5-tetrafluoroBBA (additional *para* group difference):** This pair poses a difference of an additional *para*-position fluoro group. The steric interaction imposed by this presence of the fourth fluorine atom at C4 position in the benzene ring of 2,3,4,5-tetrafluoroBBA could explain the decrease in the relative binding affinity to the tested salicylidene-3-hydroxyaniline substrate.  $K_M$  for 2,3,4,5-tetrafluoroBBA is 0.70 mM as compared with 0.43 mM, the  $K_M$  for 2,3,5-trifluoroBBA. This almost two fold change in the  $K_M$  is the main factor responsible for the decrease in the catalytic efficiency, since there is no effect on the  $k_{\text{cat}}$  ( $k_{\text{cat}}/K_M$  is 175  $\text{M}^{-1}\text{sec}^{-1}$  for 2,3,4,5-tetrafluoroBBA and 232  $\text{M}^{-1}\text{sec}^{-1}$  for 2,3,5-trifluoroBBA and 0.10  $\text{sec}^{-1}$  and 0.12  $\text{sec}^{-1}$   $k_{\text{cat}}$  values respectively) (see Table VIII). However, better and reproducible data was obtained for the 2,3,4,5-tetrafluoroBBA throughout this project which was not the case with 2,3,5-trifluoroBBA.

**Comparison of 3,4,5-trifluoroBBA and 2,3,4,5-tetrafluoroBBA (additional *ortho* group difference):** This pair poses a difference of an additional *ortho*-position fluoro group. The steric hindrance imposed by this presence of the fourth fluorine atom at C2 position in the benzene ring of 2,3,4,5-tetrafluoroBBA could explain the increase in the relative binding affinity to the tested salicylidene-3-hydroxyaniline substrate. It is shown here that one additional *ortho* fluoro group improves the binding of the catalyst to the substrate.  $K_M$  for 2,3,4,5-tetrafluoroBBA is 0.70 mM as compared with 0.85 mM, the  $K_M$  for 3,4,5-trifluoroBBA. There is also an increase in the  $k_{cat}$  values, from 0.08  $\text{sec}^{-1}$  for 3,4,5-trifluoroBBA to 0.12  $\text{sec}^{-1}$  for the 2,3,4,5-tetrafluoroBBA. These improve in the binding constant and the increase in the catalytic constant are the factors responsible for 1.5 fold increase in the catalytic efficiency.  $k_{cat}/K_M$  is 175  $\text{M}^{-1}\text{sec}^{-1}$  for 2,3,4,5-tetrafluoroBBA (1/10, BBA:substrate ratio) and 100  $\text{M}^{-1}\text{sec}^{-1}$  for 3,4,5-trifluoroBBA (1/6, BBA:substrate ratio) (see Table VIII). BBA:substrate ratios that produced these results also depict that the 2,3,4,5-tetrafluoroBBA is overall a better catalyst than the 3,4,5-trifluoroBBA. In conclusion, an *ortho*-position fluoro group renders 2,3,4,5-tetrafluoroBBA as better catalyst than 3,4,5-trifluoroBBA for the hydrolysis of the salicylidene-3-hydroxyaniline.

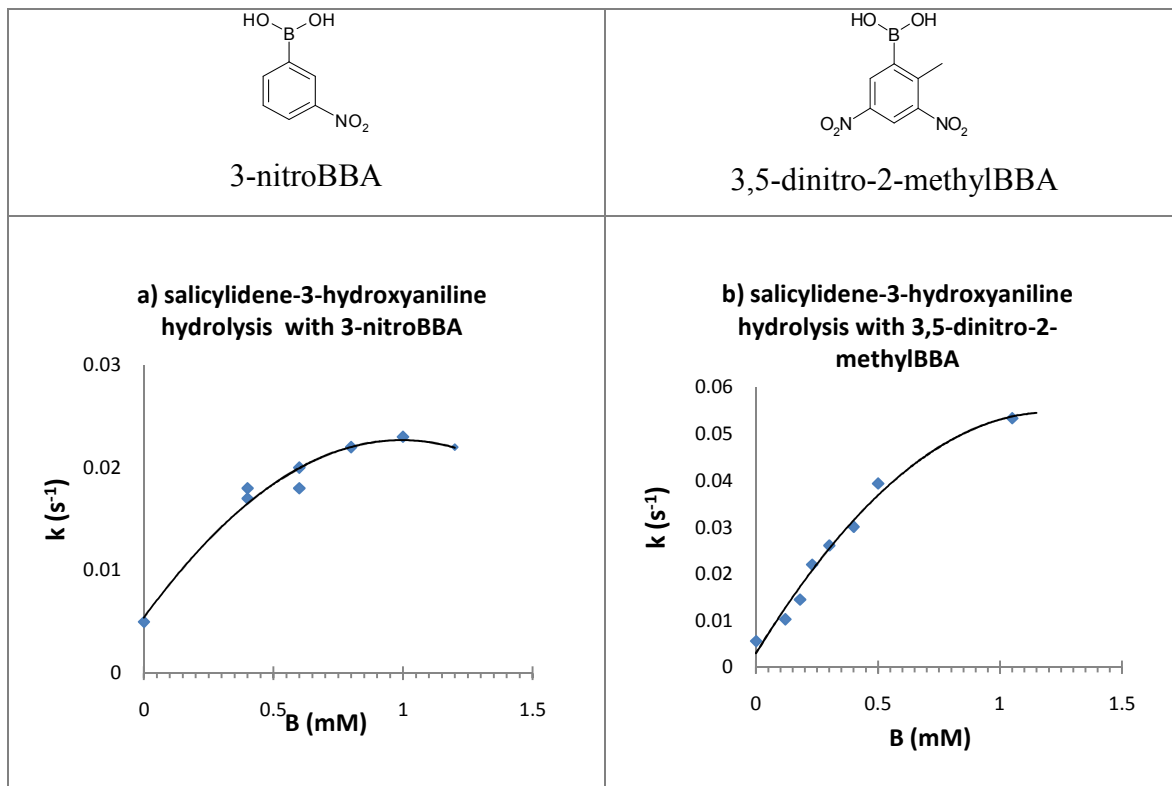
**Comparison of 2,3,5-trifluoroBBA with 3,5-bis(trifluoromethyl)BBA:** The benzenboronic acids and the imine concentration range are the same for both reactions. As can be seen from Table VIII, there are no significant differences in the relative binding affinity of BBA for the imine (the  $K_M$  for 2,3,5-trifluoroBBA and 3,5-bis(trifluoromethyl)BBA is 0.43 mM and 0.46 mM, respectively). However, there is a decrease in the  $k_{cat}$  values, from 0.1  $\text{sec}^{-1}$  for 2,3,5-trifluoroBBA to 0.05  $\text{sec}^{-1}$  for the 3,5-bis(trifluoromethyl)BBA. These changes in the  $k_{cat}$  support the view that fluoro-substitutions directly to the benzene ring are more effective than the fluorination at the alkyl side chain in the alkyl substituted BBA, in determining a higher turn-over number ( $k_{cat}$ ). The changes in the  $k_{cat}$  in this case are reflected in the two fold decrease in the  $k_{cat}/K_M$  (from 232  $\text{M}^{-1}\text{sec}^{-1}$  for 2,3,5-trifluoroBBA to 117  $\text{M}^{-1}\text{sec}^{-1}$  for 3,5-bis(trifluoromethyl)BBA).

**Comparison of 2,3,5-trifluoroBBA and 3,4,5-trifluoroBBA:** The presence of one fluoro substituent in the *ortho*-position with respect to the boron atom has some clear effects on the relative affinity ( $K_M$ ) of BBA for the imine substrate. In this case, even though the total number of fluoro substituents are the same in both compounds (i.e. three fluoro), there is no fluoro group in the *ortho*-position with respect to the boron in the case of 3,4,5-trifluoroBBA, and this could explain the two fold loss in the relative affinity for imine (0.85 mM  $K_M$  for 3,4,5-trifluoroBBA as compared with 0.43 mM  $K_M$  for 2,3,5-trifluoroBBA). Thus the changes in the  $K_M$  are reflected in the two fold lost in catalytic efficiency ( $k_{cat}/K_M$ ) ( $100 \text{ M}^{-1}\text{sec}^{-1}$  for 3,4,5-trifluoroBBA as compared with  $232 \text{ M}^{-1}\text{sec}^{-1}$  for 2,3,5-trifluoroBBA).

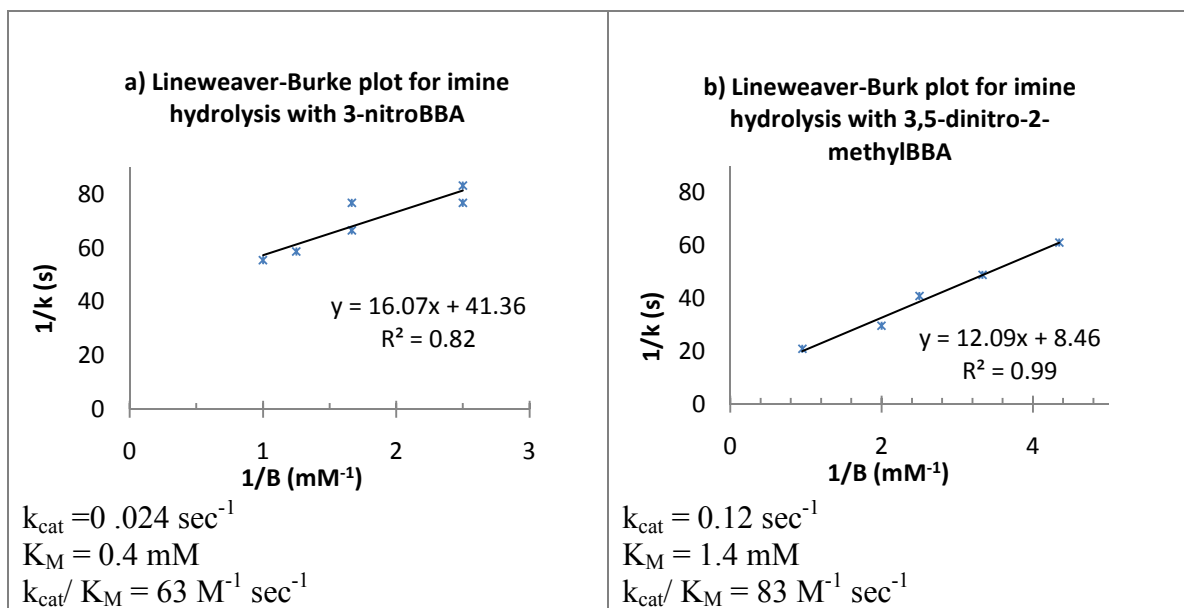
All the results presented in Table VIII proved that the fluoro-substituted benzene BA are more efficient in the hydrolysis of the imine in comparison with the unsubstituted benzene BA, except for the catalysts with two fluoro substituted in *ortho* position with respect to the boron which induced big steric hindrance effect discussed above.

### **3.2.2. The nitro substituted benzenboronic acids have higher catalytic efficiency of imine hydrolysis than the un-substituted boronic acid**

Nitro groups are also very well known electron withdrawing groups when substituted to the benzene ring. Especially, when the nitro group occupies the *meta* position, its electron withdrawing effect is enhanced. In order to gain insight into the mechanism of imine hydrolysis by nitro-substituted BBA, the focus was on two main compounds: the 3-nitro-BBA (one nitro group in *meta* position with respect to the boron) and the 3,5-dinitro-2-methylBBA (two nitro groups in *meta* position with respect to the boron). All reactions were performed at pH 6.0, as described also for many other assays.



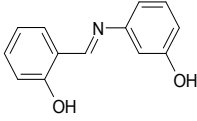
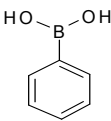
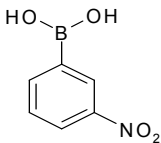
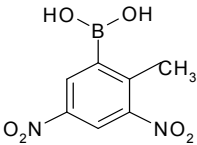
**Figure 22:**  $k$  (first order rate constant) vs.  $B$  (boronic acid concentration) plots for the hydrolysis of salicylidene-3-hydroxyaniline with different concentration of a) 3-nitroBBA and b) 3,5-dinitro-2-methylBBA at 0.1 M pH 6.0 phosphate buffer.



**Figure 23:** Lineweaver-Burk plots for the hydrolysis of salicylidene-3-hydroxyaniline with different concentration of a) 3-nitroBBA and b) 3,5-dinitro-2-methylBBA at 0.1 M pH 6.0 phosphate buffer.

As the Table IX and Figures 22, 23 show, both mono- and di-nitro substituted BBA are more efficient in hydrolyzing the imine than the unsubstituted BBA. Specifically, there is a 15 fold increase in the  $k_{\text{cat}}$  for 3-nitroBBA (at stoichiometric ratio with the imine) than for BBA(at stoichiometric ratio), while 3,5-dinitro-2-methylBBA (at substoichiometric ratios with the imine) catalyst had a 18 fold increase in the  $k_{\text{cat}}$  ( $0.12 \text{ sec}^{-1}$  for 3,5-dinitro-2-methylBBA as compared to  $0.0067 \text{ sec}^{-1}$  for BBA). This dramatic increase in the  $k_{\text{cat}}$  is also reflected in the proportional increase in the catalytic efficiency, from  $0.19 \text{ M}^{-1} \text{ sec}^{-1}$  for the unsubstituted BBA to  $52 \text{ M}^{-1} \text{ sec}^{-1}$  and  $83 \text{ M}^{-1} \text{ sec}^{-1}$  for mono- and di-nitro substituted BBA, respectively (almost 290 and 437 fold increase, respectively). In order to confirm that the sub-stoichiometric ratios of BBA/imine are the most effective in catalyzing the hydrolysis with the highest rate, I used different BBA/imine concentration ratios, as can be seen from Table IX. In most cases, the lower the amount of BBA used, the better the catalytic efficiency (as expressed in  $k_{\text{cat}}/K_M$  ratios). For comparison, analyze the  $k_{\text{cat}}/K_M$  for 3-nitroBBA at two different BBA/imine ratios:  $58 \text{ M}^{-1} \text{ sec}^{-1}$  for ratios spanning 1:1 to 5:1 BBA/imine and  $71 \text{ M}^{-1} \text{ sec}^{-1}$  for ratios spanning 1:3 to 1:1 BBA/imine concentration range. Here  $k_{\text{cat}}$  goes down about four times but  $K_M$  gets better. However, when the 3-nitroBBA and 3,5-dinitro-2-methylBBA is compared at similar ratios it can be seen that  $k_{\text{cat}}$  increases for 3,5-dinitro-2-methylBBA but  $K_M$  is not better. However,  $k_{\text{cat}}/K_M$  shows a little bit better. The fact that the binding constant  $K_M$  is not as good as with 3-nitroBBA can be explained with the methyl group at the *ortho* position for the 3,5-dinitro-2-methylBBA which could have posed some steric hindrance as well as the methyl is an electron donating group.

**Table IX:** Catalytic constants for the hydrolysis of salicylidene-3-hydroxyaniline by BBA and two different nitro substituted BBA illustrated at comparable molar ratios

 salicylidene-3-hydroxyaniline imine			$k_{\text{cat}}$ ( $\text{sec}^{-1}$ )	$K_M$ (mM)	$k_{\text{cat}} / K_M$ ( $\text{M}^{-1} \text{sec}^{-1}$ )
Imine (mM)	Boronic acid	Boronic acid concentration range (mM)			
0.75	 BBA	0.75 to 12.0	0.0067	34	0.19
1.0	 3-nitroBBA	1.0 to 4.0	0.10	2.0	52
1.2	3-nitroBBA	0.4 to 1.2	0.024	0.4	63
1.0	 3,5-dinitro-2-methylBBA	0.3 to 1.0	0.12	1.4	83

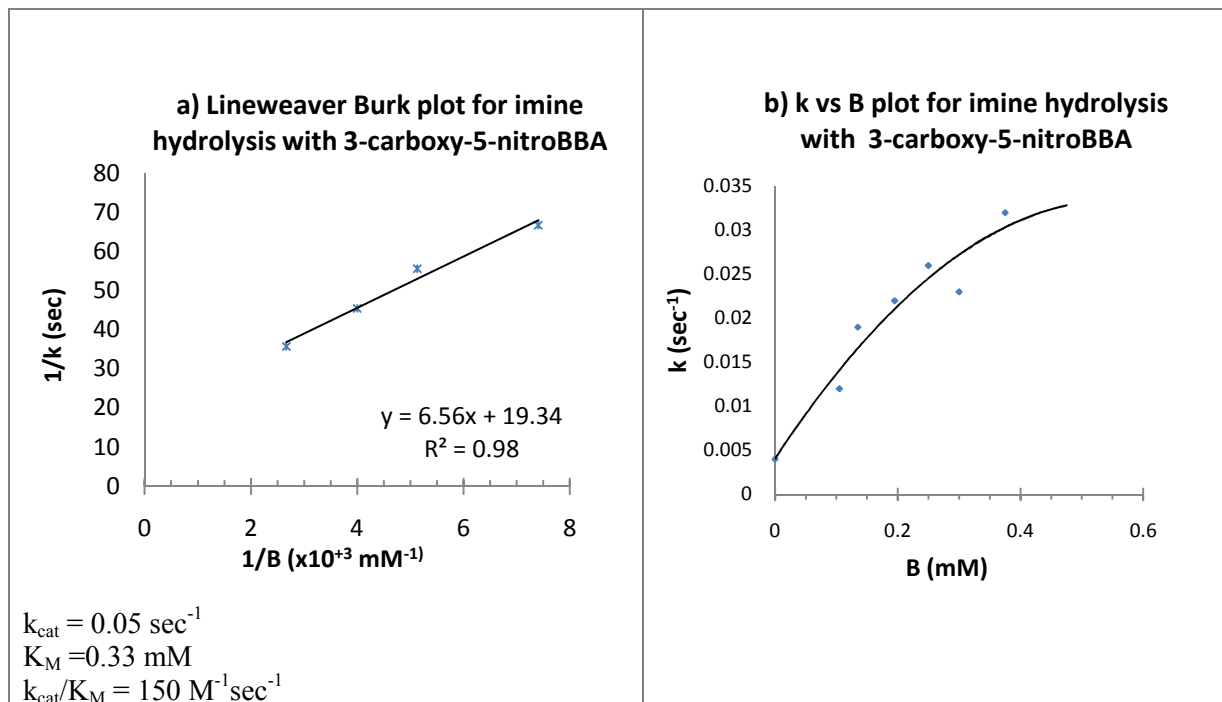
### 3.2.3. Benzeneboronic acids with mixed substitution have higher catalytic efficiency on imine hydrolysis than the unsubstituted benzeneboronic acid

Different kinds of functional groups substituted to the benzene ring of BBA other than fluoro and nitro were also explored. Among them were the amino, carboxy, amino-carboxy, nitro-carboxy, and chlorine-fluorine combinations. A common structural feature of all these compounds is the placement of all these substituents in the *meta* position with respect to the boron atom. The preference for the *meta* position and not *ortho*, was primarily determined by the previous results obtained with the fluoro-substituents (see Table VIII) where it is shown that an *ortho* substituents could exert a steric hindrance effect upon the boron, and thus could result in a dramatic lost in the catalytic efficiency (see Section 3.2.1). The results for all these combinations of substituents are presented in Table IX and in Figures 24, 25.

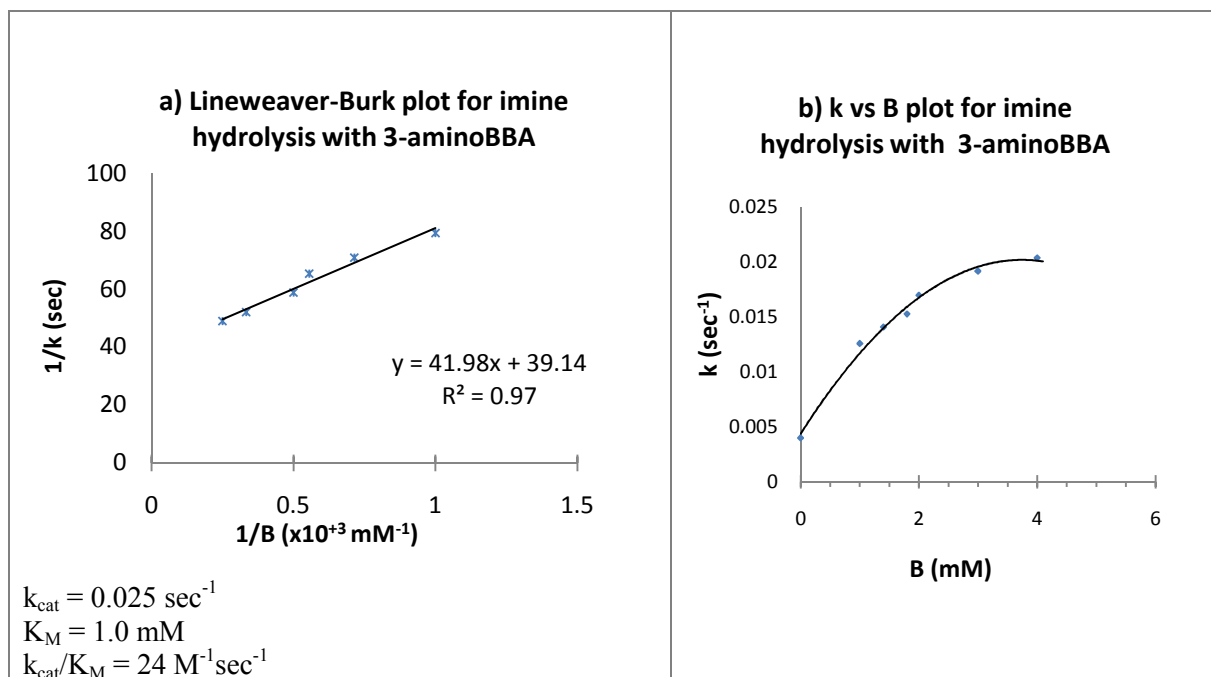
The assays were run at 1.0 mM imine while the concentration range for some of the substituted BBA were as follows: 0.40 mM up to 1.60 mM for 3-aminoBBA, i.e. at substoichiometric (one fifth from the imine concentration) or stoichiometric ratio (1:1, 3-aminoBBA : imine) (see Table X). The same concentration range was tested for the 3-amino-5-carboxyBBA compound. The concentration range for 3-carboxy-5-nitroBBA was 0.14 mM to 0.38mM which corresponds to one seventh of that of imine, up to 1:1 ratio of 3-carboxy-5-nitroBBA : imine, respectively. The 3-chloro-4-fluoroBBA concentration range was 1.0 mM to 5.0 mM, which corresponds to the 1:1 up to 5:1 of the 3-chloro-4-fluoroBBA : imine ratios. In this particular case, i.e. of 3-chloro-4-fluoroBBA, substoichiometric amounts of BBA with respect to the imine were not efficient to induce any hydrolysis reactions.

As a general observation, the most efficient catalysts were those which had substoichiometric ratios with imine. Thus, the SAR of all these different substituents highlights the new structural requirements for the benzene substitutions for achieving the highest catalytic efficiencies.

With 3-amino-5-carboxyBBA and 3-aminoBBA both stoichiometric and substoichiometric ratios were tried. 3-chloro-4-fluoroBBA was tried only at stoichiometric ratios. 3-carboxyBBA was the one also tried at substoichiometric ratios. And 3-carboxy-5-nitroBBA in this case was the best one. Note that 3,5-dicarboxyBBA could not be dissolved in the solvent.

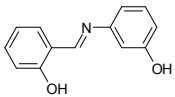
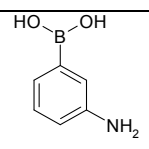
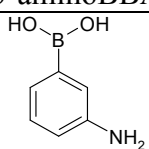
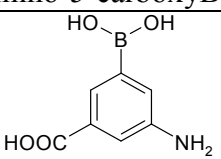
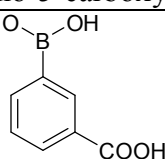
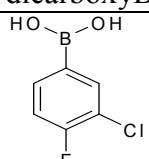
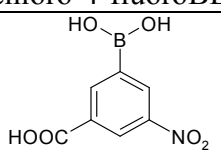


**Figure 24:** a) Lineweaver-Burk plot and b)  $k$  (first order rate constant) vs.  $B$  (boronic acid concentration) for the hydrolysis of salicylidene-3-hydroxyaniline with different concentrations of 3-carboxy-5-nitro-benzeneBBA at 0.1 M pH 6.0 phosphate buffer.



**Figure 25:** a) Lineweaver-Burk plot and b)  $k$  (first order rate constant) vs.  $B$  (boronic acid concentration) for the hydrolysis of salicylidene-3-hydroxyaniline with different concentration of 3-aminoBBA at 0.1 M pH 6.0 phosphate buffer.

**Table X:** Catalytic constants for the hydrolysis of salicylidene-3-hydroxyaniline by BBA with different substitution

 salicylidene-3-hydroxyaniline imine		$k_{cat}$ ( $\text{sec}^{-1}$ )	$K_M$ (mM)	$k_{cat}/K_M$ ( $\text{M}^{-1} \text{sec}^{-1}$ )	
Imine (mM)	Boronic acid concentration range (mM)				
1.0	 3-aminoBBA	1.0 to 4.0	0.025	1.0	24
1.0	 3-aminoBBA	0.40 to 1.60	0.033	2.8	11
1.0	3-amino-5-carboxyBBA	1.0 to 5.0	0.15	15	10
1.0	 3-amino-5-carboxyBBA	0.40 to 1.0	0.013	0.46	27
1.0	 3-carboxyBBA	0.5 to 1.0	0.0042	0.60	7
N/A*	3,5-dicarboxyBBA	N/A*	N/A*	N/A*	N/A*
1.0	 3-chloro-4-fluoroBBA	1.0 to 5.0	0.003	1.2	2.5
1.0	 3-carboxy-5-nitroBBA	0.14 to 0.38	0.05	0.33	151

\*it was not possible to dissolve in pH 6.0 buffer.

As can be seen from the Table X the combination of carboxy-nitro substituents in *meta* position with respect to the boron atom are giving the best results for  $k_{\text{cat}}$  and  $K_M$  ( $0.05 \text{ sec}^{-1}$  and  $0.33 \text{ mM}$ , respectively). This was in turn reflected in the achievement of the best catalytic efficiency, of  $151 \text{ M}^{-1}\text{sec}^{-1}$ . The other combinations of functional groups, such as amino (one group in *meta* with respect to the boron), one amino and one carboxy where each one in *meta* position with respect to the boron, or the fluoro-chloro combination that is 3-chloro-4-fluoroBBA were less effective catalysts, having six to four fold lower catalytic efficiencies ( $24 \text{ M}^{-1}\text{sec}^{-1}$  for 3-aminoBBA at stoichiometric ratio of 1:1 3-aminoBBA : imine,  $38 \text{ M}^{-1}\text{sec}^{-1}$  for 3-aminoBBA at sub-stoichiometric 1:7, 3-aminoBBA : imine,  $27 \text{ M}^{-1}\text{sec}^{-1}$  for 3-amino-5-carboxyBBA and  $2.5 \text{ M}^{-1}\text{sec}^{-1}$  for 3-chloro-4-fluoroBBA).

Since the 2,3,5-trifluoro-BBA and 2,3,4,5-tetrafluoroBBA were the best catalysts for the hydrolysis of the imine salicylidene-3-hydroxyaniline, I decided to further investigate how other structural determinants of the imine substrates could modulate the overall catalytic efficiency. Thus, I further performed other SAR for the imine substrates.

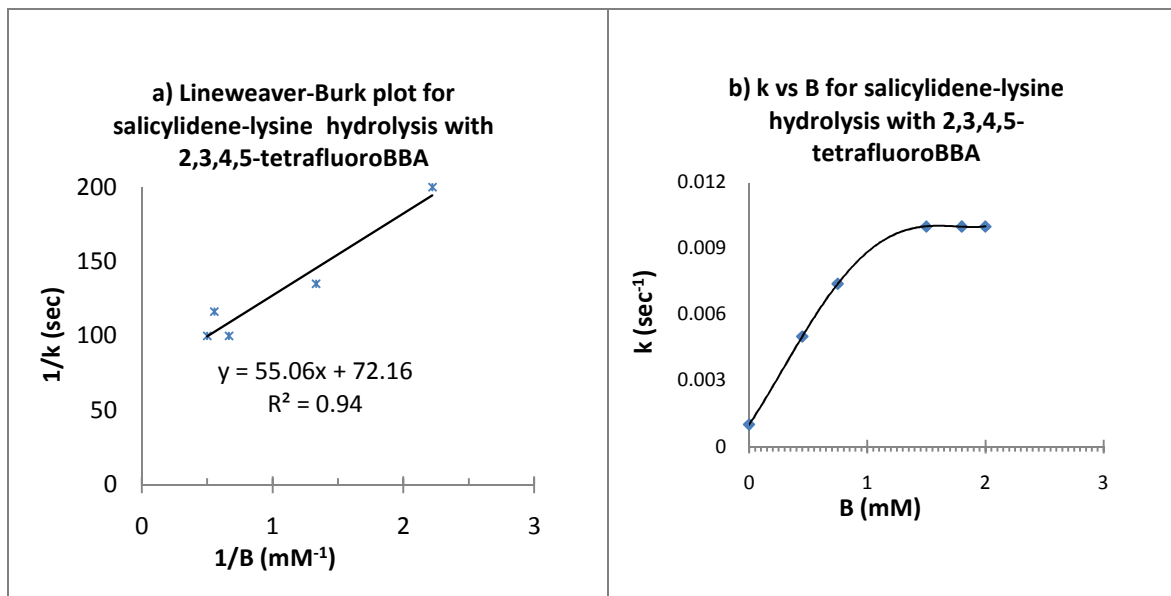
The next sections of this thesis present the SAR for the hydrolysis of different imine substrates.

### **3.3 Structure-activity relationship (SAR) of different imines substrates and their effect upon the benzenboronic acid catalytic efficiency**

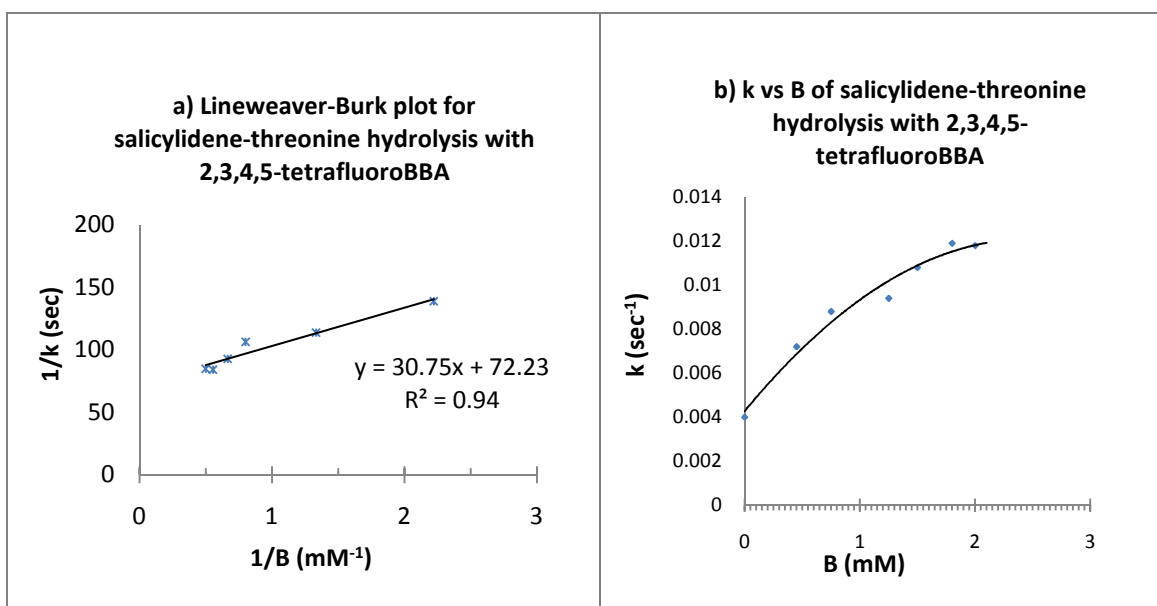
As it is determined that all the boronic acids follow a Michaelis-Menten type of kinetics with respect to the imine salicylidene-3-hydroxyaniline hydrolysis (see Sections 3.2.1 and 3.2.2), I also expanded the structural determinants of the imine substrates and further investigate the SAR of their hydrolysis. Previous studies, Rao et. al.<sup>69</sup> focused only on salicylidene-L-isoleucine imine. I developed a library of new imine substrates where other amino-acids, such as isoleucine, leucine, valine, lysine, alanyl-valine, phenylglycine, threonine etc. were used to react with salicylidene to generate the new imines, and the hydrolysis of these new substrates were investigated using 2,3,5-trifluoroBBA and 2,3,4,5-tetrafluoroBBA as catalysts.

### 3.3.1. SAR of different amino acids based imines substrates and their effect upon the benzenboronic acid catalytic efficiency

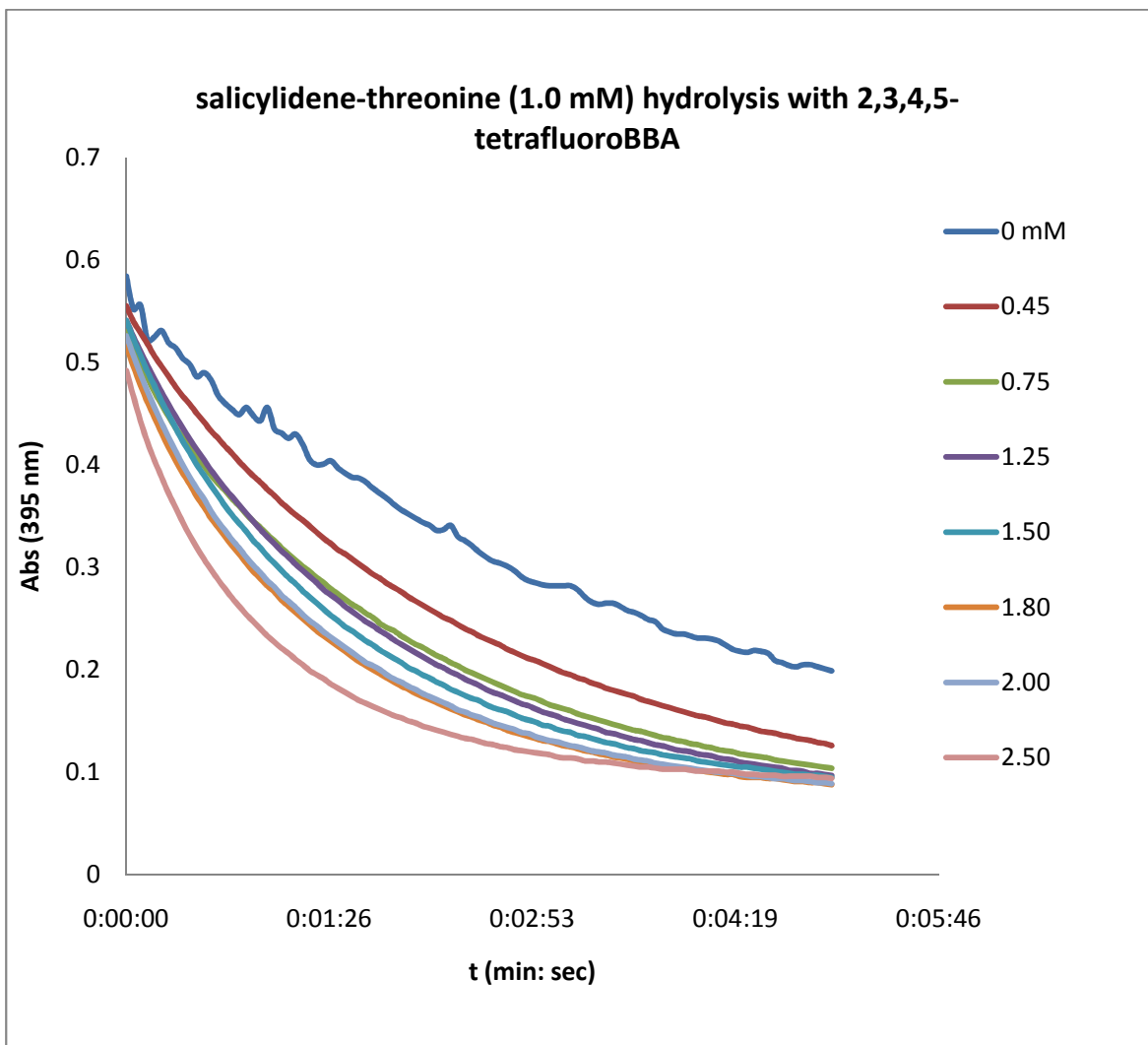
The SAR of different amino-acids based imine substrates was performed at 1:1 stoichiometric ratios of imine: 2,3,4,5-tetrafluoroBBA, in most cases. Since 2,3,4,5-tetrafluoroBBA is one of the best catalyst and produced a reproducible data, I present the results of hydrolysis of the amino acid based imines with 2,3,4,5-tetrafluoroBBA (see Table XI and Figures 26, 27 for representative kinetics runs). As can be seen from Table XI, all the aliphatic amino acids, such as valine, alanyl-valine, isoleucine, generated with salicylaldehyde imines which were not efficiently hydrolyzed by 2,3,4,5-tetrafluoroBBA as compared with the imines substrates derived from the hydroxyl-based amino acids (such as threonine and 3-hydroxy-phenylglycine) (e.g.  $k_{cat}/K_M$  is  $2\text{ M}^{-1}\text{sec}^{-1}$  for isoleucine based imine while the same catalytic efficiency is increase to  $33\text{ M}^{-1}\text{sec}^{-1}$  and  $27\text{ M}^{-1}\text{sec}^{-1}$  for threonine and 3-hydroxy-phenylglycine, respectively); the basic amino acid lysine based imine had a higher  $k_{cat}/K_M$  value (of  $17\text{ M}^{-1}\text{sec}^{-1}$ ) as compared with other alkyl-based amino-acid imines, but still lower than the catalytic efficiency obtained with the hydroxyl-based amino-acids imine. Altogether, these results suggest that the presence of hydrogen bonding donors or acceptors (hydroxy or amino groups) in the imine substrates activate the catalytic turn-over ( $k_{cat}$ ) of the benzenboronic acid catalyst (in this case, 2,3,4,5-tetrafluoroBBA), and thus increases its catalytic efficiency ( $k_{cat}/K_M$ ) as it is for an enzyme. A mechanistic explanation is yet not known for this effect, but most probably the assistance of the 2,3,4,5-tetrafluoroBBA catalyst in stabilizing the transition state by the hydrogen bonding network provided by these hydroxyl or amino groups in the substrates during the hydrolysis, could explain the five to sixteen fold increase in the  $k_{cat}/K_M$  values observed for these hydroxyl/amino based substrates.



**Figure 26:** a) Lineweaver-Burk plot and b)  $k$  (first order rate constant) vs.  $B$  (boronic acid concentration) for the hydrolysis of salicylidene-lysine with different concentration of 2,3,4,5-tetrafluoroBBA at 0.1 M pH 6.0 phosphate buffer.

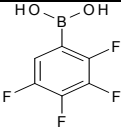
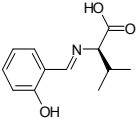
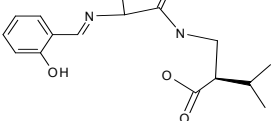
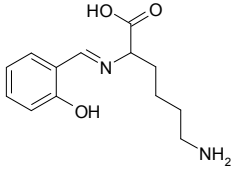
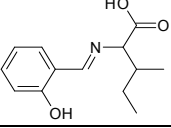
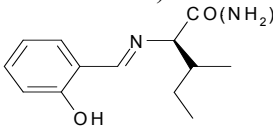
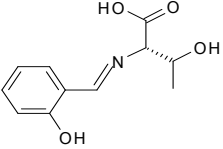
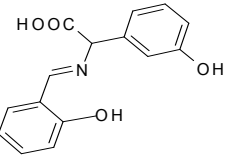


**Figure 27:** a) Lineweaver-Burk plot and b)  $k$  (first order rate constant) vs.  $B$  (boronic acid concentration) for the hydrolysis of salicylidene-threonine with different concentrations of 2,3,4,5-tetrafluoroBBA at 0.1 M pH 6.0 phosphate buffer.



**Figure 28:** Hydrolysis of salicylidene-threonine with different concentration of 2,3,4,5-tetrafluoroBBA at 0.1 M pH 6.0 phosphate buffer.

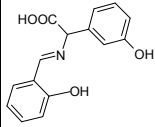
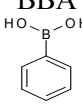
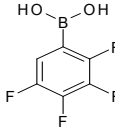
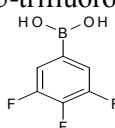
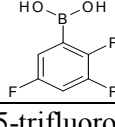
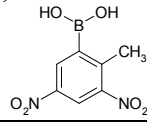
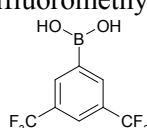
**Table XI:** 2,3,4,5-tetrafluoroBBA effect on the catalytic constants for the hydrolysis of different salicylidene-aminoacid imines (with different amino acids as the name depicts)

Imine (concentration)	 Boronic acid concentration range (mM)	$k_{\text{cat}}$ ( $\text{sec}^{-1}$ )	$K_M$ (mM)	$k_{\text{cat}} / K_M$ ( $\text{M}^{-1}\text{sec}^{-1}$ )
salicylidene-valine (0.5 mM) 	0.5 to 5.0	0.005	0.60	8
salicylidene-alanyl-valine (1.0 mM) 	1.0 to 5.0	0.02	1.6	11
salicylidene-lysine (0.5 mM) 	0.45 to 2.0	0.014	0.84	17
salicylidene-L-Isoleucine (0.60 mM) 	0.72 to 12.0	0.006	2.7	2
salicylidene-isoleucinamide (0.60 mM) 	0.60 to 12.0	0.01	8.4	1.2
salicylidene-threonine (0.5 mM) 	0.45 to 2.0	0.014	0.42	33
salicylidene-3-hydroxyphenylglycine (0.60 mM) 	0.625 to 3.75	0.044	1.6	27

### 3.3.2. The effect of *meta*-hydroxy-phenylglycine on the benzenboronic acids catalytic efficiency

Since the hydrolysis of one of the amino-acid based imine, i.e. salicylidene-3-hydroxyphenylglycine, was giving reproducible catalytic efficiencies in the presence of both 2,3,5-trifluoroBBA and 2,3,4,5-tetrafluoroBBA, I decided to test the efficiency of this substrate imine in the presence of other BBAs (Table XII). The SAR performed for this imine substrate with different BBAs is showing the importance of the fluoro and nitro substituents in enhancing the catalytic efficiency of the imine hydrolysis. The other important BBAs which gave  $k_{cat}/K_M$  values above  $20\text{ M}^{-1}\text{sec}^{-1}$ , are 3,4,5-trifluoroBBA ( $29\text{ M}^{-1}\text{sec}^{-1}$ ), 3,5-bis(trifluoromethyl)BBA ( $24\text{ M}^{-1}\text{sec}^{-1}$ ). 2,3,5-trifluoroBBA surprisingly does not produce any competitive data. In final analysis it can be said that carboxyl group on the amine part of the imine did not produce any effective H-bond interaction in the complex formation. Both substoichiometric and stoichiometric were tested for this part of the analysis.

**Table XII:** Catalytic constants of different BBA on the hydrolysis of salicylidene-3-hydroxyphenylglycine imine illustrated at stoichiometric molar ratios at 0.1 M pH 6.0 phosphate buffer

 salicylidene-3-hydroxyphenylglycine imine			$k_{cat}$ ( $\text{sec}^{-1}$ )	$K_M$ (mM)	$k_{cat} / K_M$ ( $\text{M}^{-1} \text{sec}^{-1}$ )
Imine (mM)	Benzenboronic acid	Boronic acid concentration range (mM)			
0.75	BBA 	0.78 to 6.25	0.007	1.4	5
0.60	2,3,4,5-tetrafluoroBBA 	0.62 to 3.7	0.044	1.6	27
0.80	2,3,4,5-tetrafluoroBBA	0.27 to 0.75	0.007	0.3	26
0.73	3,4,5-trifluoroBBA 	0.73 to 3.6	0.03	1.0	29
0.80	3,4,5-trifluoroBBA	0.31 to 0.8	0.007	0.34	20
0.60	2,3,5-trifluoroBBA 	0.62 to 3.7	0.055	5.0	11
0.80	2,3,5-trifluoroBBA	0.48 to 0.9	0.038	3.8	10
0.75	2,4,6-trifluoroBBA	0.78 to 4.25	0.004	7.0	6.5
0.87	3,5-dinitroBBA 	0.9 to 2.4	0.05	1.6	29
0.80	3,5-dinitroBBA	0.3 to 0.8	0.06	4.0	16
0.80	3,5-bis(trifluoromethyl)BBA 	1.0 to 5.0	0.027	1.1	24
0.80	3,5-bis(trifluoromethyl)BBA	0.15 to 0.8	0.028	1.4	20

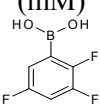
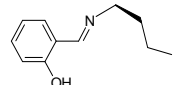
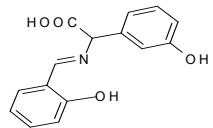
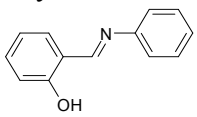
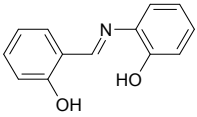
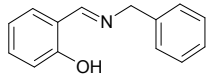
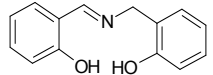
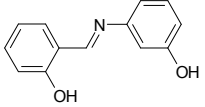
### 3.3.3. SAR of different primary organic amines based imine substrates and their effect upon the benzenboronic acids catalytic efficiency

Table XI shows that salicylidene-*meta*-hydroxyphenylglycine gave highest  $k_{cat}$  value (of  $0.044 \text{ sec}^{-1}$ ) and a very good  $k_{cat}/K_M$  ( $27 \text{ M}^{-1}\text{sec}^{-1}$ ), ranking the second highest in this group. This result led me to further investigate whether other aromatic amines would the same relative high efficiency in their catalysis by different boronic acids. Thus aromatic amines that I used were aniline and benzylamine. In addition of being an aromatic amine based imine, salicylidene-*meta*-hydroxyphenylglycine has a hydroxyl group at the *meta* position of the benzene ring. Therefore, I considered that it would be of valuable interest to perform the SAR of different hydroxyl-substituted aromatic amines, and thus, I synthesized salicylidene-aniline, salicylidene-2-hydroxyaniline, salicylidene-benzylamine, salicylidene-2-hydroxybenzylamine, salicylidene-3-hydroxyaniline. In order to better gain insight into the mechanism of hydrolysis of the aromatic-amine based imines I used as a reference for the amine part of the imine, an aliphatic amine, i.e. salicylidene-*n*-butyl, and I compared the  $k_{cat}$ ,  $K_M$ , and  $k_{cat}/K_M$  values obtained for all these imines substrates which are presented in the Tables XIII and XIV. These imine substrates were proved to be efficiently hydrolyzed by both 2,3,5-trifluoroBBA and 2,3,4,5-tetrafluoroBBA. Table XIII presents the catalytic constants for the imine hydrolysis by 2,3,5-trifluoroBBA while Table XIV shows the catalytic constants for the same imine hydrolysis by 2,3,4,5-tetrafluoroBBA.

A careful analysis of the results presented in Table XIII outlines the importance of the hydroxyl-substituted aromatic amine in augmenting the catalytic efficiency of the 2,3,5-trifluoroBBA, the best being the case of salicylidene-2-hydroxyaniline ( $55 \text{ M}^{-1}\text{sec}^{-1}$ ) and salicylidene-3-hydroxyaniline ( $40 \text{ M}^{-1}\text{sec}^{-1}$ ). Also, the data presented in the same table support the hydroxyl-aniline based imines as better substrates for 2,3,5-trifluoroBBA than the benzylamine-based imines. All benzylamine-imines are characterized by lower catalytic efficiencies of their hydrolysis by 2,3,5-trifluoroBBA than the anilines-imines ( $4 \text{ M}^{-1}\text{sec}^{-1}$  for the benzylamine-imine and  $24 \text{ M}^{-1}\text{sec}^{-1}$  for the 2-hydroxyl-benzylamine-imine). Altogether, the results provided by the Table XIII highlight the importance of the hydroxyl group substituted to the benzene ring in aniline or benzylamine based imines in determining a better catalytic

efficiency for their hydrolysis by the 2,3,5-trifluoroBBA. Also, n-butyl based imine has almost the same catalytic efficiency of hydrolysis as the previously tested *meta*-hydroxyphenylglycine substrate (11-12 M<sup>-1</sup>sec<sup>-1</sup>), lower than any of the hydroxyl-substituted aromatic amines, aniline or benzylamine-imines.

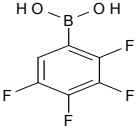
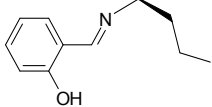
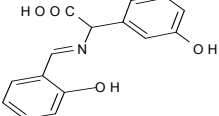
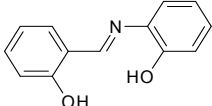
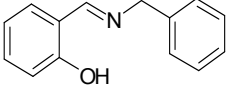
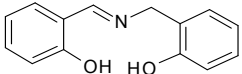
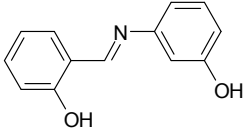
**Table XIII:** 2,3,5-trifluoroboronic acid effect on the catalytic constants for the hydrolyses of different imines between salicylidene and primary organic amines at 0.1 M pH 6.0 phosphate buffer

Imine (concentration)	Boronic acid concentration range (mM) 	$k_{cat}$ (sec <sup>-1</sup> )	$K_M$ (mM)	$k_{cat} / K_M$ (M <sup>-1</sup> sec <sup>-1</sup> )
salicylidene-n-butylamine (0.50 mM) 	1.0 to 6.0	0.07	5.7	12
salicylidene-3-hydroxyphenylglycine (0.60 mM) 	0.6 to 3.7	0.055	5.0	11
salicylidene-aniline 	N/A*	N/A*	N/A*	N/A*
salicylidene-2-hydroxyaniline (0.50 mM) 	0.1 to 0.4	0.01	0.19	55
salicylidene-benzylamine (0.50 mM) 	0.7 to 5.0	0.156	34	4
salicylidene-2-hydroxybenzylamine (0.50 mM) 	0.50 to 5.0	0.18	0.78	24
salicylidene-3-hydroxyaniline (0.60 mM) 	0.60 to 1.8	0.20	5.0	40
salicylidene-3-hydroxyaniline (1.0 mM)	0.20 to 1.0	0.14	0.87	166
salicylidene-3-hydroxyaniline (1.0 mM)	0.10 to 1.0	0.10	0.43	232

\*insoluble state in buffer pH 6.0 made the hydrolysis run impossible.

Since the 2,3,4,5-tetrafluoroBBA ranked as the second next best BBA in catalyzing the salicylidene-3-hydroxyaniline, I performed the same type of SAR for different imine substrates as I did with 2,3,5-trifluoroBBA. The data for the hydrolysis of different imines having alkyl or aromatic and hydroxyl substituted aromatic structural units are presented in the Table XIV. Comparing these data with those presented in the Table XIII, it can be noted that it had the same trend in the efficiency of the imines hydrolysis by the 2,3,4,5-tetrafluoroBBA. Specifically, the hydroxyl-substituted aromatic amine are powerful activators on the catalytic efficiency of 2,3,4,5-tetrafluoroBBA, the best being the case of salicylidene-2-hydroxy aniline ( $55 \text{ M}^{-1}\text{sec}^{-1}$ ) and salicylidene-3-hyaniline ( $67 \text{ M}^{-1}\text{sec}^{-1}$ ). Also, the data presented in the same tables support the hydroxyl-aniline based imines as better substrates for 2,3,4,5-tetrafluoroBBA than the benzylamine-based imines, having the same type of reactivity observed with 2,3,5-trifluoroBBA. All benzylamine-imines are characterized by lower catalytic efficiencies of their hydrolysis by 2,3,4,5-tetrafluoroBBA than the anilines-imines (so far no reactivity for the benzylamine-imine and  $18 \text{ M}^{-1}\text{sec}^{-1}$  for the 2-hydroxyl-benzylamine-imine). Altogether, the results provided by the Table XIV highlight the importance of the hydroxyl group substituted to the benzene ring in aniline or benzylamine based imines in determining a better catalytic efficiency for their hydrolysis by the 2,3,4,5-tetrafluoroBBA. Also, n-butylamine based imine has a lower catalytic efficiency of hydrolysis than the previously tested *meta*-hydroxy-phenylglycine substrate ( $11 \text{ M}^{-1}\text{sec}^{-1}$  as compared with  $27 \text{ M}^{-1}\text{sec}^{-1}$  for the *meta*-hydroxy-phenylglycine substrate), and a lower reactivity toward 2,3,4,5-tetrafluoroBBA than any of the hydroxyl-substituted aromatic amines, aniline or benzylamine-imines.

**Table XIV:** 2,3,4,5-tetrafluoroBBA effect on the catalytic constants for the hydrolysis of different imines between salicylaldehyde and primary organic amines at 0.1 M pH 6.0 phosphate buffer

Imine (concentration)	Boronic acid concentration range (mM) 	$k_{cat}$ ( $\text{sec}^{-1}$ )	$K_M$ (mM)	$k_{cat} / K_M$ ( $\text{M}^{-1} \text{sec}^{-1}$ )
salicylidene-n-butylamine (0.50 mM) 	0.45 to 2.0	0.25	22.5	11
salicylidene-3-hydroxyphenylglycine (0.50 mM) 	0.45 to 1.80	0.044	1.6	27
salicylidene-2-hydroxy aniline (0.50 mM) 	0.45 to 2.5 0.09 to 0.50	0.077 0.036	1.77 0.64	43 55
salicylidene-benzylamine 	N/A*	N/A*	N/A*	N/A*
salicylidene-2-hydroxybenzylamine (0.75 mM) 	0.67 to 2.25	0.15	8.0	18
salicylidene-3-hydroxyaniline (0.60 mM) 	0.54 to 1.44	0.24	3.6	67
salicylidene-3-hydroxyaniline (1.0 mM)	0.20 to 1.0	0.27	1.9	142

\*there is no detected hydrolysis

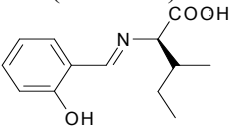
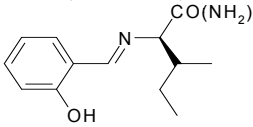
Other related aromatic imines were tested also with 2,3,4,5-tetrafluoroBBA and no reactivity was observed. It can be seen that other substituted aromatic imines, such as benzaldehyde derivatives, or methoxy substituted benzene, etc, were not efficient substrates for 2,3,4,5-tetrafluoroBBA. The following imines were tested: p-hydroxybenzaldehyde-n-butylamine, p-hydroxy benzaldehyde-3-hydroxyaniline, 2,2'-dihydroxybenzophenone-nbutylamine, o-methoxy benzaldehyde-3-hydroxyaniline, p-methoxybenzaldehyde-3-hydroxyaniline, salicylidene-2-aminohexanol.

#### **3.4.1. Effect of carboxyl group of imines on the catalytic efficiencies of benzeneboronic acids**

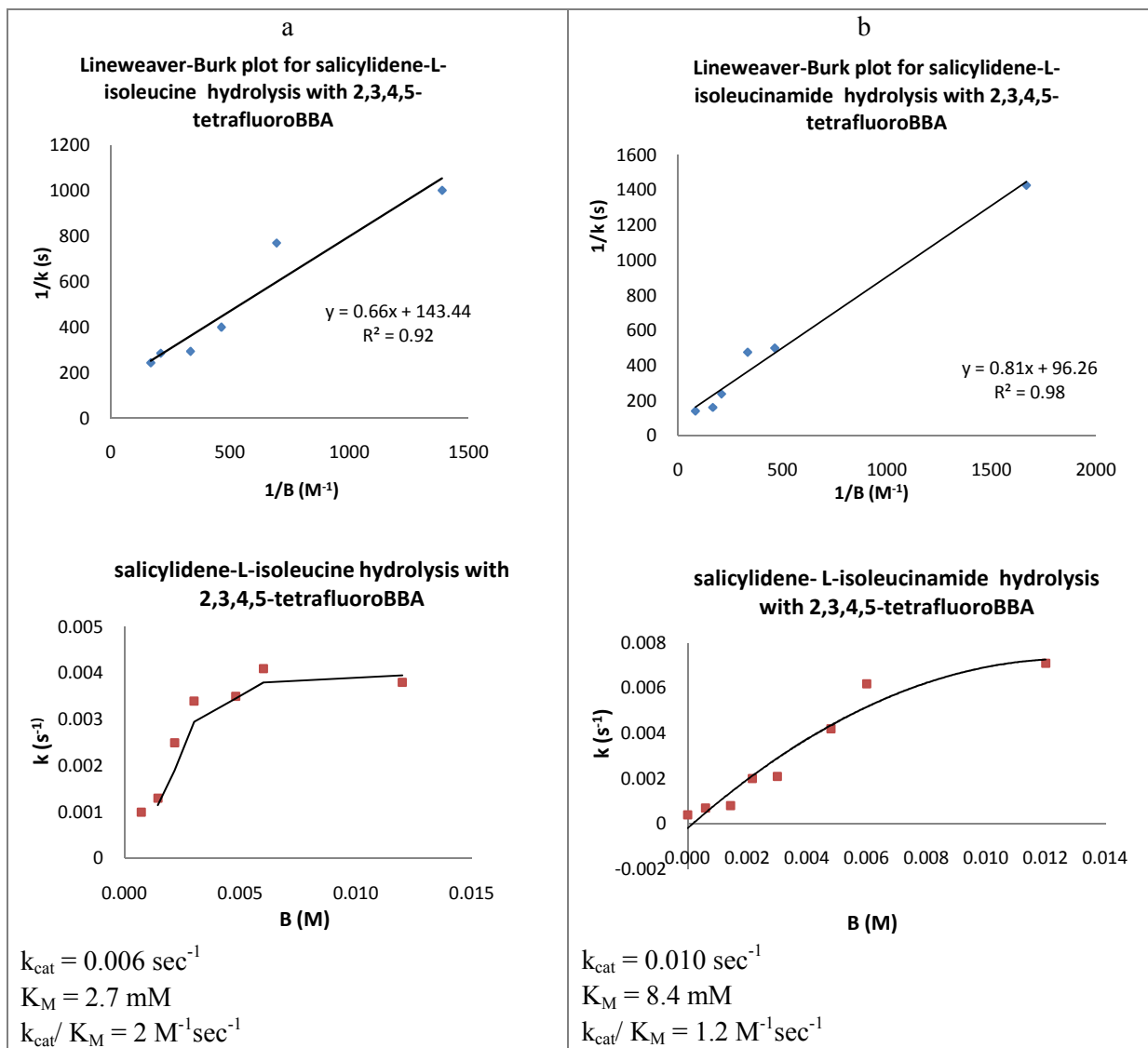
In order to explore the contribution of other chemical functional groups from the amine side of the imine, carboxyl and amide groups based imines were separately analyzed and their hydrolyses were performed in the presence of the best investigated BBAs, i.e. 2,3,5-trifluoroBBA and 2,3,4,5-tetrafluoroBBA. The first two imines investigated were salicylidene-L-isoleucine and salicylidene-L-isoleucinamide.

In all these experiments the imine concentration was maintained constant (0.6 mM), while the concentration of the 2,3,4,5-tetrafluoroBBA catalyst was varied so that stoichiometric ratios of imine:BBA were attained. Alternatively, the reactions were run with excess of 2,3,4,5-tetrafluoroBBA. Specifically, the 2,3,4,5-tetrafluoroBBA concentrations were 0.72 to 12.0 mM toward salicylidene-L-isoleucine substrate and 0.60 to 12.0 mM toward the salicylidene-L-isoleucinamide substrate (see Table XV). Figure 29 shows Lineweaver-Burk plot and the  $k$  vs.  $B$  plot of the above mentioned reaction.

**Table XV:** Catalytic constants for the 2,3,4,5-tetrafluoroBBA mediated hydrolysis of carboxyl and carboxylamide substituted imines stoichiometric molar ratios at 0.1 M pH 6.0 phosphate buffer

Imine (concentration)	2,3,4,5-tetrafluoroBBA concentration range (mM)	$k_{cat}$ (sec <sup>-1</sup> )	$K_M$ (mM)	$k_{cat}/K_M$ (M <sup>-1</sup> sec <sup>-1</sup> )
salicylidene-L-isooleucine (0.60 mM) 	0.72 to 12.0	0.006	2.7	2.0
salicylidene-L-isooleucinamide (0.60 mM) 	0.6. to 12.0	0.01	8.4	1.2

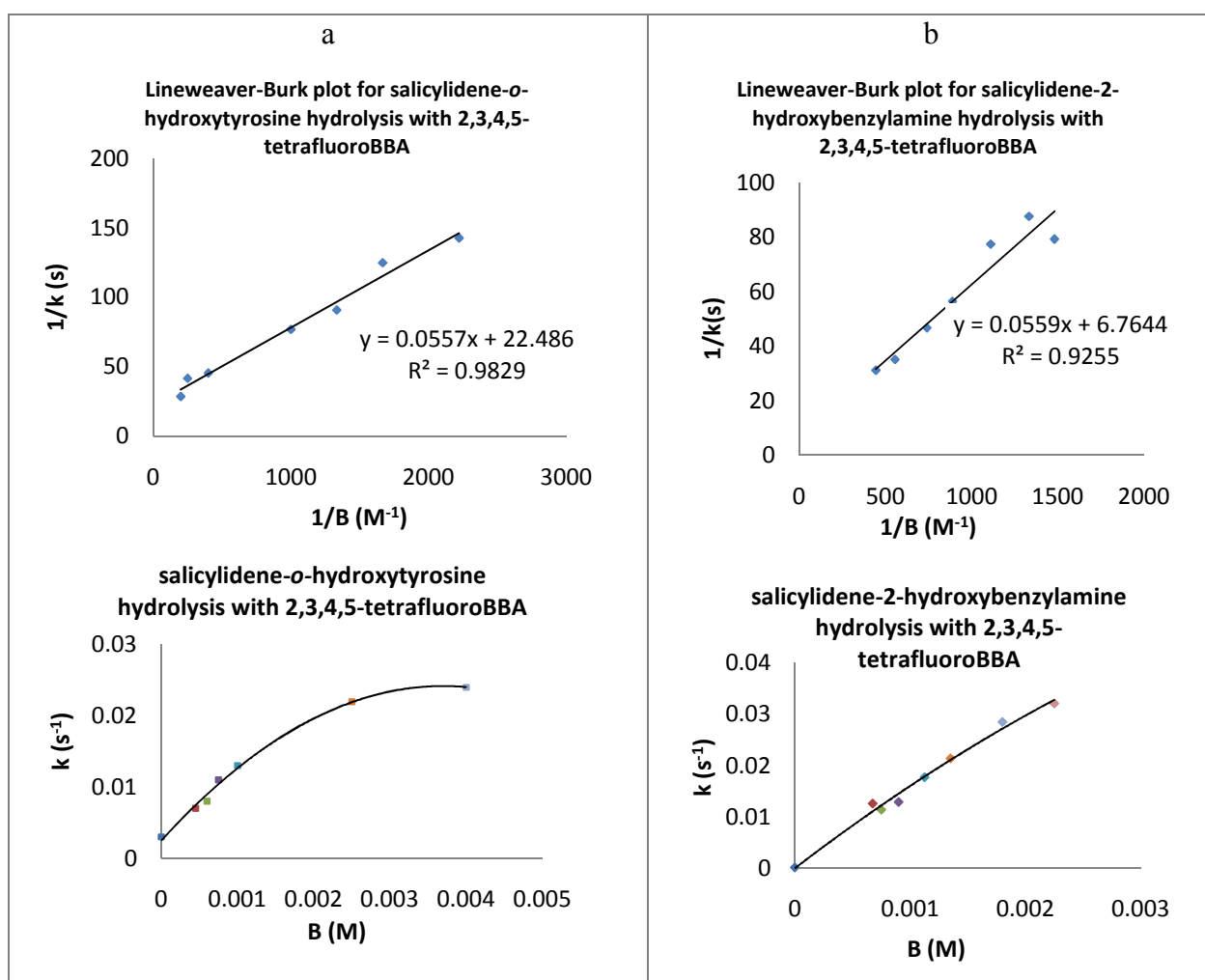
The results presented in Table XV demonstrate that salicylidene-isooleucine has a higher affinity for the 2,3,4,5-tetrafluoroBBA catalyst as compared with the salicylidene-isooleucinamide ( $K_M$  values were 2.7 mM for the salicylidene-isooleucine imine and 8.4 mM for the salicylidene-isooleucinamide). However, the later has a higher catalytic turn over ( $k_{cat}$ ) than the former one that is 0.01 sec<sup>-1</sup> for the salicylidene-isooleucinamide as compared to 0.006 sec<sup>-1</sup> for the salicylidene-L-isooleucine. These results suggest that the carboxyl group might help in binding of the imine to the 2,3,4,5-tetrafluoroBBA but may not be efficient in the activation of the hydrolysis rate. Altogether, none of the investigated carboxyl or amide based salicylidene imines were efficient substrates for 2,3,4,5-tetrafluoroBBA, as compared with all the aromatic and hydroxyl aromatic base imines presented in the previous Section 3.3.3. Thus, the catalytic efficiencies for the hydrolysis of these imines were as low as 2 M<sup>-1</sup>sec<sup>-1</sup>, dozen and hundreds of time less than other imine substrates tested in the previous sections.



**Figure 29:** Lineweaver-Burk and  $k$  (rate constant) vs.  $B$  (boronic acid concentration) plots for the hydrolysis of a) salicylidene-L-isoleucine b) salicylidene-L-isoleucinamide with different concentration of 2,3,4,5-tetrafluoroBBA at 0.1 M pH 6.0 phosphate buffer. Catalytic constants are included in Table XV.

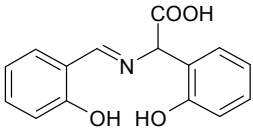
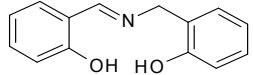
Another independent set of imines substrates carrying carboxyl groups were tested with both 2,3,5-trifluoroBBA and 2,3,4,5-tetrafluoroBBA. The imines were salicylidene-2-hydroxytyrosine and salicylidene-2-hydroxybenzylamine.

Table XVI and Table XVII present the results of these two imines hydrolysis by 2,3,4,5-tetrafluoroBBA and 2,3,5-trifluoroBBA. The imine salicylidene-*ortho*-hydroxytyrosine concentration was 0.50 mM while that of the 2,3,4,5-tetrafluoroBBA catalyst was varied again to obtain stoichiometric or excess of catalyst, i.e. 0.45mM to 5.0mM. The salicylidene-2-hydroxybenzylamine concentration was 0.75 mM while that of 2,3,4,5-tetrafluoroBBA catalyst was varied between 0.67 to 2.25 mM. Almost the same trend in the concentration range was tested for the 2,3,5-trifluoroBBA with the same set of imines (see Table XVII). Figure 30 shows hydrolyses run for the above mentioned reactions. Analysis of the results follows.

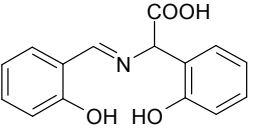
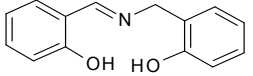


**Figure 30:** Lineweaver-Burk and  $k$  (rate constant) vs.  $B$  (boronic acid concentration) plots for the hydrolysis of (a) salicylidene-*o*-hydroxytyrosine (b) salicylidene-2-hydroxybenzylamine with different concentration of 2,3,4,5-tetrafluoroBBA at 0.1 M pH 6.0 phosphate buffer. Catalytic constants are included in Table XVI.

**Table XVI:** Catalytic constants for the 2,3,4,5-tetrafluoroBBA mediated hydrolysis of two related imines at stoichiometric molar ratio at 0.1 M pH 6.0 phosphate buffer

Imine (concentration)	Boronic acid concentration range (mM)	$k_{cat}$ (sec <sup>-1</sup> )	$K_M$ (mM)	$k_{cat}/K_M$ (M <sup>-1</sup> sec <sup>-1</sup> )
Salicylidene- <i>o</i> -hydroxytyrosine (0.50 mM) 	0.45 to 5.0	0.044	2.4	18
Salicylidene-2-hydroxybenzylamine (0.75 mM) 	0.67 to 2.25	0.150	8.1	18

**Table XVII:** Catalytic constants for the 2,3,5-trifluoroBBA mediated hydrolyses of two related imines at stoichiometric molar ratios at 0.1 M pH 6.0 phosphate buffer

Different Imines and 2,3,5-trifluoroBBA		$k_{cat}$ (sec <sup>-1</sup> )	$K_M$ (mM)	$k_{cat}/K_M$ (M <sup>-1</sup> sec <sup>-1</sup> )
Imine (concentration)	Boronic acid concentration range (mM)			
Salicylidene- <i>o</i> -hydroxytyrosine (0.5 mM) 	0.5 to 5.0	0.047	3.0	15
Salicylidene-2-hydroxybenzylamine (0.5 mM) 	0.5 to 5.0	0.185	7.8	24

The analysis of the results presented in the Table XVI shows that the turn over numbers,  $k_{\text{cat}}$  for salicylidene-*o*-hydroxytyrosine and the salicylidene-2-hydroxybenzylamine were  $0.044 \text{ sec}^{-1}$  and  $0.15 \text{ sec}^{-1}$  respectively, whereas the  $K_{\text{M}}$  values were 2.4 mM and 8.1 mM, respectively. These data show that the affinity of 2,3,4,5-tetrafluoroBBA for salicylidene-*o*-hydroxy tyrosine was higher than that for salicylidene-2-hydroxybenzylamine.

The analysis of the structural features of the imines used here suggests that the presence of the carboxyl group in salicylidene-*o*-hydroxytyrosine may be the major determinant in the observed differences in the hydrolyses mediated by 2,3,4,5-tetrafluoroBBA. The first order rate constant is better for salicylidene-2-hydroxybenzylamine which has no carboxyl group. The  $k_{\text{cat}}/K_{\text{M}}$  for both imines are the same, i.e.  $18 \text{ M}^{-1}\text{sec}^{-1}$ .

Figure 31 and Table XVII shows the results with 2,3,5-trifluoroBBA for the hydrolysis of salicylidene-*o*-hydroxytyrosine and salicylidene-2-hydroxybenzylamine where the carboxyl group in salicylidene-*o*-hydroxytyrosine improves the affinity of the substrate for the 2,3,5-trifluoroBBA catalyst (lower  $K_{\text{M}}$  value), but it decreases the  $k_{\text{cat}}$  values.

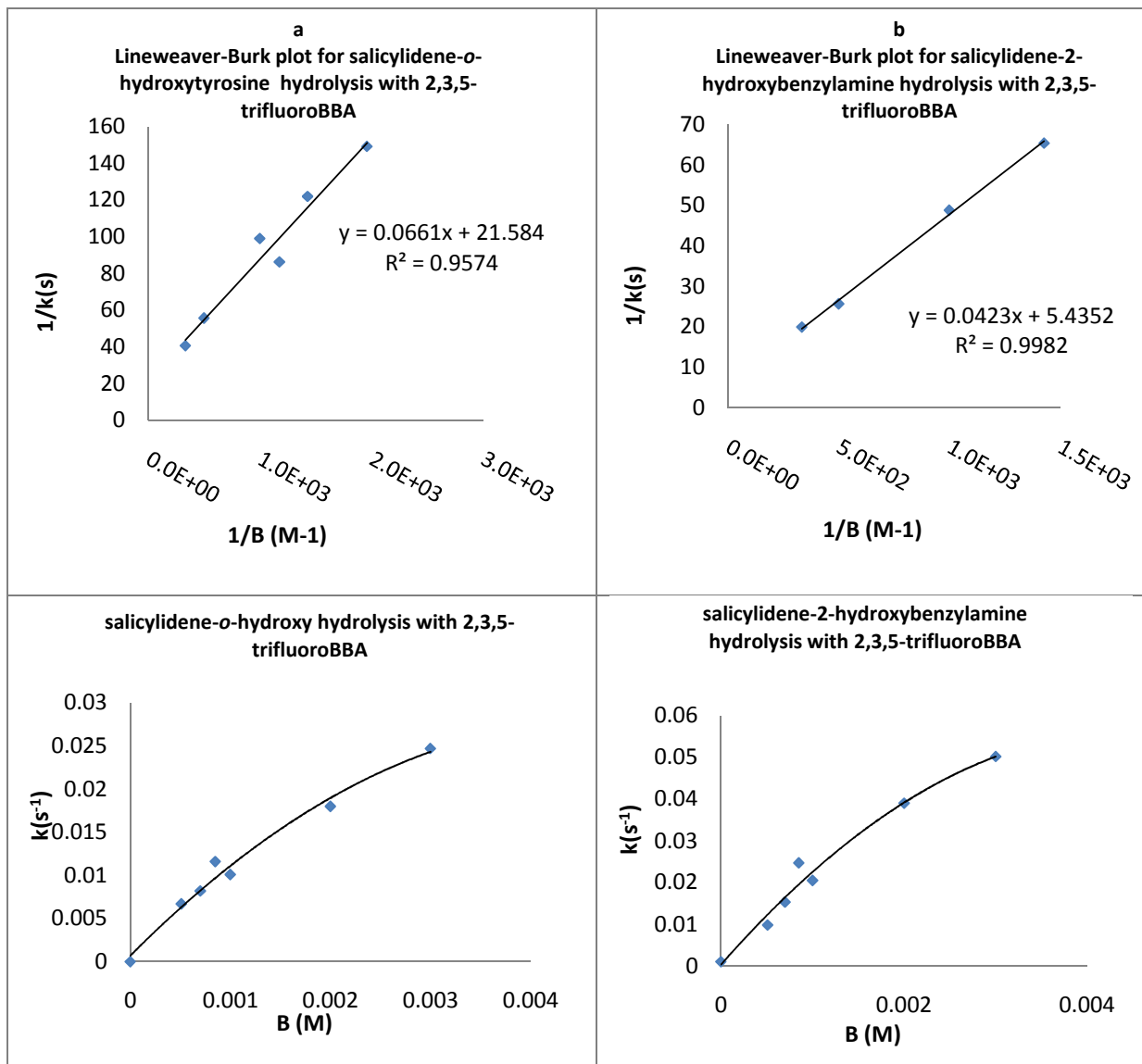


**Figure 31:** Lineweaver-Burk and  $k$  (rate constant) vs.  $B$  (boronic acid concentration) plots for the hydrolysis of a) salicylidene-*o*-hydroxytyrosine b) salicylidene-2-hydroxybenzylamine with different concentration of 2,3,5-trifluoroboronic acid at 0.1 M pH 6.0 phosphate buffer. Catalytic constants are included in Table XVII.

In summary, if I compare salicylidene-2-hydroxybenzylamine with salicylidene-*o*-hydroxy-tyrosine, it can be observed that in a very reproducible manner, there is at least three fold increased catalytic turn over number ( $k_{cat}$ ) for the hydrolysis of the imine lacking the carboxyl group (i.e. salicylidene-2-hydroxybenzylamine).

However, the relative affinity for each of the two BBA catalysts used (as is determined by their  $K_M$  values) is three fold higher for salicylidene-*o*-hydroxytyrosine, which has the carboxyl group present on the amine side of the imine (i.e.  $K_M$  for this imine is three fold lower than that obtained for the salicylidene-2-hydroxybenzylamine).

Thus, the results highlight the importance of the carboxyl group in improving the binding of the substrate to the BBA catalyst, but at the same time reveal that this functional group reduces the catalytic turn-over. In other words, carboxyl group constitute to be a better binding group but a participant of poorer catalysis by the BBA.

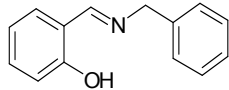
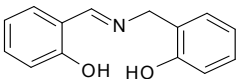
### **3.4.2. Effect of hydroxyl containing imine on the benzenboronic acid catalytic efficiency**

The results presented in Tables XVIII and Table XIX shows that the hydroxyl group substituted to the aromatic amine are an important structural element in enhancing the catalytic efficiency for the imine hydrolysis by 2,3,5-trifluoroBBA and 2,3,4,5-tetrafluoroBBA. The position of the hydroxyl group (2-hydroxyl vs. 3-hydroxyl) substituted to the benzene ring with respect to the  $NH_2$  (amino) group profoundly affect the catalytic efficiency. 3-hydroxyl substituent outrank 2-hydroxyl substituents for catalytic efficiency.

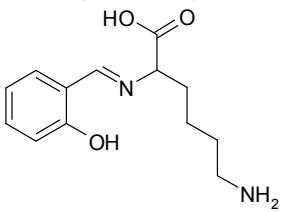
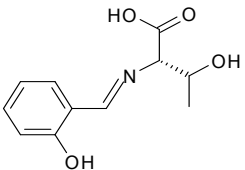
Moreover, the catalysis of the 3-hydroxyl-aromatic based imines are more efficient when it is mediated by 2,3,5-trifluoroBBA than by the 2,3,4,5-tetrafluoroBBA.

In summary, to better understand the effect of the imine hydroxyl group on the catalytic efficiency for imine hydrolyses, Tables XVIII – XXI are constructed which contrast the SAR of different hydroxyl-substituted aniline and benzylamine containing imine. As mentioned above, all the hydroxyl containing imine made the imine substrates more efficient towards hydrolysis by 2,3,4,5-tetrafluoroBBA or 2,3,5-trifluoroBBA catalysts. In addition to the case of the aromatic amines substituted with hydroxyl groups at different positions, the lysine and the threonine amine based imine also provide a insightful examples for the enhancement of the catalytic efficiency by the hydroxy group (see Table XIX).

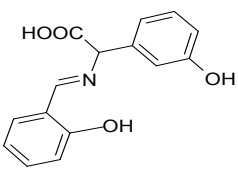
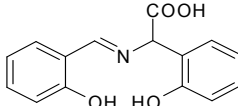
**Table XVIII:** 2,3,4,5-tetrafluoroBBA catalytic constants for the hydrolysis of two hydroxyl functional group related imines at stoichiometric molar ratios at 0.1 M pH 6.0 phosphate buffer

Imine (concentration)	Boronic acid concentration range (mM)	$k_{cat}$ ( $sec^{-1}$ )	$K_M$ (mM)	$k_{cat}/K_M$ ( $M^{-1}sec^{-1}$ )
salicylidene-benzylamine (0.50 mM) 	0.7 to 5.0	0.15	34	4
salicylidene-2-hydroxybenzylamine (0.5 mM) 	0.7 to 5.0	0.20	8	25

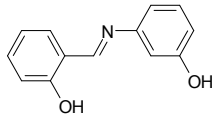
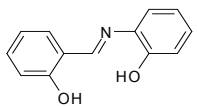
**Table XIX:** Kinetic constants for the 2,3,4,5-tetrafluoroBBA catalyzed hydrolysis of two hydroxyl functional group related imines at stoichiometric molar ratios at 0.1 M pH 6.0 phosphate buffer

Imine (concentration)	Boronic acid concentration range (mM)	$k_{cat}$ ( $sec^{-1}$ )	$K_M$ (mM)	$k_{cat}/K_M$ ( $M^{-1}sec^{-1}$ )
salicylidene-lysine (0.50 mM) 	0.45 to 2.5	0.014	0.84	17
salicylidene-threonine (0.50 mM) 	0.45 to 0.5	0.014	0.42	33

**Table XX:** Kinetic constants for the 2,3,4,5-tetrafluoroBBA catalyzed hydrolysis of two hydroxyl functional group related amino acid imines at stoichiometric molar ratio ratios at 0.1 M pH 6.0 phosphate buffer

Imine (concentration)	Boronic acid concentration range (mM)	$k_{cat}$ (sec <sup>-1</sup> )	$K_M$ (mM)	$k_{cat}/K_M$ (M <sup>-1</sup> sec <sup>-1</sup> )
salicylidene-3-hydroxyphenylglycine (0.60 mM) 	0.63 to 3.7	0.044	1.6	27
Salicylidene-2-hydroxytyrosine (0.50 mM) 	0.45 to 5.0	0.044	2.4	18

**Table XXI:** Kinetic constants for the 2,3,4,5-tetrafluoroBBA catalyzed hydrolysis of two hydroxyl functional group related imines at stoichiometric molar ratios at 0.1 M pH 6.0 phosphate buffer

Imine (concentration)	Boronic acid concentration range (mM)	$k_{cat}$ (sec <sup>-1</sup> )	$K_M$ (mM)	$k_{cat}/K_M$ (M <sup>-1</sup> sec <sup>-1</sup> )
Salicylidene-3-hydroxyaniline (0.50 mM) 	0.09 to 0.50	0.130	1.0	94
Salicylidene-2-hydroxyaniline (0.5mM) 	0.09 to 0.50	0.035	0.6	55

A comprehensive representation of the hydroxy effect upon the catalytic efficiency of imine hydrolyses are shown in Figure 32.

As discussed earlier in this section, the bar graphs focus on the SAR for the position of the hydroxy-group (2-hydroxyl vs. 3-hydroxyl substituted to the benzene ring with respect to the amino group and its effect upon  $k_{cat}/K_M$  (Figure 32) and upon  $K_M$  and  $k_{cat}$  obtained in the presence of 2,3,4,5-tetrafluoroBBA catalyst.

In conclusion, the hydroxy group provides the major structural determinant for the catalytic efficiency and its position as a substituent in the benzene ring has the highest effect upon the  $k_{cat}/K_M$ , 3-hydroxyl group outranking 2-hydroxyl substituents.

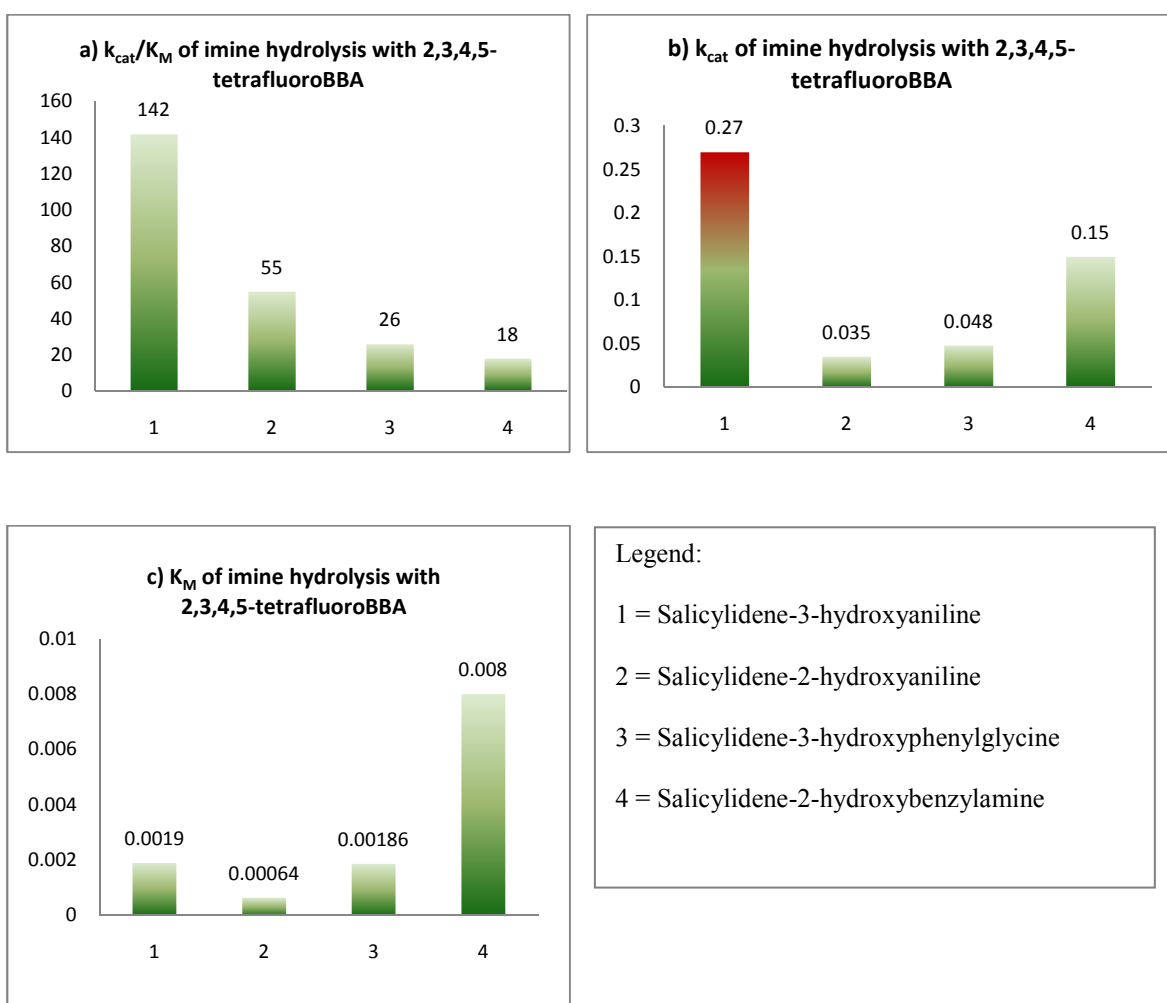


**Figure 32:** Bar graph depicting a)  $k_{cat}/K_M$  b)  $k_{cat}$  c)  $K_M$  for the hydrolysis of different imines with the catalyst 2,3,4,5-tetrafluoroBBA.

### 3.5. Effect of substituents of benzenboronic acid on the rate of imine hydrolysis

#### Hammett plot analysis of different benzene substituents in the boronic acid catalysts

The Hammett  $\rho$  values for different substituents of benzenboronic acids catalysts were determined at pH 6.0 at which the BBAs have the best catalytic activities. Previous studies of Rao *et al.*<sup>69</sup> have shown that the electron-withdrawing substituents stabilize the anionic tetrahedral boronic acid-imine complex, whereas the boronic acids with electron-donating groups destabilize such a complex. Based on these previous studies, I further investigated the effect of different electron withdrawing and electron donating groups of new benzenboronic acid catalysts on the hydrolysis of salicylidene-3-hydroxyaniline imine (see Table XXII).

The Hammett plot of  $\text{Log}(K_M)$  vs. the substituent constant (Figure 34) shows the dependency of  $K_M$  as a function of different electronic structures substituted to the benzene ring of BBA catalyst. It can be seen that almost all BBAs with electron withdrawing groups (3-chloro-4-fluoro-, 3-nitro, 3,4,5-trifluoro, 3-carboxy-5-nitro-BBA) show  $\text{Log}(K_M)$  values that vary linearly with the Hammett sigma value. Deviation from this linearity was observed for some BBAs that have side chain group that can engage in proton transfer reaction (such as 3-carboxy-5-amino, 3-amino, 3-carboxy BBAs). The fitted straight line gave a slope ( $\rho$  value) of  $-2.01 \pm 0.10$ , with the highest sigma values being obtained for 3,4,5-trifluoro BBA which had also one of the lowest  $K_M$  in the plot. These data suggest that electronic withdrawing groups help BBAs to have a higher binding affinity for their imine substrates. It also shows that there is a tighter complex between the BBA and the imines for the BBAs with the higher Hammett substituent constants as compared to the unsubstituted BBA. The results obtained here are very similar with those published by Rao *et al.* and those obtained with the substituted BBAs to serine proteases, where the electron withdrawing groups induced tighter binding by forming a strong complex with the active site serine hydroxyl group.<sup>50,97</sup> However, if the unsubstituted BBA was excluded, both the electronic withdrawing and electron donating groups shows no trend or hierarchy in the binding affinity for the imine substrate ( $\text{Log}(K_M)$  values vs. Hammett sigma fall on a straight). This also shows that BBAs with side chain groups that can engage in proton transfer reactions do not necessarily obey the Hammett relationship.

When the logarithm (Log) of  $k_{\text{cat}}$  for the hydrolysis of the imine salicylidene-3-hydroxyaniline by BBA vs. sigma (substituent constant) are plotted (Figure 33), all boronic acids including one with sigma of negative value (3-carboxyBBA with  $\sigma$  of -0.10) fall on a straight line with a positive slope ( $\rho$  value) of  $+1.36 \pm 0.01$ . This suggests that BBAs with electron withdrawing substituents are more efficient in the catalysis of imine hydrolysis. It can also be seen that 3-carboxy-5-amino and 3-amino substituted BBA deviate from the linear relationship of Log ( $k_{\text{cat}}$ ) vs. sigma, supporting the fact that these electron donating groups decrease the catalytic efficiency of imine hydrolyses.

When the Log ( $k_{\text{cat}}/ K_M$ ) vs.  $\sigma$  is plotted (see Figure 35) it can be seen that the data fall on a straight line with the positive slope of  $3.33 \pm 0.05$ , where the second order rate constants,  $k_{\text{cat}}/ K_M$ , are higher in the cases of BBAs with electronic withdrawing substituents as compared to the BBAs with electron donating groups. These results confirmed that the electron withdrawing substituents have a significant effect on the imine hydrolysis. However, by comparison with the unsubstituted BBA, both the electron donating and electronic withdrawing groups had higher second order catalytic constants.

As a general outcome, it can be concluded that higher sigma values for the substituted BBAs (which was always determined for the substituted BBAs with electron withdrawing groups) are directly linked with both higher  $k_{\text{cat}}$  and  $k_{\text{cat}}/ K_M$  values. Also, the higher sigma values were correlated with lower  $K_M$  values, meaning higher affinity for the imine substrate (see Table XXII).

**Table XXII:** Hammett relationship values for the hydrolysis of salicylidene-3-hydroxyaniline by various BBAs

Benzeneboronic Acid (BBA)	Total $\sigma$	Log ( $k_{cat}$ )	Log ( $K_M$ )	Log ( $k_{cat}/ K_M$ )
BBA	0.00	-2.17	1.53	-1.66
3,5-bis(trifluoromethyl)BBA	0.86	-1.301	-0.337	4.76
3,4,5-trifluoroBBA	0.74	-1.09	-0.071	4.61
3-amino-5-carboxyBBA	-0.26	-1.87	-0.301	3.26
3-aminoBBA	-0.16	-1.60	-0.244	1.58
3-carboxy BBA	-0.10	-2.37	-2.22	0.845
3-chloro-4-fluoroBBA	0.43	-0.25	0.079	3.22
3-carboxy-5-nitroBBA	0.61	-1.306	-0.481	5.01
3-nitroBBA	0.71	-1.09	0.230	4.34

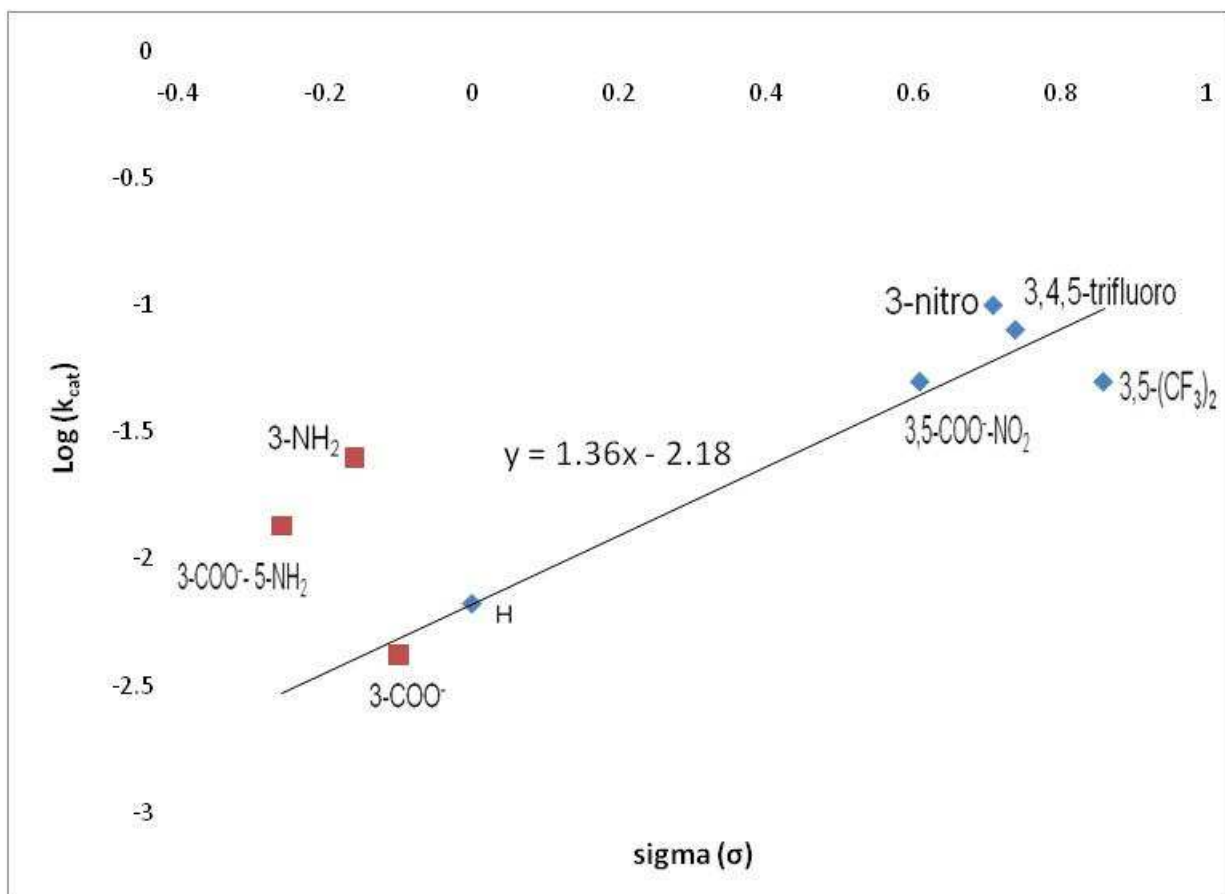


**Figure 33:** A Hammett plot relating Log ( $k_{cat}$ ) values and  $\sigma$  for the hydrolysis of salicylidene-3-hydroxyaniline by different substituted benzeneboronic acids at 30°C in 0.1 M phosphate buffer of pH 6.0. Benzeneboronic acids with 3-amino and 3-carboxy-5-amino substituents show systemic deviation from others and thus were not included in the regression analysis. The  $\rho$  value is  $+1.36 \pm 0.01$ .

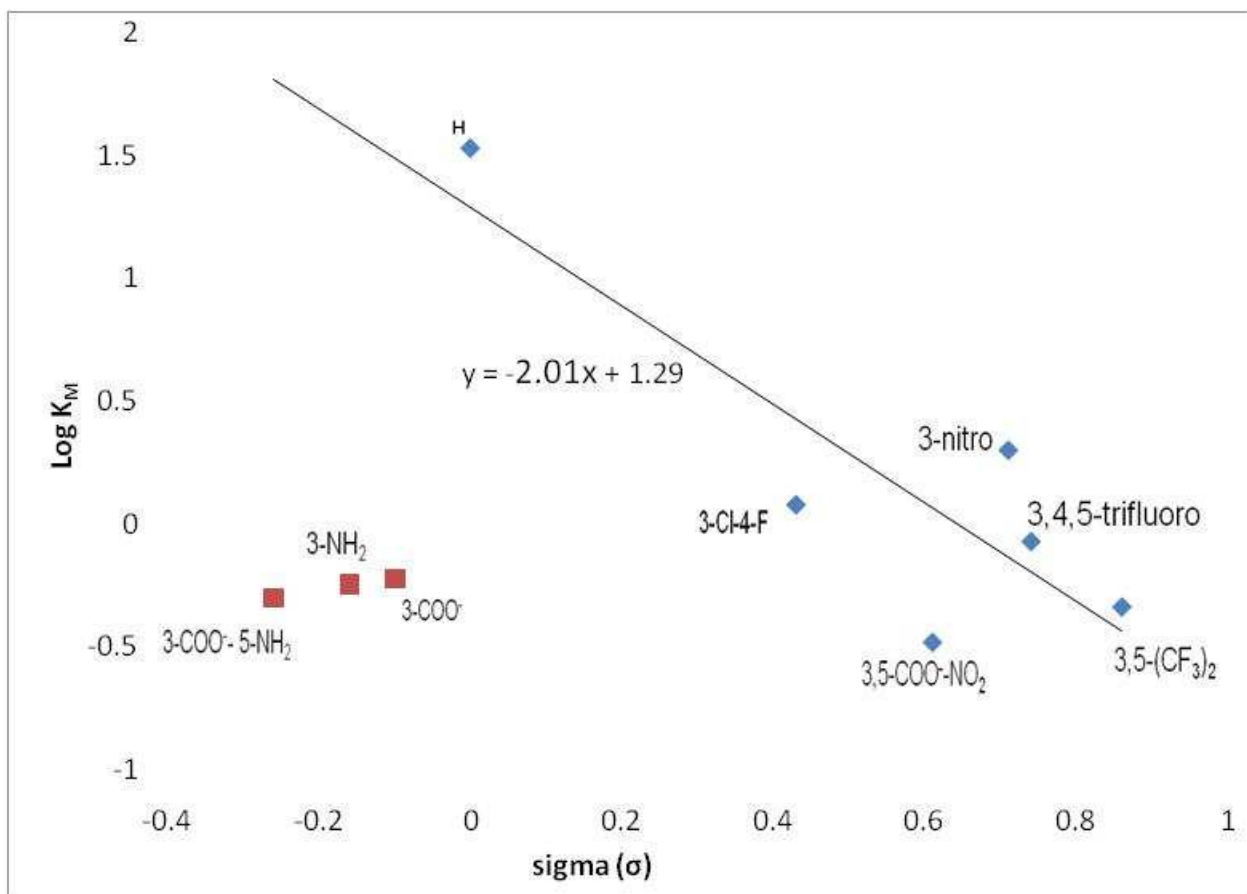


**Figure 34:** A Hammett plot relating Log ( $K_M$ ) values and  $\sigma$  for the hydrolysis of salicylidene-3-hydroxyaniline by different substituted benzenboronic acids in at 30°C in 0.1 M phosphate buffer of pH 6.0. Benzenboronic acids with 3-carboxy and 3-amino and 3-carboxy-5-amino substituents show systemic deviations from others and thus were not included in the regression analysis. The  $\rho$  value is  $-2.01 \pm 0.1$ .

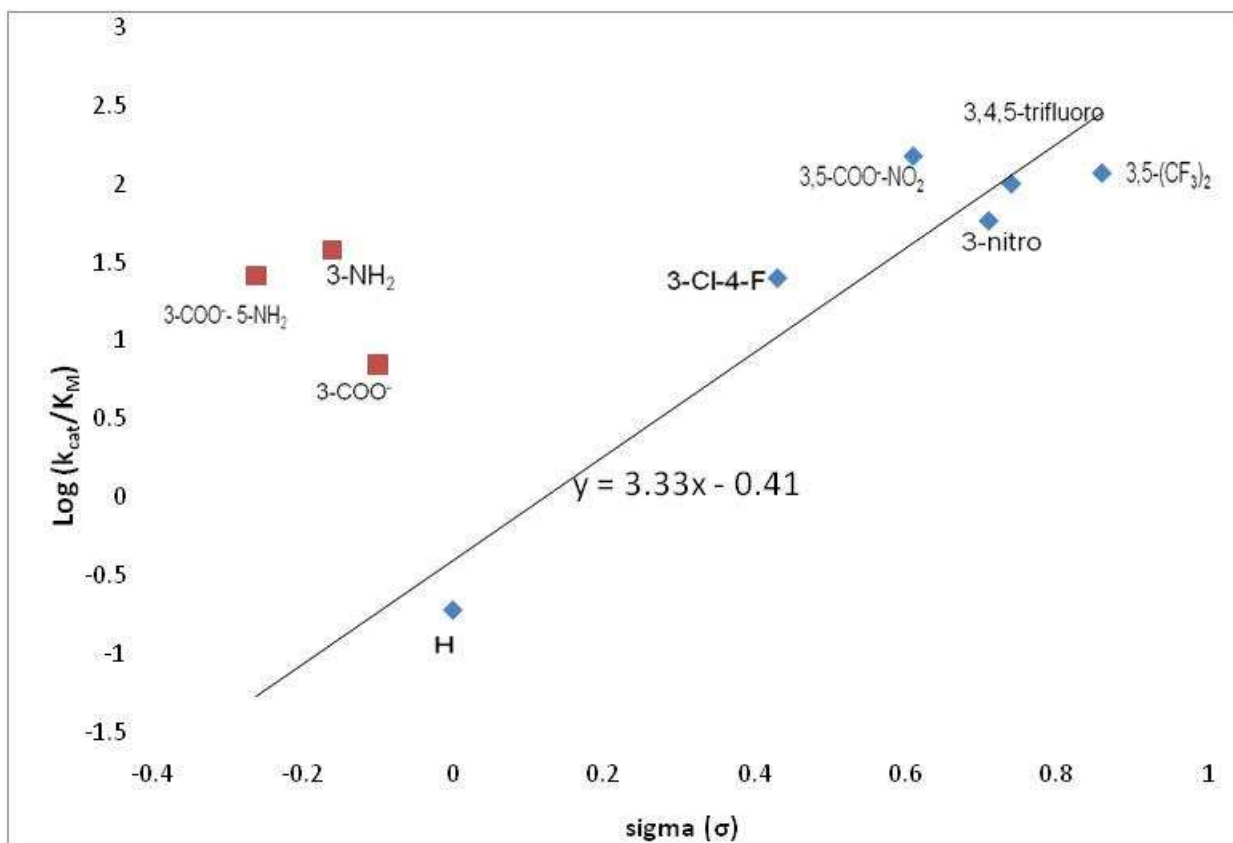


**Figure 35:** A Hammett plot relating  $\text{Log}(k_{\text{cat}}/K_M)$  values and  $\sigma$  for the hydrolysis of salicylidene-3-hydroxyaniline by different substituted benzeneboronic acids at 30°C in 0.1 M phosphate buffer of pH 6.0. Benzeneboronic acids with 3-carboxy and 3-amino and 3-carboxy-5-amino substituents show systemic deviations from others and thus were not included in the regression analysis. The  $\rho$  value is  $+3.33 \pm 0.05$ .

### 3.6. Sculpt Results

In order to assess the relationship between the structures of different imines substrates and their relative affinity for different boronic acids catalysts, I used a docking procedure in which the complex between BBAs and the imine was preformed, and imported in the docking software Sculpt, and then minimized using the built-in MMFF94 force field to assess the relative energy associated with the complex formation. The software allowed the prediction of both steric fitness based on the van der Waals interactions of the two target components in the complex and their electrostatic contacts as predicted by the Coulombic electrostatic term of the MMFF force field.

Table XXIII presents the major investigated complexes between different BBAs, primarily 2,3,5-trifluoroBBA and 2,3,4,5-tetrafluoroBBA and their imines substrates. The table presents the predicted relative affinity between the BBA and the imine substrate, based on the assessment of both electrostatics and van der Waals interactions, as they are the major read-out from the Sculpt analysis of the docking experiments. In addition, the combined steric fitness and the electrostatic interactions between the BBAs and the imines are shown in the last column of the table.

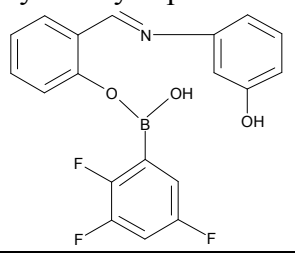
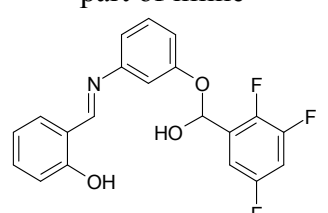
The results presented in Table XXIII support the idea that the electrostatic interactions between BBAs and the selected imines substrates increase the relative stability between these complexes, while the steric fitness based on van der Waals interactions impose restrictions to the covalent and non-covalent interactions between the BBAs and the imines. Thus, all tested complexes between BBAs and imines were characterized by a negative electrostatic term. This energy term is even more favorable for the complex between the two BBAs and the 3-hydroxy group of the aniline in the imine substrate. However, in terms of steric fitness, the more stable complexes were those between the selected BBAs and the salicylidene-3-hydroxyaniline mediated by the ester bond with the salicylaldehyde hydroxyl group.

When the combined electrostatic and van der Waals interactions were used to predict the relative stability of the selected complexes, the read-out shown in the last column of Table XXIII suggests that the most stable complex is between 2,3,5-trifluoro-BBA and the salicylidene-3-hydroxyaniline. This complex was mediated by the ester bond with the salicylaldehyde hydroxyl group. The predicted free energy of interaction is -1160 kcal/mol).

The complex between the 2,3,4,5-tetrafluoroBBA and salicylidene-3-hydroxyaniline is predicted to have very low stability when compared with the complex between 2,3,5-trifluoroBBA and salicylidene-3-hydroxyaniline (only -6.0 kcal/mol). The data presented in Table XXIII also suggest that the complexes between the selected BBAs and the salicylidene-3-hydroxyaniline were not favorable when mediated by the ester bond with 3-hydroxy group of aniline. Table XXIII also show that both of the BBA when ester bonded with 3-hydroxy group of aniline produced positive predicted free energy of interaction.

The major complexes between the BBAs and the imines are depicted in Figure 36 using the visual tools from Sculpt.

**Table XXIII:** SCULPT-derived interaction energies and structural images for complexes of BBAs with salicylidene-3-hydroxyaniline

Benzeneboronic acid	Bond between BBA and Imine	van der Waal and Electrostatic Forces (kcal/mol)
2,3,5-trifluoroBBA	No ester bond	-10
	Ester bond with hydroxyl group on salicylaldehyde part of imine 	-1160
	Ester bond with hydroxyl group of the aniline part of imine 	+50
2,3,4,5-tetrafluoroBBA	Ester bond with hydroxyl group on salicylaldehyde part of imine	-6
	Ester bond with hydroxyl group of the aniline part of imine	+30

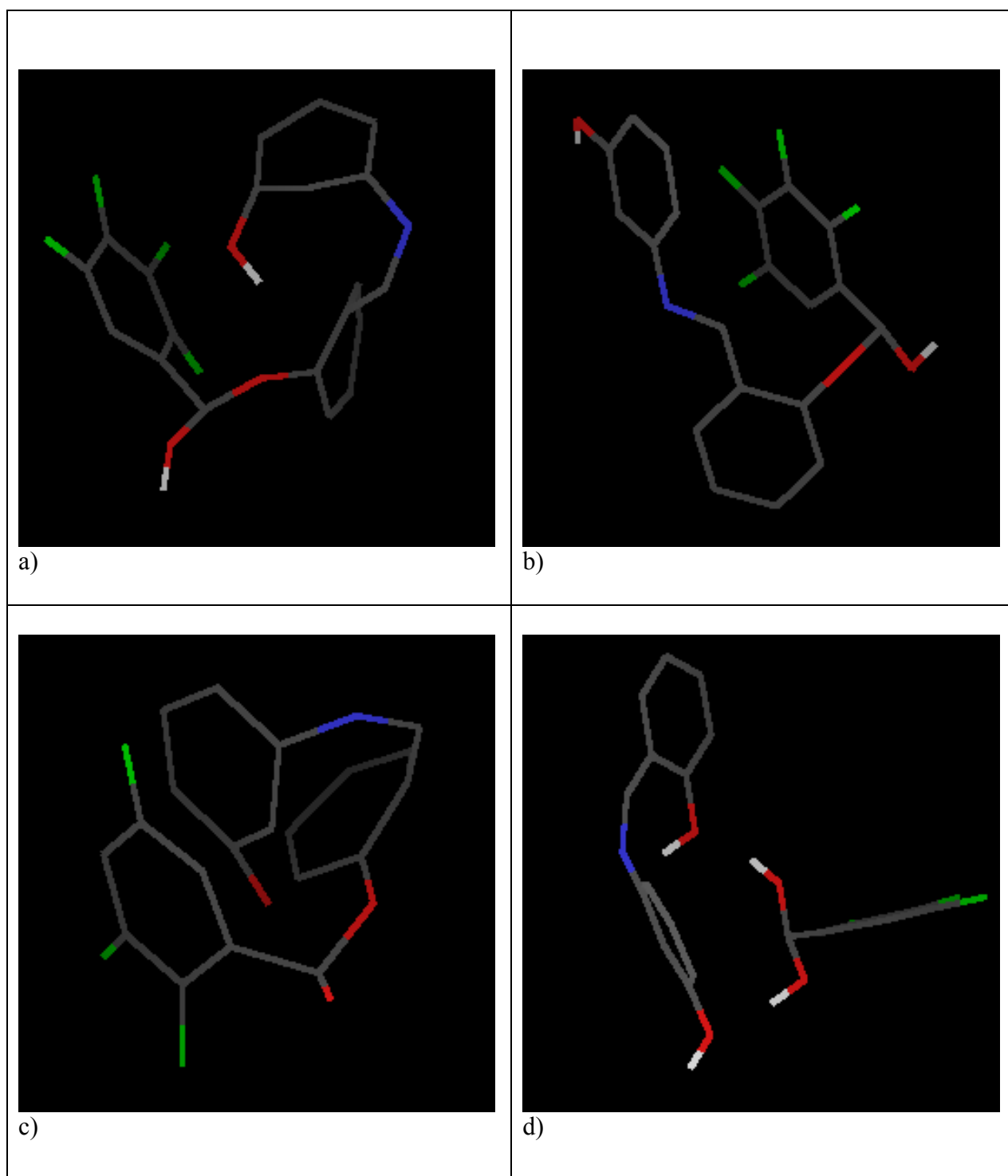


**Figure 36:** SCUPLT modeling with (a,b) 2,3,4,5-tetrafluorobBA (c,d) 2,3,5-trifluorobBA and the salicylidene-3-hydroxyaniline.

### 3.7.1. Effect of pH on the hydrolysis of salicylidene-3-hydroxy aniline by different boronic acids

In order to gain some mechanistic insights for the BBA mediated hydrolysis of imine presented in other sections the second- order rate constants ( $k_{\text{cat}}/ K_M$ ) for the hydrolysis of the salicylidene-3-hydroxy aniline imine by 2,3,4,5-tetrafluoroBBA, 2,3,5-trifluoroBBA, 3,4,5-trifluoroBBA, 3,5-dinitro-2-methylBBA and 3,5-bis(trifluoromethyl)BBA are plotted as a function of pH (see Figure 37). All points on the pH-rate profile were corrected for the spontaneous hydrolysis of imine at the same buffer concentration. The pH profile was plotted in the 6.0-9.0 range.

The results presented herein show that the rates of this imine hydrolysis obtained with different boronic acids are maximal at lower pH ranges (6.0-7.5) and decreases with increasing pH. pH profiles are consistent with the hypothesis that single-proton ionizations control the catalyzed hydrolysis of the imine (see Figure 37 and Table XXIV).

**Table XXIV:** pK values derived from pH profiles for the hydrolysis of salicylidene-3-hydroxyaniline with different BBAs

BBA	pK
2,3,4,5-tetrafluoroBBA	7.6
2,3,5-trifluoroBBA	7.8
3,5-dinitro-2-methylBBA	7.8
3,4,5-trifluoroBBA	8.3
3,5-bis(trifluoromethyl)BBA	8.3

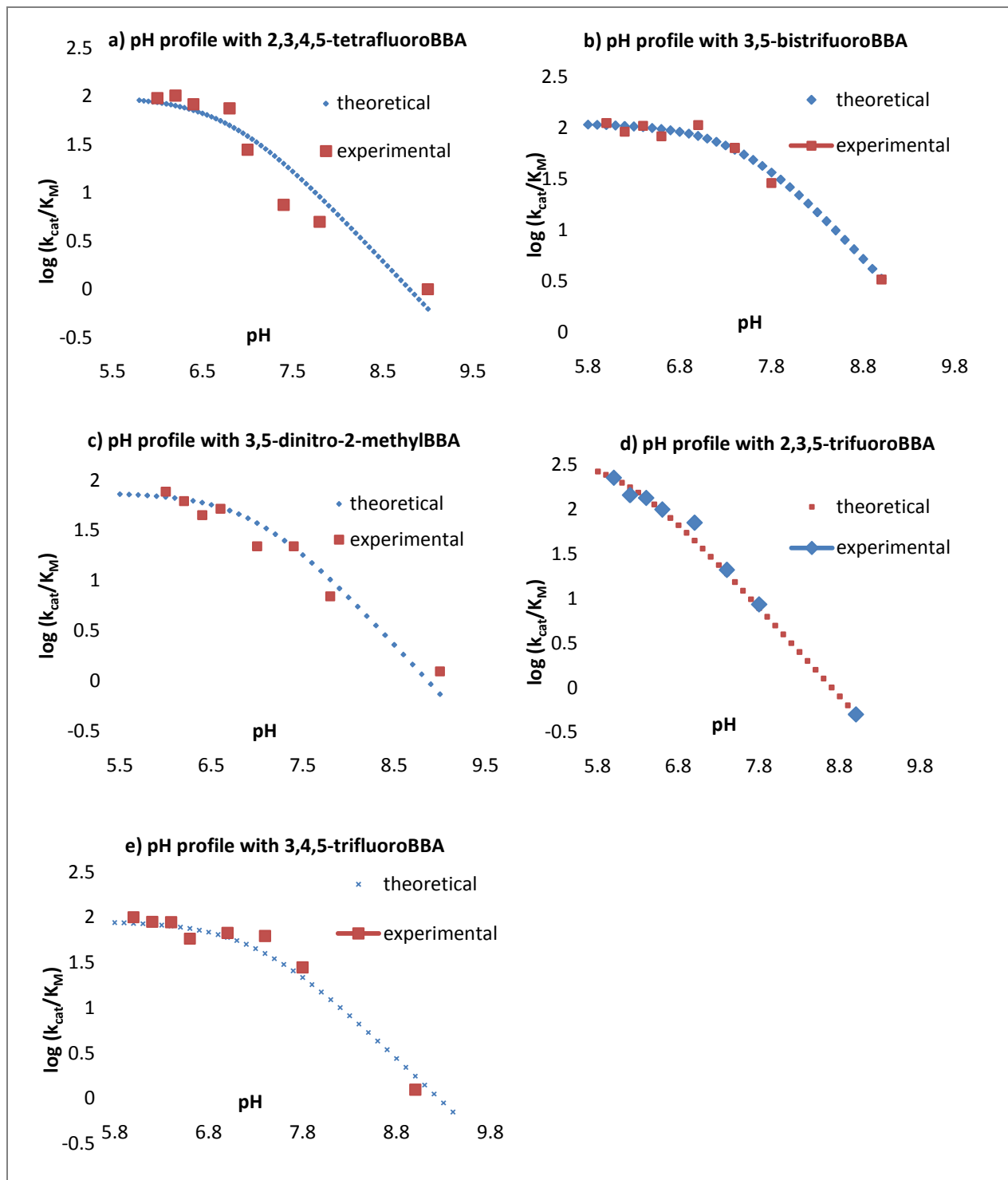


**Figure 37:** pH dependent hydrolysis of the salicylidene-3-hydroxyaniline with a) 2,3,4,5-tetrafluoroBBA, b) 3,5-bistrifluoromethylBBA, c) 3,5-dinitro-2-methylBBA, d) 2,3,5-trifluoroBBA, e) 3,4,5-trifluoroBBA.

The observed pH profiles may reflect the ionization of the BBAs that are used. The pK obtained from the experimental theoretical curves are close to the pK of the boronic acids.<sup>91,92,93</sup> These results are consistent with the pH profile observed for the boric acid-catalyzed hydrolysis of a hydroxyl imine.<sup>94</sup> It is also consistent with the pH profile observed for the 3-nitro-BBA catalyzed hydrolysis of the salicylidene-L-isoleucine imine by Rao and Philipp.<sup>69</sup>

Rao *et al.* investigated the pH profile for the catalysis of salicylidene-L-isoleucine by un-substituted BBA. They reported that this pH profile has shifted from the one obtained with the 3-nitroBBA and the extrapolated pK was 8.96, which is nearly identical with the reported value in the literature of 8.8, the pK for BBA<sup>95</sup>. The results reported by Rao et.al. are thus in agreement with the findings, that during the imine hydrolysis there is one single step of ionization, and that one is entirely due to the hydroxylation of the BBA catalyst. These results demonstrate that there is no other ionization event related to the imine itself which could affect the final catalytic efficiency.

Similarly, pH profiles observed for the five different benzenboronic acids catalyzed hydrolysis of the salicylidene-3-hydroxyaniline imine gave different pKs whereas pK for salicylidene-3-hydroxyaniline is 4.17<sup>96</sup>. These results proved that the ionizable groups in the salicylidene-3-hydroxyaniline are not responsible for the pK values determined from the pH profiles. Altogether, these data reinforced the previous findings, showing that the variable pKs extrapolated from the pH profiles are due entirely to the ionization of the boronic acids catalysts.

In addition, this conclusion is also supported by the finding of a low pK of 4.70<sup>97</sup> for the phenolic hydroxyl group in salicylidene-2-aminopropane substrate, which doesn't match any of the above pKs determined from pH profiles (see Table XXIV). It may be assumed that the phenolic hydroxy groups of salicylidene-3-hydroxyaniline is ionized in the entire pH range (6.0-9.5) used in this study.

### 3.7.2. The pH dependence of $k_{\text{cat}}$ and $K_{\text{M}}$ in the hydrolysis of the imine by the boronic acids

The pH profiles presented in the Section 3.7.1 do not explain the mechanism underlying the decrease in imine hydrolysis with increasing pH. It is not known whether it is due to poor binding or lower catalytic rate constants at higher pHs. The pH dependencies shown in those pH profiles (Figure 37a, 37b, 37c, 37d, 37e) indicate that the un-ionized boronic acids are effective catalysts in this system. These studies were done using the composite second order rate constant  $k_{\text{cat}}/K_{\text{M}}$ . The decrease in the imine hydrolysis at higher pH's could be due either to poorer binding of the imine substrate to the BBAs catalysts or to lower catalytic rate constants ( $k_{\text{cat}}$ ).

In order to gain insight for the possible mechanism that modulates the second-order rate constants ( $k_{\text{cat}}/K_{\text{M}}$ ) values of imine hydrolysis at higher pH, I further determined the changes in the kinetic constants,  $k_{\text{cat}}$  and  $K_{\text{M}}$  as a function of pH. Specifically I measured the  $k_{\text{cat}}$  and  $K_{\text{M}}$  values at pH 6.0, and 7.8 using 2,3,4,5-tetrafluoroBBA, 2,3,5-trifluoroBBA, 3,4,5-trifluoroBBA, 3,5-dinitro-2-methylBBA and 3,5-bistrifluoromethylBBA for catalyzing the hydrolysis of salicylidene-3-hydroxyaniline.

Table XXV presents the  $k_{\text{cat}}$  and  $K_{\text{M}}$  values determined for the above mentioned hydrolyses reactions and the extrapolated pK values from the associated graphs. It can be seen that  $k_{\text{cat}}$  values do not change with pH. In conclusion, the  $K_{\text{M}}$  values obtained from the same type of measurements are radically different as the pH increases for all tested BBAs. If one look specifically to the case of 2,3,5-trifluoroBBA, it can be seen from Table XXV that  $K_{\text{M}}$  is increase from 0.4 mM (at pH 6.0) to 12 mM (at pH 7.8). The same increase in the  $K_{\text{M}}$  values with the increasing pH values was obtained for other BBAs investigated. These results support the view that higher pH (>7.0), stabilize an ionized BBA species that has a lower binding affinity for the imine substrate than the conjugated acid form that exists at lower pH. It is also observed that for the same 2,3,5-trifluoroBBA, the catalytic rate constant,  $k_{\text{cat}}$  for imine hydrolysis is the same at pH 6.0 and pH 7.8 (i.e.  $0.1 \text{ sec}^{-1}$ ).

**Table XXV:** Comparison of  $k_{cat}$  and  $K_M$  at different pH value for different BBAs

Benzeneboronic acid (BBA)	$k_{cat}/K_M$	pK from pH profile (Fig. 37)	$k_{cat}$ at pH 6.0	$k_{cat}$ at pH 7.8	$K_M$ at pH 6.0	$K_M$ at pH 7.8
2,3,4,5-tetrafluoroBBA	175	7.6	0.17	0.19	0.80	8
2,3,5-trifluoroBBA	232	7.8	0.10	0.10	0.40	12
3,5-dinitro-2-methylBBA	100	7.8	0.20	0.20	1.3	6
3,4,5-trifluoroBBA	117	8.3	0.07	0.06	0.70	2
3,5-bis(trifluoromethyl)BBA	116	8.3	0.04	0.04	0.46	1

### 3.8. NMR analysis for the structure determination

In this section I present NMR spectra for structural analysis. The two structures shown below are salicylidene-3-hydroxyaniline imine in an ionic form (on the left) and salicylaldehyde (on the right). The letters a, b, c, d, & e are placed next to the appropriate hydrogen atoms in these structures and in the NMR spectra. Unlabeled peaks between 6 to 8 ppm belong to aromatic hydrogen atoms. Other peaks between 2 and 4 ppm result from the DMSO-d (dimethyl sulfoxide) solvent. In the NMR spectrum of salicylidene-3-hydroxyaniline in Figure 37a, the peaks a and b are absent which were present in the spectrum

of salicylaldehyde in Figure 37b. These data demonstrate the formation of the imine salicylidene-3-hydroxyaniline.

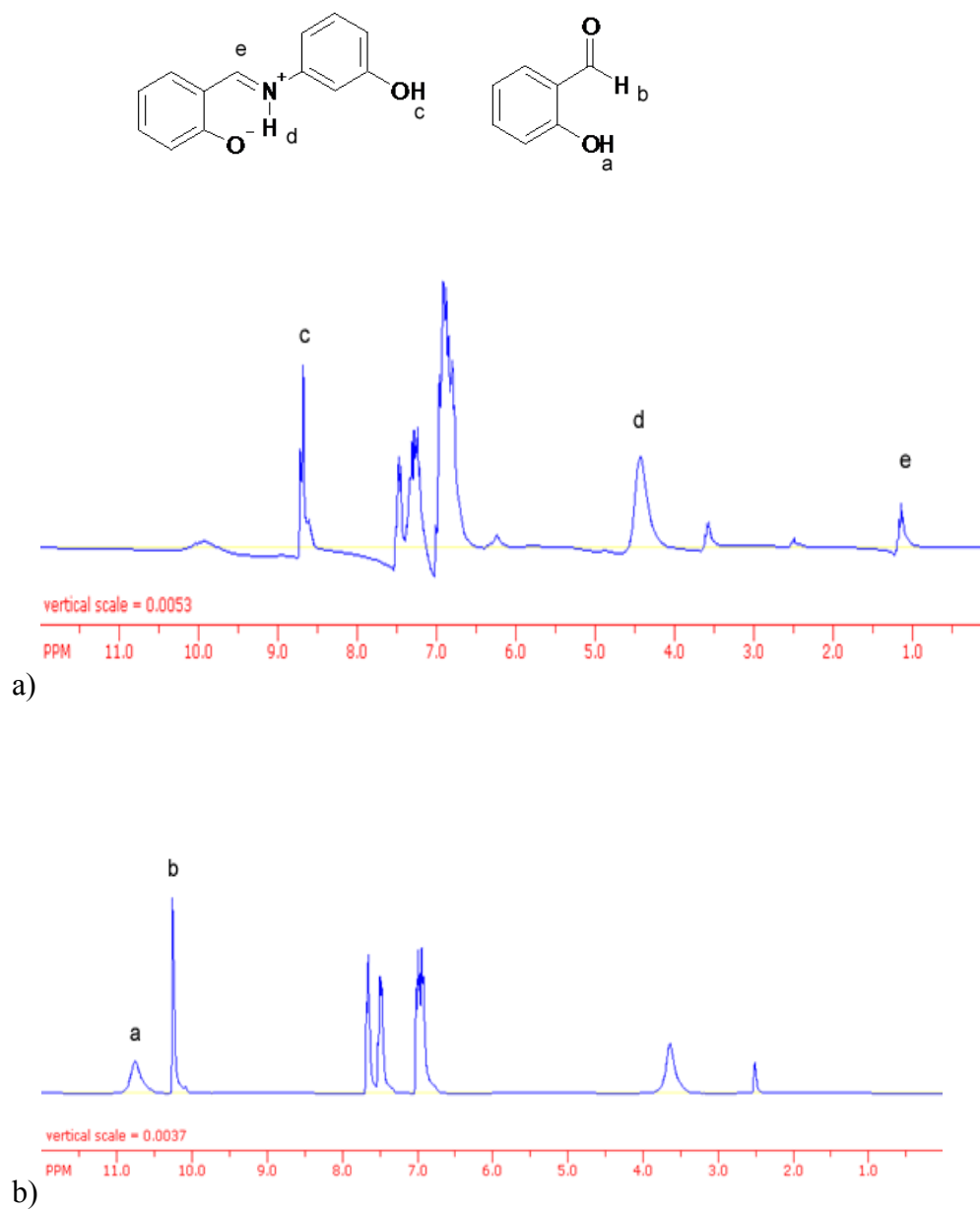


**Figure 38:** <sup>1</sup>H-NMR spectra corresponds to a) salicylidene-3-hydroxyaniline and b) salicylaldehyde in DMSO-d.

## 4. Conclusions

Arylboronic acids accelerate the hydrolysis of the Schiff's bases derived from salicylaldehyde and different primary amines. The acceleration of the Schiff's bases must be due to the complex formation between the boronic acid and the imines followed by the breakdown of the complex to products. If the benzenboronic acid complexes with the imines, then the imine increasingly saturates as the concentration of the boronic acid raises: eventually the rate of hydrolysis should remain steady when the imine is completely saturated.

The research presented herein presents results which showed that a hyperbolic curve is obtained when first-order rate constants are plotted as a function of BBA (Figures 19a, 19b, 22a, 22b, 24b, 25b, 26b, 27b, 29a, 29b, 30a, 30b). It indicates that this system follows Michaelis-Menten kinetics through the formation of a boronic acid-imine base complex. The linearity of Lineweaver-Burk plots (Figures 14b, 16b, 20a, 20b, 21a, 21b etc.) also support the formation of a Michaelis-Menten complex between BBA and the imine substrate.

It has been known that boric acid esterifies with the phenolic hydroxy group of salicylaldehyde, salicylamide<sup>98</sup> and salicylaldehyde oxime.<sup>99</sup> It was concluded that the boronic acids complex with the imine through esterification of phenolic hydroxy group of the imine. Rao *et al.* showed that there is no effect on the hydrolysis of the imine that was derived from 4-hydroxybenzaldehyde and L-isoleucine. These results further support that the boronic acid form a complex with the phenolic hydroxy group of the Schiff's base and that the boronic group in the complex facilitates the hydrolysis of the imine by forming a six-membered ring involving either imine carbon or nitrogen.

In the case of 4-hydroxybenzylidene-L-isoleucine, the boronic group is far away from the imine nitrogen or carbon in the complex and it may not be possible for the boronic group to form a cyclic structure like the one possible in the case of imines with the salicylaldehyde.

It is known that the hydrolysis of an imine was subjected to general acid catalyst at lower pHs.<sup>89</sup> It may be possible that the boronic acid acts as general acid in the hydrolysis of the Schiff's base and proton transfer is involved in the rate determining step. But Rao *et al.* showed that there is no solvent deuterium isotope effect on the hydrolysis of the imine catalyzed by BBA. The rate constants obtained in D<sub>2</sub>O as well as in H<sub>2</sub>O at pH 6.0 and 6.6 were the same and the ratio of  $k(\text{H}_2\text{O})/k(\text{D}_2\text{O})$  was close to unity. If proton transfer is involved in the transition

state, then the ratio of  $k(\text{H}_2\text{O})/k(\text{D}_2\text{O})$  is close to unity. If proton transfer is involved in the transition state, then the ratio of  $k(\text{H}_2\text{O})/k(\text{H}_2\text{O})$  would have been higher than one. But the ratio obtained from the experiments of Rao et. al.<sup>69</sup> was close to unity which suggests that the proton transfer is not involved in the transition state, and that the boronic acid does not act as a general acid during hydrolysis of an imine.

In order to better understand the mechanism involved in the imine hydrolysis by Boronic acids, I performed an advanced structure-activity relationship (SAR) of different substituted benzenboronic acids (BBAs) and structured the SAR for different imine substrates undergoing hydrolysis. I presented the most important aspects of these SAR studies on both the catalysts (BBAs) and on their imines substrates. The pH effects on the catalytic constants for imine hydrolysis by different substituted BBAs were also stretched in detail. The Hammett plot analysis of these catalytic constants as a function of the electronic withdrawing or electron donating groups substituted on the benzene ring of BBAs revealed new mechanistic insights for imine hydrolyses.

One of the most important contributions of this research is the establishment of the major factors leading the SAR of BBAs and SAR of imines which are summarized in the following sections.

### **1. The ratio of BBAs: imine substrate has a significant effect on the hydrolysis rate**

It can be seen from Table VII that varying the molar ratios of catalyst: substrate had a significant effect on the catalytic efficiency ( $k_{\text{cat}}/K_M$ ) for BBA mediated the imine hydrolysis by. Sub-stoichiometric ratios of BBA: imine (i.e. 1/10 and 1/5 of BBA/imine) allowed the achievement of the lowest  $K_M$  values (0.7 mM) and an intermediate  $k_{\text{cat}}$  value (0.12  $\text{sec}^{-1}$ ). Obtaining the lowest  $K_M$  value at sub-stoichiometric molar ratios of the catalyst : imine support the view that the BBA is more efficient in binding the imine substrate under these conditions. This is also a condition for being a good catalyst. In turn, the highest catalytic efficiency ( $k_{\text{cat}}/K_M$ ) was achieved at substiochiometric BBA : imines ratios, for the best tested BBAs. These results made it possible to show that changes in the structural features of both the benzenboronic catalysts and the imines substrates could determine the achievement of different catalytic efficiencies.

## 2. SAR of different substituted BBAs with respect to their catalytic efficiency for imine hydrolysis

In order to better understand the mechanism of imine hydrolysis by different substituted BBAs focus was specifically given to the level of substitution of these catalysts with electron withdrawing groups (such as fluoro, chloro, nitro, carboxyl) and I performed experiments with the aim to understand the relationship between the type and the position of the substituents on the benzene ring and the rate of imine hydrolysis. I further compared the effects obtained with the substituted BBA containing electronic withdrawing groups with those gained with electron donating groups and the unsubstituted BBA.

The main hypothesis was that the electron withdrawing groups would enable the BBA to be more easily deprotonated, thus becoming a very good hydrogen bonds donor.

The Section 3.2 presented the results for the hydrolysis of the salicylidene-3-hydroxy aniline imine obtained with different benzenboronic acid derivatives catalysts in which the benzene ring was substituted with fluoro, nitro, carboxy or mixed combination of these electronic withdrawing groups. SAR experiments conducted with different fluoro-substituted benzenboronic acids showed that all fluoro-BBAs have higher catalytic efficiency of imine hydrolysis than the un-substituted boronic acid except for the catalysts with two fluoro substituted in *ortho*- position with respect to the boron which induced the steric hindrance effect (see Section 3.2.1).

Nitro groups are very well known electronic withdrawing groups when substituted to the benzene ring. Especially when the nitro group occupies the *meta* position, its electronic withdrawing effect is enhanced. Following the same trend observed for the fluoro-substituted BBAs, the nitro substituted benzenboronic acids have a much higher catalytic efficiency of imine hydrolysis than the un-substituted boronic acid (Section 3.2.2).

In addition to the nitro and fluoro-substituents, the SAR of mixed functional-substituted benzenboronic acids showed these compounds to have higher catalytic efficiency of imine hydrolysis than the un-substituted boronic acid (see Section 3.2.3).

A common structural feature of all these compounds was the placement of all these substituents in the *meta* position with respect to the boron atom. The preference for the *meta* position and not *ortho*, was originally determined by the previous results obtained with the

fluoro-substituents (see Table VIII) where I showed that *ortho* substituents could exert a steric hindrance effect upon the boron atom, and thus could result in a dramatic loss in catalytic efficiency (see Section 3.2.2).

Thus, the SAR of all these different substituents highlights the new structural requirements for the benzene substitutions for achieving the highest catalytic efficiencies. The best catalysts for the hydrolysis of salicylidene-3-hydroxyaniline imine were 2,3,5-trifluoroBBA and 2,3,4,5-tetrafluoroBBA. Thus, decision was taken to further investigate the major structural determinants of the imine substrates that modulate the overall catalytic efficiency of imine hydrolysis and other SAR for the imine substrates were performed.

### 3. SAR of different substituted imine substrates

The structure-activity relationship (SAR) of different imine substrates and their effect upon the BBA-imine complex formation and rate of imine hydrolysis was presented in Section 3.3 and Section 3.4. The most important contributions to the efficiency of imine hydrolysis are the hydrogen bonding donors or acceptors (hydroxy or amino groups) in the imine substrates which were shown to activate the catalytic turnover ( $k_{cat}$ ) of the benzene-boronic acid catalyst (like 2,3,4,5-tetrafluoroBBA). A mechanistic explanation is yet not known for this effect. It is proposed that the hydrogen bonding network provided by the hydroxyl or amino groups in the imine substrates during the hydrolysis could assist the BBAs catalysts in binding tighter to the substrate, which in turn, is reflected in higher catalytic efficiency (five to sixteen fold increase in the  $k_{cat}/K_M$  values observed for these hydroxyl/amino based substrates as compared with the imines lacking the hydroxy or amino groups). In Section 3.4.1 it is established that carboxyl group on amine help in binding but not in hydrolysis (see Table XV and Table XVI). Altogether, the results provided by the Tables XVII, XVIII, XIX and XXI compares salicylidene-valine and salicylidene-isoleucine to salicylidene-lysine, salicylidene-threonine and salicylidene-3-hydroxyphenylglycine imines. These comparisons together with the Section 3.4.2, highlight the importance of the hydroxyl group substituted to the benzene ring in aniline or benzylamine based imines in determining a better catalytic efficiency for their hydrolysis by the 2,3,5-trifluoroBBA.

#### 4. pH effects on catalytic constants

The pH dependence of the salicylidene-3-hydroxyaniline hydrolysis by different BBAs showed that the rate constants are maximal at lower pH and decrease with increasing pH (Figures 37a, 37b, 37c, 37d, 37e, and Section 3.7.2). These results demonstrate that there is no other ionization event related to the imine itself which could affect the final catalytic efficiency as already discussed in Section 3.7.

The analysis of the  $k_{\text{cat}}$ ,  $K_{\text{M}}$  and  $k_{\text{cat}}/K_{\text{M}}$  dependence with the pH (see Figures 37a, 37b, 37c, 37d, 37e, and Table XXV, Section 3.7.1, Section 3.7.2) prompted to another conclusion, that  $k_{\text{cat}}$  is independent of pH which indicates the absence of specific acid or base (i.e. hydroxide ion or hydronium ion) involvement in the hydrolysis.

In addition, the data presented in the Table XXV support the idea that the binding between BBA and the imine substrate becomes poorer with increasing pH, indicating that ionized boronic acids do not form a complex with the imine.

The data described for the pH dependence of the  $K_{\text{M}}$ ,  $k_{\text{cat}}$  and  $k_{\text{cat}}/K_{\text{M}}$  discussed in the Section 3.7.2 leads to further conclude that:

1. The *un-ionized* boronic acid reversibly esterifies with the phenolic hydroxyl group of the imine in the first step of the reaction.
2. The boronic acid complexes to the imine when the acid is in the trigonal, neutral configuration.
3. While binding is controlled by the boronic acid ionization, catalysis is independent of pH.

Previous studies of Rao *et al.* involving the solvent deuterium isotope effects on the hydrolysis of imine by BBAs prompted also the conclusion that there is no proton transfer in the rate-determining step.

## 5. Hammett plot analysis and linear free energy relationships

The Hammett plot of  $\text{Log}(K_M)$  vs. substituent constants (Figures 33, 34, 35) indicates that  $K_M$  is dependent on substituent groups present in the benzenboronic acids. Boronic acids with electron-withdrawing substituents stabilize the tetrahedral form or negative charge in the boronic acid-imine complex, whereas boronic acids with electron-donating substituents destabilize the complex. That is why binding is better in the cases of BBA with electron withdrawing substituents compared to benzenboronic acids with electron-donating substituents. These results are consistent with the results observed by Torssell *et al.*<sup>100</sup> where they found that electron-withdrawing groups on benzene ring increase the stability of the complexes of BBA with sugars compared to electron-donating substituents. Similar results were observed in the cases of enzyme-catalyzed reactions with boronic acids as inhibitors.<sup>48,101</sup>

## 6. Modeling of BBAs and imines complexes support the proposed mechanism of imine hydrolysis by BBA

Table XXIII and Figures (36a, e) show that there is a preference for the type of ester covalent bond between the BBA and imine which would enable the best stability of the complex. Thus, when the complex formation between the BBA and the imine is mediated by the ester bond with the salicylaldehyde hydroxyl group of the imine, the relative stability of the complex has the highest stability, as it is predicted by the docking experiments performed with Sculpt software. The most stable complex is between 2,3,5-trifluoro-BBA and the salicylidene-3-hydroxyaniline with a relative free energy of interaction of “-1160 kcal/mol” based on both van der Waals and electrostatic interactions.

Another important chemical signature that characterizes the stability of the complex between BBA and the imine, which is predicted by the docking experiments, is the presence of one fluorine functional group in the *ortho* position on the BBA side, which helps the binding of the imine substrate in the active site, and which, in turn, enables the activation of the imine hydrolysis. The lack of electronic withdrawing groups from the BBA side inhibits the formation of any stable complex between the BBA and the imine.

## 7. Mechanism of BBAs catalyzed hydrolyses of different imine substrates

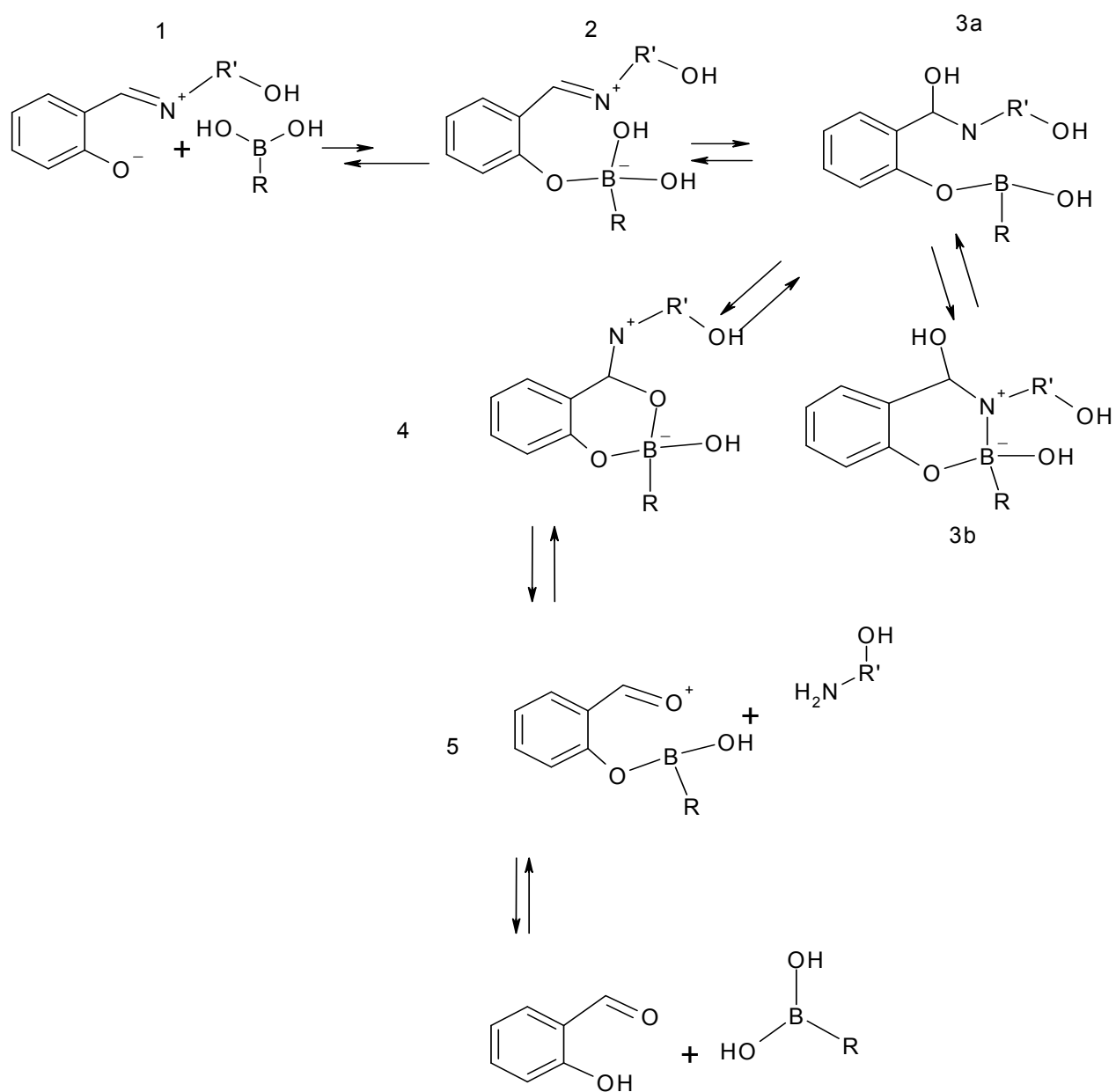
The major steps for the imine hydrolysis by BBAs are depicted in the Scheme I as follows:

1. The first step in the mechanism is the esterification of unionized boronic acid with the ionized phenolic hydroxy group of the Schiff's base. This step may be very rapid as observed in the esterification of boric acid with polyols<sup>102</sup>. In the second step, the nucleophilic oxygen of the hydroxyl group, attached to the boron, attacks the imine carbon and forms a six-membered ring as shown in 4. It is also possible that a six-membered ring 4 form through a carbinolamine intermediate 3a, which in turn forms from 2 by intramolecular transfer of hydroxyl group of the boronic group to the imine carbon. The six-membered ring 4 has a negative charge on the boron which is stabilized by electron-withdrawing substituents on benzene ring, whereas electron-donating substituents destabilize it. This could explain the better binding observed in the cases of arylboronic acids with electron-withdrawing substituents compared to electron-donating substituents. In subsequent steps, the six-membered ring breaks- down followed by the hydrolysis to give products.
2. It is also possible that a different six-membered ring 3b forms involving the imine nitrogen from carbinolamine intermediate 3a. This type of bicyclic structure was known with salicylamide<sup>89</sup>. The formation of this ring may be non-productive as it does not lead to products.
3. The rate-determining step is the break-down of six-membered ring 4 to another intermediate 5. No solvent deuterium-isotope effect in the experiment means that there is no proton transfer in this step. The boron atom does not change much electronically going from six-membered ring 4 to another intermediate 5, as it carries negative charge in both structures. That is why there is no substituent effect on this step. The catalytic rate constant is independent of pH as this step does not require any hydroxide ion or hydronium ion. Certainly, the hydroxyl group on the imine helps the complex formation when it is available. If the hydrolysis of intermediate 4 is the rate-determining step, then it would be expected that pH and substituent groups will have an effect on the catalytic rate constant. But there were no such effects observed in the experiments and it excludes the possibility of the

hydrolysis of intermediate 5 is the rate-determining step. Based on the above results, it may be concluded that the rate-determining step is the break-down of the six-membered ring 4.

4. This mechanism also explains the reversible reaction i.e. the formation of a Schiff's base.<sup>62</sup> In the reverse reaction, the boronic acid forms a complex with salicylaldehyde, the boron in the complex acts as a Lewis acid and coordinates to the carbonyl oxygen and makes the carbonyl carbon electron deficient facilitating the nucleophilic attack of an amine. The boron atom here acts like a metal ion in the hydrolysis of esters. In the hydrolysis of amino esters by metal ions, the metal ion coordinates to the carbonyl oxygen and facilitates the nucleophilic (OH<sup>-</sup>) attack on the carbonyl carbon.<sup>103</sup> In fact it has been shown that borate also acts in the same way in the hydrolysis of phenyl salilate.<sup>57</sup> The rate-determining step in the formation of a Schiff's base may be the attack of an amino on the carbonyl carbon.
5. The results presented here clearly indicate that different arylboronic acids are very good catalysts for hydrolyses of imines. Substrate binding is an important factor in the catalyzed reactions and if the binding is not good, then catalysis requires high concentration of catalysts or substrates which are the cases in some of these hydrolysis studies. Enzymes generally catalyze the reactions in the micromolar concentration range as binding of enzymes with substrates is good.
6. Studies with these arylboronic/benzenboronic acids provide additional support with the involvement of the hydroxyl group of the imine and provide solid support for the mechanism proposed earlier. Finally, it can be concluded that many arylboronic acids pose as one of the best enzyme models for the imine hydrolysis.

**Scheme I: Mechanistic scheme for the hydrolysis of the imine by BBA**



R, R' = substituted or unsubstituted aromatic hydrocarbon.

## References:

---

- <sup>1</sup> R. Pascal, *European Journal of Organic Chemistry* (10), 21, 1813-1824 (2003).
- <sup>2</sup> J. Steinhardt and C. H. Fugitt, *J. Res. Natl. Bur. Std. A.* 29, 315 (1942). Cited in *Bioorganic Mechanisms* by T. C. Bruice and S. Benkovic, Benjamin, New York, 2, 201 (1966).
- <sup>3</sup> H. Ladenheim, E. M. Loebel, and H. Morawetz, *J. Am. Chem. Soc.*, 81, 20 (1959).
- <sup>4</sup> H. Ladenheim and H. Morawetz, *J. Am. Chem. Soc.*, 81, 4860 (1959).
- <sup>5</sup> R. L. Letsinger and I. Klaus, *J. Am. Chem. Soc.*, 86, 3884 (1964)..
- <sup>6</sup> C. G. Overberger and J. C. Salamone. *Acc. Chem. Res.*, 2, 217 (1969).
- <sup>7</sup> H. C. Kiefer, W. I. Congdon, I. S. Scarapa, and I.M. Klotz, *Proc Nat. Acad Sci, USA*, 69, 2155 (1972).
- <sup>8</sup> G. Wulff. *Chem. Rev.*, 102(1), 1-28 (2002).
- <sup>9</sup> E. F. J. Duynstee and E. Grunwald, *J. Am. Chem. Soc.*, 81, 4540, 4542 (1959).
- <sup>10</sup> J. G. Fullington and E. H. Cordes, *Proc. Chem. Soc.* 224 (1964).
- <sup>11</sup> R. G. Shorestein, L. S. Pratt, C. J. Hsu, and T. E. Wagmer. *J. Am. Chem. Soc.*, 900, 6199 (1968).
- <sup>12</sup> C. A. Bunton, L. Robinson, and M. F. Stam. *Tetrahedron Lett.*, 121 (1971).
- <sup>13</sup> R. A. Moss. Y. S. Lee, and T. J. Luks, *J. Am. Chem. Soc.*, 101, 2499 (1979).
- <sup>14</sup> A. C. Dash, B. Dash, D. Panda. *J. Org. Chem.*, 50 (16), 2905–2910 (1985).
- <sup>15</sup> N. Hennrich and F. Cramer, *J. Am. Chem. Soc.*, 87, 1121 (1965).
- <sup>16</sup> R. L. VanEtten, J. F. Sebastian, G. A. Clowes, and M. L. Bender, *J. Am. Chem Soc.*, 89, 3242 (1967).

- 
- <sup>17</sup> R. L. VanRtten. G. A. Clowes, J. F. Sebastian, and M. L. Bender, *J. Am. Chem. Soc.*, 89, 3253 (1967).
- <sup>18</sup> R. Breslow and P. Campbell, *J. Am. Chem. Soc.*, 91, 3085 (1969).
- <sup>19</sup> K. Flohr, R. M. Paton, and E. T. Kaiser, *J. Am. Chem. Soc.*, 97, 1209 (1975).
- <sup>20</sup> R. Breslow, M. Hammond, and M. Lauer, *J. Am. Chem. Soc.*, 102, 421 (1980).
- <sup>21</sup> R. Breslow, J. B. Doherty, G. Guillot and C. Lipsey, *J. Am. Chem. Soc.*, 100, 3227 (1978).
- <sup>22</sup> I. Tabushi, Y. Kuroda, and A. Mochizuki, *J. Am. Chem. Soc.*, 102, 1152 (1980).
- <sup>23</sup> C. J. Pedersen, *J. Am. Chem. Soc.*, 89, 7017 (1967).
- <sup>24</sup> Y. Chao and D. J. Cram, *J. Am. Chem. Soc.*, 98, 1015 (1976).
- <sup>25</sup> J. M. Lehn and C. Sirlin, *Chem. Commun.*, 949 (1978).
- <sup>26</sup> J. Sunamoto, H. Kondo, H. Okamoto, and Y. Murakami, *Tetrahedron Lett.*, 1329 (1977).
- <sup>27</sup> T. R. Cech, A. J. Zaug, P. J. Grabowski, *Cell*, 27, 487 (1981).
- <sup>28</sup> K. Kruger, P. J. Grabowski, A. J. Zaug, J. Sands, D. E. Gottschling, and T. R. Cech, *Cell*, 31, 147 (1982).
- <sup>29</sup> G. Garriga and A. M. Lambowitz, *Cell*, 39, 631 (1984).
- <sup>30</sup> A. J. Zaug and T. R. Cech, *Nucleic Acids Res.*, 10, 2823 (1982).
- <sup>31</sup> T. R. Cech, *Ann. Rev. Biochem.* 59, 543 (1990).
- <sup>32</sup> A. J. Zaug and T. R. Cech, *Science*, 231, 470 (1986).
- <sup>33</sup> T. Shimidzu and R. L. Letsinger, *Bull. Chem. Soc. Jpn.* 44, 584 (1971).
- <sup>34</sup> T. Shimidzu and R. L. Letsinger, *Bull. Chem. Soc. Jpn.* 46, 3270 (1979).
- <sup>35</sup> Z. Tang and A. Marx, *Angewandte Chemie International Edition*, 46, 38, 7297 (2007).

- 
- <sup>36</sup> X. Li, D. R. Liu, *Angew. Chem.* 2004, 116, 4956. *Angew. Chem. Int. Ed.*, 43, 4848 (2004).
- <sup>37</sup> J. B. Doyon, T. M. Snyder, D. R. Liu, *J. Am. Chem. Soc.*, 125, 12372 (2003).
- <sup>38</sup> Z. J. Gartner, M.W. Kanan, D. R. Liu, *J. Am. Chem. Soc.*, 124, 10304 (2002).
- <sup>39</sup> Z. J. Gartner, B. N. Tse, R. Grubina, J. B. Doyon, T. M. Snyder, D. R. Liu, *Science*, 305, 1601. (2004).
- <sup>40</sup> J. O. Edwards, G. C. Morrison, V. Ross, and J. W. Schultz, *J. Am. Chem. Soc.*, 77, 266 (1955).
- <sup>41</sup> J. Boeseken, *Adv. Carbohydr. Chem.*, 4, 189 (1949).
- <sup>42</sup> H. Steinberg and D. L. Hunter, *Ind. Eng. Chem.*, 49, 174 (1957).
- <sup>43</sup> K. Kustin and R. Pizer, *J. Am. Chem. Soc.*, 91, 317 (1957).
- <sup>44</sup> S. Friedman, B. Pace, and R. Pizer, *J. Am. Chem. Soc.*, 96, 5381 (1974).
- <sup>45</sup> G. Lober and R. Pizer, *Inorg. Chem.*, 15, 978 (1976).
- <sup>46</sup> S. Friedman and R. Pizer, *J. Am. Chem. Soc.*, 97, 6059 (1975).
- <sup>47</sup> R. Pizer and L. Babcock, *Inorg. Chem.*, 16, 1677 (1977).
- <sup>48</sup> L. Babcock and R. Pizer, *Inorg. Chem.*, 19, 56 (1980).
- <sup>49</sup> H. L. Weith, J. L. Weibers, and P. T. Gilham, *Biochemistry*, 9, 4396 (1970).
- <sup>50</sup> K. Torssel, *Arkiv Kemi*, 10, 529 (1957).
- <sup>51</sup> M. Philipp and M. L. Bender, *Proc. Nat. Acad. Sci. USA*, 68, 478 (1971).
- <sup>52</sup> C. A. Kettner and A. B. Shenvi, *J. Biol. Chem.*, 259, 15106 (1984).
- <sup>53</sup> M. Philipp, G. Claeson, D. S. Matteson, T. Desoyza, E. Agner, and M. Sadhu, *Federation Proceedings*, 46, 2223 (1987).

- 
- <sup>54</sup> K. A. Koehler and G. E. Lienhard, *Biochemistry*, 10, 2477 (1971).
- <sup>55</sup> H. G. Peer, *Rec. Trav. Chim.*, 79, 825 (1960).
- <sup>56</sup> W. P. Jencks, *Catalysis in Chemistry and Enzymology*, McGraw-Hill, Inc., 30-32 (1969).
- <sup>57</sup> R. L. Letsinger, S. Dandegaonker, W. J. Vulio and J. D. Morrison, *J. Am. Chem. Soc.*, 85, 2223 (1963).
- <sup>58</sup> R. L. Letsinger and J. D. Morrison, *J. Am. Chem. Soc.*, 85, 2227 (1963).
- <sup>59</sup> R. L. Letsinger and D. B. Maclean, *J. M. Chem. Soc.*, 85, 2230 (1903).
- <sup>60</sup> B. Capon and B. C. Ghosh, *J. Chem. Soc. (B)*, 472 (1966).
- <sup>61</sup> T. Okuyama, H. Nagamatsu, and T. Fueno, *J. Org. Chem.*, 46, 1336 (1981).
- <sup>62</sup> H. Matsuda, H. Nagamatsu, T. Okuyama, and T. Fueno, *Bull. Chem. Soc. Jpn*, 57, 500 (1984).
- <sup>63</sup> H. Matsuda, H. Nagamatsu, T. Okuyama and T. Fueno, *Bull. Chem. Soc. Jpn*, 57, 500 (1984).
- <sup>64</sup> H. Nagamatsu, T. Okuyama and T. Fueno, *Bull. Chem. Soc. Jpn*, 57, 2502 (1984).
- <sup>65</sup> H. Nagamatsu, T. Okuyama and T. Fueno, *Bull. Chem. Soc. Jpn*, 57, 2508 (1984).
- <sup>66</sup> V. K. Antonov. T. V. Ivaniva. L .V. Brezin and K. Martinek. *Dokl. Akad Nauk. SSSR*. 183, 284 (1968).
- <sup>67</sup> I. Georgiou, G. Ilyashenko and A. Whiting. *Acc. Chem. Res.*, 42 (6), 756–768 (2009).
- <sup>68</sup> K. Ishihara, S. Ohara, and H. Yamamoto, *J. Org. Chem.*, 61 (13), 4196–4197 (1996).
- <sup>69</sup> G. Rao, M. Philipp, *J. Org. Chem.*, 56 (4), 1505–1512 (1991).
- <sup>70</sup> R. W. Layer, *Chem. Rev.*, 63 (5), 489–510 (1963).

- 
- <sup>71</sup> C. M. Metzler, A. Cahill, D. E. Metzler, *J. Am. Chem. Soc.*, 102 (19), 6075–6082 (1980).
- <sup>72</sup> H. Liu, H. Zheng, W. Miao and X. Du, *Langmuir*, 25 (5), 2941-2948 (2009).
- <sup>73</sup> S. S. Hindo, R. Shakya, N. S. Rannulu, M. M. Allard, M. J. Heeg, M. T. Rodgers, S. R. P. da Rocha and C. N. Verani, *Inorg. Chem.*, 47 (8), 3119–3127 (2008).
- <sup>74</sup> Choi KH, Lai V, Foster CE, Morris AJ, Tolan DR, Allen KN. *Biochemistry*, 45, 8546-8555 (2006).
- <sup>75</sup> T. Soeta, M. Kuriyama, and K. Tomioka. *J. Org. Chem.*, 70 (1), 297–300 (2005).
- <sup>76</sup> P. Marcazzan, C. Abu-Gnim, K. N. Seneviratne, and B. R. James. *Inorg. Chem.*, 43 (16), pp 4820–4824 (2004).
- <sup>77</sup> Kambli, D. K., Patil, I. R., Laxmeshwar, N. B., and Prabhu, D. V., *Asian J. Chem.*, 11, 189 (1999).
- <sup>78</sup> Echevarria-Gorostidi, G. R., Perez, M. P. M., Santos, J. G., and Blanco, F. G., *Helv. Chim. Acta*, 82,769 (1998).
- <sup>79</sup> Ming-Dong Zhoua, Shu-Liang Zang, E. Herdtweck and F. E. Kühn, *Journal of Organometallic Chemistry*. 693, 15, 2473-2477 (2008).
- <sup>80</sup> Ho-hi Lee and T. Kitagawa, *Bull. Chem. Soc. Jpn.*, 59, 2897-2898 (1986).
- <sup>81</sup> A. A. Soliman, *Spectrochimica Acta Part A* 53, 509-515 (1997).
- <sup>82</sup> L.I. Kozhevina, E.B. Prokopenko, V.I. Rybachenko, E.V. titov. *Spectrochimica Acta Part A* 51 (1995) 2517-2523.
- <sup>83</sup> J.J. Charette and E. de Hoffmann. *J. Org. Chem.*, Vol. 44, No. 13, 2256-2262 (1979).
- <sup>84</sup> C. Hansch, A. Leo, W. Taft, *Chem. Rev.*, 91, 165-195 (1991).
- <sup>85</sup> L. P. Hammett, *Chem. Rev.*, 17 (1), 125-136 (1935).
- <sup>86</sup> S. L. Keenan, K.P. Peterson, K. Peterson, and K. Jacobson, *J. Chem. Ed*, 85(4) (2008).
- <sup>87</sup> R. F. Cookson. *Chem. Rev.* 74, 5 (1974).
- <sup>88</sup> C. Long, *Biochemists' Handbook*, Van Nostrand Reinhold Comp., pages 30-42.

- 
- <sup>89</sup> F. J. Kezdy and M. L. Bender, *Biochemistry*, 1, 1097 (19962).
- <sup>90</sup> El-Taher, M. A., *J. Chin. Chem. Soc. (Taipei)*, 45, 815 (1998); *Chem. Abs.*, 130, 153278 (1999).
- <sup>91</sup> T. D. James, P. Linnane, S. Shinkai, *Chem. Commun.*, 281-288 (1996).
- <sup>92</sup> W. Wang, X. Gao, B. Wang, *Curr. Org. Chem.* 6, 1285-1317 (2002).
- <sup>93</sup> J. G. Yan, S. Springsteen, B. Deeter, 11205-11209 (2004).
- <sup>94</sup> J. Hoffman, V. Sterba, *Collect. Czech. Chem. Commun.* 37, 2043 (1972).
- <sup>95</sup> H. Nakatani, T. Morita, and K. hiromi, *Biochim. Biophys. Acta*, 525, 423 (1978).
- <sup>96</sup> *Chemical Principles: The Quest for Insight*. Peter Atkins, Loretta Jones, Macmillan, (2007).
- <sup>97</sup> R. Herscovitch, J. J. Charette, and E. de Hoffmann, *J. Am. Chem. Soc.*, 96, 4954 (1974).
- <sup>98</sup> D. W. Tanner and T. C. Bruice, *J. Am. Chem. Soc.*, 89, 6954 (1967).
- <sup>99</sup> V. R. Ripan, G. Kiss-imreh, and Z. Szekely, *Rev. Roum. Chim.*, 10, 965 (1965).
- <sup>100</sup> K. Torssell, J. H. McClendon, and G. M. Somers, *Acta Chem. Scand.*, 12, 1373 (1953).
- <sup>101</sup> I. Tsai and M. L. Bender, *Arch. Biochem. Biophys*, 228, 555 (1984).
- <sup>102</sup> G. L. Roy, A. L. Laferriere, and J. O. Edwards, *J. Inorg. Nucl. Chem.*, 4, 106 (1957).
- <sup>103</sup> M. L. Bender and B. W. Turnquest, *J. Am. Chem. Soc.*, 79, 1889 (1957).